

**IMPROVING FOREST FRAGMENTATION DETECTION IN MEXICO,
AND ASSESS JAGUAR HABITAT IN CENTRAL MEXICO**

By

Carlos Daniel Ramirez Reyes

A dissertation submitted in partial fulfillment of
the requirements for the degree of

Doctor of Philosophy

(Forestry)

at the

UNIVERSITY OF WISCONSIN-MADISON

2016

Date of final oral examination: 8/30/2016

The dissertation is approved by the following members of the Final Oral Committee:

Volker C. Radeloff, Department of Forest and Wildlife Ecology

Jennifer Alix-Garcia, Department of Agriculture and Applied Economics

Mutlu Ozdogan, Department of Forest and Wildlife Ecology

Tim Van Deelen, Department of Forest and Wildlife Ecology

Alberto Vargas, Latin American and Caribbean Studies

IMPROVING FOREST FRAGMENTATION DETECTION IN MEXICO, AND ASSESS JAGUAR HABITAT IN CENTRAL MEXICO

Carlos Daniel Ramirez Reyes

Under the supervision of Professor Volker Radeloff
at the University of Wisconsin-Madison

Abstract

Deforestation decreases both biodiversity and other ecosystem services that forests provide, such as climate regulation and water regulation. Given high rates of deforestation across the world, especially in tropical forests, international efforts have implemented forest protection programs to offer payments for ecosystem services (PES). Monitoring the performance of these programs over large areas can be difficult, especially in areas with limited satellite data availability. Furthermore, even when deforestation data is available, it is often unclear how deforestation has affected levels of forest fragmentation or habitat availability for wildlife species including predators. The goal of this dissertation was to monitor forest fragmentation and deforestation in tropical forests, and to map potential habitat and its connectivity for jaguars. I found a gradient of forest fragmentation across Mexico, moving from lower levels of fragmentation in the north, to higher levels of fragmentation in the south and east of the country. The highest levels of forest core were lost within tropical forests. Forests that were enrolled in the PES program had less fragmentation than those that were not. To improve detection of deforestation, I combined Landsat and MODIS images to assess deforestation in areas with strong phenology, and where original Landsat imagery was lacking. From this

assessment, I calculated deforestation rates across Mexico, which confirmed the gradient of low deforestation in the north to high deforestation in the south. At the local level, I generated a potential habitat suitability map for jaguars in the Sierra Gorda Biosphere Reserve in Central Mexico and identified the areas that were most important for habitat connectivity. Moreover, I developed new methods to identify optimal thresholds of minimum patch size and habitat suitability for connectivity analyses. My approaches can be easily transferred to other systems where there is a need to assess deforestation with limited imagery, forest fragmentation, and habitat connectivity.

Acknowledgements

This work has my name on the cover, but from its conception and until its finishing details required the work, feedback and support from many people. Naming everybody that in a direct or indirect way contributed to this work and my formation as a professional would take many pages but certainly there are people I want to show my appreciation. First, I want to thank my advisor Volker Radeloff, who have both guided me and contributed actively to this dissertation. Thank you for having welcomed me both to the lab and also to your house, for the multiple walks we had, shared experiences, and advices. I also want to thank the members of my committee, who helped me to focus and complete this dissertation. Jennifer Alix-Garcia, was a key person since she invited me to be part of the project in Mexico. I learned a lot of new approaches, suggestions, and she was a great collaborator. Mutlu Ozdogan, was always willing to help in my endeavors, I really appreciate his follow through my sporadic but urgent requests, and also for stopping to check in by to my former office. Tim Van Deelen, provided me with ground thinking and valuable comments of my work. I really enjoyed his personal, ecological and management chats during trips around the state. Alberto Vargas was a great person to ask for a fresh and external point of view to my work. Alberto was always eager to help and provided useful comments to improve the scope of the dissertation.

My work included a lot of feedback from my collaborators Elizabeth Shapiro and Katherine Sims, thank you for the professionalism. I want to acknowledge the Mexican National Forest Commission, in particular Efrain Abundio, Jesus Gutierrez, Carmen Meneses, Adriana Saldaña, and Rodolfo Valdez. Thanks also to the people from the Grupo Ecologico Sierra Gorda, and Jaime Lagunas from the Sierra Gorda Reserve, who

graciously guided me to collect field data. I am very thankful to Glen Aronson and Emily Duerr for their help during the early stages of the research. Also to Jeff Wala and multiple students that helped me digitize data. I am most grateful to the funding agencies that allowed me to make this work, including the International Initiative for Impact Evaluation and NASA Earth and Space Science Fellowship. The University of Wisconsin- Madison provided me with great facilities and resources to succeed academically and personally, it certainly became my second alma mater.

During my time in Madison I have been part of the Silvis lab, with which I have shared both office time and also interpersonal relationships. From my arrival, the lab was a great group of smart, knowledgeable, and friendly people. I really enjoyed that our lab meetings often looked like an UN assembly, with people with many diverse backgrounds and experiences. During my years as a student in the lab I have met over 30 Silvis lab members and visitors. Thank you all for being great company in this trip, share your laughter, beer, games, space, food and camaraderie. A special ode to Dave Helmers, who introduced me to Wisconsin fine beers, bowling skills, and downhill sledding survival skills; and also solved my processing needs along my research. Special thanks to Anita, Catalina, Chris, Genia, Isabel, Johanna, Konrad, Martina, Max, Naparat, Patricia, and Sebastian for daring and surviving my culinary attempts, and also for join me to experience Madison city. I am very happy I crossed wonderful people also outside from the lab, and I want to thank Arnoldo, Brian, Carlos, Carlyne, Dennisse, Erika, Eve, Hector, Jesus, Jianxiao, Lauren, Michael, Ken, Omar, Oscar, Paulina, Ricky, Sarahy,

Shai, and the wonderful people I met in Madison, those that are gone in the ones that stay to enjoy this great town.

I want to recognize my mother Yolanda Reyes Vilchis, a marvelous loving entity I always admire; my brother, Marco Ramirez, who always supports, and Sandra Ramirez, whose laughter is comforting and contagious. Distance is large, their love is larger.

Thanks to Ali, whose love, shared adventures, patience, support, and encouragement during happy and stressing times, made this work possible. Finally, my writing would not be finished without Alejandro Mora, the person that checked with me more often and also checked constantly the progress of my dissertation.

Table of Contents

Chapter 1: Payments for ecosystem services in Mexico reduced forest

fragmentation	30
1-1 Abstract	30
1-2 Introduction	32
1-3 Methods	34
1-3.1 Study area	34
1-3.2 Data	34
1-3.3 Forest morphology	35
1-3.4 Microlandscapes	36
1-3.5 Matching microlandscapes	37
1-4 Results	38
1-4.1 Forest morphology in Mexico	38
1-4.2 Fragmentation according the forest types	39
1-4.3 Fragmentation in PES areas	40
1-4.4 Fragmentation in protected areas	40
1-5 Discussion	41
1-6 Conclusion	45
1-7 Literature cited	46

1-8 Tables	57
1-9 Figures.....	60
Chapter 2: Spectral Mixture Analysis of STARFM fusion images improves deforestation assessments of diverse forest types in Mexico	66
2-1 Abstract	66
2-2 Introduction	68
2-3 Methods.....	71
2-3.1 Study area.....	71
2-3.3 Relative radiometric normalization.....	73
2-3.4 STARFM.....	73
2-3.5 Spectral Mixture Analysis.....	74
2-3.6 Deforestation estimation	74
2-3.7 Accuracy assessment.....	75
2-4 Results.....	76
2-5 Discussion	79
2-6 Conclusions	82
2-7 Literature cited	83
2-8 Tables	91
2-9 Figures.....	95

Chapter 3: Effects of habitat suitability and minimum patch size thresholds on the assessment of landscape connectivity for jaguars in the Sierra Gorda, Mexico	101
3-1 Abstract	101
3-2 Introduction	103
3-3 Methods	106
3-3.1 Study area	106
3-3.2 Input data: jaguar occurrences and environmental data	107
3-3.3 Potential habitat modeling	108
3-3.4 Connectivity analysis	109
3-3.5 Identification of the optimal combination of thresholds	110
3-4 Results	111
3-4.1 Threshold selection	112
3-4.2 Habitat connectivity	113
3-4.3 The optimal combination of thresholds	113
3-5 Discussion	114
3-6 Literature cited	120
3-7 Tables	132
3-8 Figures	133

List of figures

Figure 1-1: Our study area in Mexico, including the properties enrolled in the PES between 2003 and 2010, as well as the north, central, southwest and southeast zones that we used for our analysis.....	60
Figure 1-2: Example of forest morphology analysis. Depending on the neighborhood cover type, forested pixels will be assigned to different categories.	61
Figure 1-3: Percent change for the main forest morphology categories for all of Mexico.	62
Figure 1-4: Top: Map of vegetation type in Mexico in which we only include forests types. Bottom: Forest morphology changes in each vegetation type (proportion of the total of forest per category in 2000).....	63
Figure 1-5: Comparison between forest morphology changes in PES and non-PES microlandscapes. We calculated the changes in relation to the total forest area in category in 2000, and conducted the analysis for each zone.	64
Figure 1-6: Comparison between forest morphology changes in PES areas and the National Protected Areas System. We calculated the changes in relation to the total forest area in category in 2000, and conducted the analysis for each zone.	65
Figure 2-1: Study area. The three squares represent the northern, central and southeastern Landsat footprints that we analyzed in Mexico. We include the path and row for each of the footprints.....	95
Figure 2-2: Endmembers used in the spectral unmixing process.	96

Figure 2-3: Correlation between the vegetation fraction maps produced with T_0 raw surface reflectance values of the T_1 fraction maps produced with a) raw surface reflectance, b) radiometric normalization and c) STARFM fusion image. We show the r^2 value of the regression lines. The grey area represents a confidence interval for the fitted values of the model. 97

Figure 2-4: Changes between vegetation fraction maps T_1 and T_0 and the corresponding deforestation validation points, where 1 corresponds to a deforested pixel and 0 to an intact forest pixel. 98

Figure 2-5: Example of the deforestation found using 0.1, 0.2 and 0.3 threshold values for the difference in vegetation fraction maps. This area corresponds to a large deforested area in the northern footprint. 99

Figure 2-6: Example of the deforestation detected using a STARFM fusion image. The images correspond to a) the surface reflectance in 2001, b) surface reflectance in 2012, and c) surface reflectance in 2012, with the mapped deforestation in orange. 100

Figure 3-1: Sierra Gorda Biosphere Reserve in Central Mexico. The core zones are located at the margins of the reserve. 133

Figure 3-2: Flow diagram of the approach that we developed to identify the best thresholds for habitat suitability index, HSI, and minimum patch size, MPS. We evaluated the performance of each combination of thresholds to describe connectivity based on the area under the curve, AUC. The processes are mentioned on the right while

the tools used at each step are mentioned on the left. Only a few examples from the total of 45 combinations that we evaluated are shown here. 134

Figure 3-3: Habitat suitability in the study area as determined by our model. The most suitable areas are in the central-eastern part of the reserve and in the south. 135

Figure 3-4: Figure 4: Performance of the integral index of connectivity, dIIC, obtained with different habitat suitability thresholds and minimum patch size for the jaguar presence points. Patches with dark colors provide better connectivity for the patch network. For display purposes we do not include all the different combinations tested at different habitat suitability indexes and minimum patch size. No patches remained at a HSI larger than 0.8. 136

Figure 3-5: Landscape configuration metrics for different habitat suitability index, HSI, and minimum patch size, MPS. Both the color and size of the circles are proportionate to their respective metric score. 137

Figure 3-6: Performance of the integral index of connectivity obtained with different habitat suitability thresholds, and minimum patch size for the jaguar presence points. A better model has a higher area under the curve (AUC), and therefore a lighter color. No patches were left with a HSI larger than 0.8. 138

Figure 3-7: Connectivity of the potential habitat for jaguars in the reserve using the combination of thresholds for habitat suitability index 0.3 and a minimum patch size of 2km^2 . The habitat areas that are most important for the connectivity of the area are located in the eastern portion of the reserve 139

Overview

Conservation of forest ecosystems is important, as these areas host a number of wildlife species and regulate surface energy, water, and greenhouse gas fluxes (Foley et al., 2005). Deforestation is of great concern across the globe, because it leads to negative effects such as loss in biodiversity, destruction of the hydrological cycle, altered regional climate, decreased water quality, and accelerated soil erosion (Broadbent et al., 2008; Geist and Lambin, 2002; Huppe, 2008). In addition, deforestation can lead to environmental and economic costs both in the areas where it occurs and also in downstream areas that no longer receive the benefits of forest services (Metzger et al., 2006). Globally, nearly 40% of all forests have been lost over the last two centuries (Shvidenko, 2008). In recent decades, deforestation in tropical areas has been especially high, with rates of 4.04×10^6 ha yr⁻¹ during the 1990s and 6.54×10^6 ha yr⁻¹ in the 2000s (Kim et al., 2015).

Deforestation leads to forest fragmentation by increasing edge habitat and changing the configuration of remaining forest patches, thereby exposing ecosystems to external forces that could degrade them (Harper et al., 2005). While forest fragmentation can lead to increased habitat for certain generalist species and shade intolerant species (Tabarelli et al., 2012), fragmentation has many negative consequences for forest ecosystems. Fragmentation can lead to species isolation, reduction of prey species, change in species composition, establishment of invasive species, and changes in the physical environment that ultimately affect ecosystem services (Haddad et al., 2015; Harper et al., 2005; Lindenmayer and Fischer, 2013). Hence, measures of fragmentation can provide a proxy to assess ecosystem services (Dobbs *et al.*, 2011). The fate of forest

core areas is especially important, as they provide unique conditions that many species require to survive and reproduce (Vogt et al., 2007a). Forest edges are more susceptible to edge effects such as tree mortality, changes in species composition and invasions by exotic species (Harper et al., 2005).

Despite the importance of ecosystem services provided by forests, forest owners often receive few direct benefits from forest conservation. The reason is that these benefits are frequently of less monetary value than the ones of alternative land uses, such as conversion to cropland or pasture (Castillo et al., 2005). In such cases, payments for ecosystem services (PES) can help to make conservation a more attractive option for landowners, by offering them incentives to protect their forests (Pagiola et al., 2005). In order to reduce high deforestation rates, the Mexican National Forest Commission, CONAFOR, established a PES program in 2003. The aim was to provide forest landowners with economic incentives to maintain forests on their land, thereby benefitting watershed protection (Alix-Garcia et al., 2005; Corbera et al., 2009). Since 2003, the program was gradually expanded, and more than 2.3 million ha were enrolled by 2011 (CONAFOR, 2012). The PES program works in coordination with the United Nations as part of their Reducing Emissions from Deforestation and Forest Degradation (REDD) initiative in developing countries, which aims to mitigate greenhouse emissions by enhancing forest management in developing countries. Similar economic incentive programs are becoming increasingly popular as a way to manage ecosystems (Farley and Costanza, 2010), making Mexico's PES an important benchmark for learning from its experience.

Although individual properties receiving funds from the program are being monitored to verify their eligibility after 3 years of being enrolled, measuring the effects at large scales is complicated because of the large magnitude of the PES program. Multiple studies have measured the performance of the PES program at the local level, putting emphasis on evaluating particular elements of the environment such as water quality (Martínez et al., 2009), local economies (Bautista and Torres, 2003; Corbera et al., 2009), and cultural perceptions (Kosoy et al., 2008). These local studies have reported a range of failures and successes. For instance, individual properties or small groups of properties have not complied with the program rules (Costedoat et al., 2015; Le Velly et al., 2015). On the other hand, other studies reported good performance in terms of preventing forest loss and also a satisfactory perception of the people participating in the PES (Caro-Borrero et al., 2015; Manzo-Delgado et al., 2014; Rico García-Amado et al., 2013). More recently, extensive nation-wide evaluations found that Mexico's PES program has been successful in preventing deforestation (Sims and Alix-Garcia, 2015) and poverty alleviation (Alix-Garcia et al., 2015). Although these assessments have highlighted the effectiveness of the PES for preventing forest loss, we remain uncertain of the patterns that deforestation has created in the landscapes, which could affect the provision of ecosystem services.

Monitoring deforestation and fragmentation at large scales is best done using remote sensing, and is facilitated by increasing data availability and computer processing power (Hansen and Loveland, 2012). However, despite recent advances in remote sensing to investigate land cover change patterns (Aide et al., 2013; Hansen et al., 2013),

there is still uncertainty about forest cover changes in areas with challenging environmental conditions, such as mixed and deciduous forests, high cloud persistence, and pronounced topography. This problem is amplified if there is not enough image availability to capture similar phenological conditions when making comparisons between two or more dates. Thus, in order to overcome low image availability, new methods have been designed to combine different types of satellite imagery (Gao et al., 2006). These image fusion analyses can combine coarse images with high temporal resolution, such as MODIS, with images that have lower temporal but higher spatial resolution, like Landsat. This combination of MODIS and Landsat imagery allows us to capture smaller deforestation events (Hilker et al., 2009; Jia et al., 2014).

Another consideration is that deforestation assessments are mostly done in a binary way, where forest is either present or absent, and do not capture intermediate events such as partial tree removal. Binary deforestation evaluations are common because it is difficult to capture changes in vegetation that are smaller than the unit of analysis, which is dictated by the pixel size of the image used. For this purpose, sub-pixel analysis techniques are available, such as spectral mixture analysis, which assess the proportion of a pixel that is occupied by a particular land cover type (Adams et al., 1986). Although spectral mixture analysis has been known for some time and has provided good evaluations of forest cover in different landscapes (Dawelbait and Morari, 2012; Matricardi et al., 2010; Yang et al., 2012), we are not aware of any prior studies that applied spectral mixture analysis to fusion images, which could potentially fill a gap in forest degradation analysis.

Besides impacts on ecosystem service provision, deforestation often affects wildlife populations, as species depend on specific conditions to survive, and deforestation diminishes the habitat in which species live, feed, and reproduce (Haines-Young, 2009). Large predators are particularly important to study because they can be indicators of the health of ecosystems. These species often occupy large areas for their biological needs including hunting, nesting, and reproduction (Woodroffe, 2000). Moreover, the presence of predators can indicate the presence of the species that they feed on (Lantshener *et al.*, 2012). Because of deforestation in central Mexico, jaguar populations (*Panthera onca*) have shrunk. Jaguar populations were once widespread across Mexico, but few suitable habitat areas in the central region remain. It is therefore important to locate the remaining habitat for this species and to evaluate the connectivity of this habitat. In addition, by looking at the configuration of the potential habitat of this species, we could also learn about this predator's responses to fragmentation.

The overarching goal of my dissertation research was to identify strategies to monitor forest fragmentation in tropical forests. This goal was especially important because many other developing countries are either considering or applying forest protection as part of the REDD+ and other global efforts to limit carbon emissions due to deforestation (Kemkes *et al.*, 2010; Kanowski *et al.*, 2011). My specific research questions were:

1. What are the patterns of forest fragmentation in Mexico and did the Payment for Ecosystems Services program limit fragmentation?

2. Does combining MODIS and Landsat satellite imagery, and applying spectral mixture analysis improve deforestation detection?

3. Where is the potential habitat for jaguars in the Sierra Gorda Biosphere Reserve and how well is it connected?

These questions correspond to three different levels of analysis: country level, regional level and local level. In order to address these questions, I divided this dissertation into three chapters. In the following pages I provide a synopsis for each of the chapters.

Chapter 1 summary

Research question: What are the patterns of forest fragmentation in Mexico and did the Payment for Ecosystems Services program limit fragmentation?

Given high deforestation rates over the past decades in Mexico, the Mexican government implemented a payment for ecosystem services program in 2003. Although overall deforestation rates have decreased in PES areas, measuring levels of forest fragmentation would provide another indication of the performance of the program to prevent ecological damages at the national level. By measuring rates of forest fragmentation across Mexico, it would be possible to determine which regions and forest types are subject to greater land use change.

My goal for this chapter was to determine whether areas enrolled in the PES program had lower rates of forest fragmentation than areas that did not participate in the program. I was particularly interested in: a) calculating the differences in forest morphological patterns in Mexico, b) identifying the forest types that are most affected by fragmentation, c) measuring the performance of the PES to prevent fragmentation, and d) comparing the differences between PES areas and protected areas to prevent fragmentation.

I generated forest fragmentation maps for all of Mexico based on global forest cover assessments between 2000 and 2012 (Hansen et al., 2013). I divided the country into a grid of 1.98-km resolution microlandscapes for making comparisons. For each cell in the grid, I calculated the occupancy of multiple forest categories, based on morphological spatial pattern analysis and fragmentation metrics. By comparing grid

cells with similar characteristics, I was able to compare forest changes between PES areas and non-PES areas, as well between PES areas and protected areas.

My analyses showed both that the majority of Mexico's forests are within core areas, and that the majority of the deforestation occurred in these core areas. I also found that, on average, properties that received PES support had lower forest fragmentation compared to the properties that did not receive protection funds. These differences were strongest in the south of the country, and minimal in the north. Among forest types, mid and high-stature tropical forest experienced the highest rates of forest conversion, while oak and pine forests had the lowest. Compared to protected areas of Mexico's National Protected Area System, the properties with PES status had a similar performance to general protected areas, but lower performance than the strict core areas within biosphere reserves.

Overall, core forest in Mexico showed high fragmentation rates in the southern regions of the country, where the tropical forests occur. The PES reduced fragmentation in areas of high deforestation, but did not stop it completely. The PES program performed similarly to other established protected areas, so a combination of both strategies could extend protection in sensitive regions. In this context, there are opportunities to target areas with higher deforestation risk in the southern part in the country for conservation, while other areas in the north may not represent big risks for forest fragmentation.

Resulting paper: Ramirez-Reyes, C., Sims, K., and Radeloff, V.C. Payment for ecosystem services in Mexico reduced forest fragmentation. Anticipated submission: Sep 2016 to Landscape Ecology

Chapter 2 summary

Research question: Does combining MODIS and Landsat satellite imagery, and applying spectral mixture analysis improve deforestation detection?

Mexican forests are diverse, with multiple vegetation types including deciduous and mixed forest. During the growing season, there is often a constant cloud cover over many of Mexico's forests, making detection of forest change difficult. While medium resolution satellites like Landsat are good sources of imagery for detecting vegetation change, the frequent cloud cover in Mexico leads to a small pool of images that can be used for forest change detection, and even fewer available images at the same phenological stages. New algorithms have been developed to combine higher acquisition frequency images from MODIS, with less frequent Landsat images. However, we do not know whether or not these fusion images can be used to detect small vegetation changes at the subpixel level, which would improve deforestation detection in areas with low image availability.

My goal was to evaluate the performance of fusion images for detecting deforestation in Mexico. I was interested in: a) measuring deforestation rates in different areas of Mexico, and b) evaluating the potential use of Landsat-MODIS combined imagery as a basis for spectral mixture analysis.

I evaluated the potential use of fusion imagery as a basis for spectral mixture analysis by comparing a) surface reflectance images, b) radiometric normalized images and c) fusion images. I compared results from the three image types for both 2000 and 2010 in a northern, central, and southern Landsat footprint. Based on the resulting

images, I generated vegetation fraction maps, and used sensitivity analysis to calculate deforestation rates. In this sensitivity analysis, I determined the threshold at which differences in vegetation fraction maps could be considered deforestation events.

I found that by using these predicted Landsat images, the assessment of deforestation improved in areas where original Landsat imagery was lacking. This method allowed us to compare images with similar phenological development. However, when Landsat imagery was available to make comparisons at times with similar phenology stages, the use of original Landsat images was best for identifying deforestation. The deforestation rates that I obtained had a north-to-south gradient, where southern areas experienced the largest forest changes.

In conclusion, my research showed that the combination of Landsat-MODIS fusion imagery can improve the accuracy of deforestation estimates, particularly in areas where phenological differences are pronounced, and where Landsat images are scarce. This opens the possibility of using similar approaches to study forest cover loss in a continuous way, rather than the frequently used binary forest-non-forest approach.

Resulting paper: Ramirez-Reyes, C., and Radeloff V. C. Use of Spectral Mixture Analysis in STARFM fusion images to assess deforestation in diverse forest types in Mexico. Anticipated submission: Sep 2016 to Remote Sensing of Environment

Chapter 3

Research question: Where is the potential habitat for jaguars in the Sierra Gorda Biosphere Reserve and how well is it connected?

Habitat loss is one of the major causes of declining wildlife populations. A decrease in habitat has many potential negative consequences for species, such as limiting their range, limiting food sources, and increasing exposure to diseases. Moreover, changes in habitat configuration can diminish the connectivity among areas occupied by different populations of a given species. This is why there is an interest in locating and protecting the remaining habitat of species. Predators are particularly interesting, because they are species whose presence can indicate healthy ecosystems.

My goal was to assess potential habitat for jaguars (*Panthera onca*) and its connectivity in the Sierra Gorda Biosphere Reserve in central Mexico. I was interested in examining the effects of different thresholds of both habitat suitability and minimum patch size on resulting habitat connectivity. I sought to develop a new approach for identifying the optimal combination of these thresholds.

I first generated a potential habitat model for jaguars in the Sierra Gorda reserve and its surroundings, based on a database of the occurrences of jaguars in the region, and the environmental conditions that could explain the presence of these felines. Since my connectivity analysis required a binary habitat no-habitat map, I conducted a sensitivity analysis to determine the optimal thresholds of habitat suitability and minimum patch size. I then described the connectivity of the potential habitat using the map resulting from the best combination of thresholds.

I found that jaguar's potential habitat was primarily within oak and pine forests in the reserve. The best-connected areas were the large habitat patches located in the central and eastern parts of the reserve. These potential habitat areas were predominantly within the buffer zone of the reserve, while the highly protected core areas showed little suitability for the species. Based on the connectivity assessments, I determined that jaguars can occupy potential habitat areas as small as 2 km², and that a 0.3 threshold for the habitat suitability model best described the presence data.

From these results, I concluded that minimum patch size and habitat suitability thresholds greatly affect subsequent connectivity analysis. Therefore, it is important to apply a sensitivity analysis to determine the appropriate thresholds to use. Jaguars generally prefer large habitat areas, but they can also occupy smaller habitat patches in fragmented landscapes. Although the conditions may not be optimal, the buffer zones of the Sierra Gorda Biosphere Reserve could potentially host jaguars, with opportunities for increased protection outside of the reserve in highly suitable areas.

Resulting paper: Ramirez-Reyes, C., Bateman, B. L., and Radeloff V. C. Effects of habitat suitability and minimum patch size thresholds on the assessment of landscape connectivity for Jaguars in the Sierra Gorda, Mexico. *Biological Conservation*. Under review

Overall significance

The PES program in Mexico is one of the largest and oldest of the world. It is thus important to evaluate its performance. As such, my work provides useful information to the program's managers, so they can modify and potentially improve it. CONAFOR is making an effort to evaluate landcover changes in relation to the PES program, and my study provides a broad assessment by identifying fragmentation both in areas receiving funds from the program and in areas that did not. Moreover, with the growing increase of conservation efforts, there is also an increasing need of outcome evaluations. Therefore my work builds on these efforts to improve forest change detection using fusion imagery. Finally, my work contributes to wildlife management needs, as it provides a way to improve potential habitat and connectivity assessments.

My research goal and objectives are important for several fields because I addressed questions of interest to specialists in remote sensing, conservation biology, environmental management and local and international actors. Thus, my research made contributions in three dimensions: Scientific, methodological and also in terms of conservation.

Scientific contributions

In Chapter 1, I contributed to the understanding of the relationships between incentive programs for environmental protection and forest fragmentation. This work also illustrated how deforestation rates are translated into fragmentation rates, and also how different vegetation types are more subject to fragmentation processes. **In Chapter 2**, I demonstrated how different image products produced deforestation estimations. I

explored avenues to use fusion imagery to overcome low image availability in the assessment of forest degradation. This analysis could be particularly important for dry ecosystems and forest where cuts occur progressively. In **Chapter 3**, I demonstrated how different thresholds for minimum patch size affect the extent and configuration of potential habitat. The variation of these will greatly affect further connectivity analysis.

Methodological contribution

Mexico's latitude, topography and closeness to oceans are the cause for very complex ecosystems that provide challenging conditions for remote sensing analysis and wildlife studies. For this reason there were numerous methodological opportunities to advance in remote sensing science and wildlife habitat modeling. In **Chapter 1**, I analyzed worldwide assessment of deforestation via image morphology analysis to generate forest fragmentation maps. In **Chapter 2**, I tested the use of fusion images in spectral mixture analysis to improve deforestation detection. This opened opportunities to study forest degradation using fusion imagery. In **Chapter 3**, I developed a new method to identify optimal thresholds for both minimum patch area and habitat suitability. This technique can be applied to other places where minimum patch size is critical for the species of interest.

Conservation and applied research contribution

My work has direct applications for CONAFOR, which is restructuring its PES program. In **Chapter 1**, I assessed the performance of the PES program in preventing forest fragmentation. The results could give this Mexican agency an indicator of the

performance of the program to prevent deforestation and forest fragmentation at broad spatial scales. In **Chapter 2**, I analyzed deforestation rates based on fusion images, which could provide the images needed to measure forest cover and partial tree removal in areas where images are lacking. In **Chapter 3**, I provided a map of potential habitat that the conservation NGO Grupo Ecologico Sierra Gorda could use when taking decision regarding the protection of the species. This NGO is interested in having an assessment of jaguar habitat beyond the borders of the reserve and thus could benefit from my habitat estimation both within the reserve as well as in the surrounding area.

Literature cited

- Adams, J.B., Smith, M.O., Johnson, P.E., 1986. Spectral mixture modeling: A new analysis of rock and soil types at the Viking Lander 1 Site. *J. Geophys. Res.* 91, 8098–8112. doi:10.1029/JB091iB08p08098
- Aide, T.M., Clark, M.L., Grau, H.R., López-Carr, D., Levy, M.A., Redo, D., Bonilla-Moheno, M., Riner, G., Andrade-Núñez, M.J., Muñiz, M., 2013. Deforestation and Reforestation of Latin America and the Caribbean (2001-2010). *Biotropica* 45, 262–271. doi:10.1111/j.1744-7429.2012.00908.x
- Alix-Garcia, J., Janvry, A. de, Sadoulet, E., 2005. A Tale of Two Communities: Explaining Deforestation in Mexico. *Institutional Arrange. Rural poverty Reduct. Resour. Conserv.* 33, 219–235. doi:10.1016/j.worlddev.2004.07.010
- Alix-Garcia, J.M., Sims, K.R.E., Yañez-Pagans, P., 2015. Only one tree from each seed? Environmental effectiveness and poverty alleviation in Mexico's payments for ecosystem services program. *Am. Econ. J. Econ. Policy* 7, 1–40. doi:10.1257/pol.20130139
- Bautista, H., Torres, J., 2003. Valoración económica del almacenamiento de carbono del bosque tropical del ejido Noh Bec, Quintana Roo, México. *Rev. Chapingo* 9, 69–75.
- Broadbent, E.N., Asner, G.P., Keller, M., Knapp, D.E., Oliveira, P.J.C., Silva, J.N., 2008. Forest fragmentation and edge effects from deforestation and selective logging in

- the Brazilian Amazon. *Biol. Conserv.* 141, 1745–1757.
doi:10.1016/j.biocon.2008.04.024
- Caro-Borrero, A., Corbera, E., Neitzel, K.C., Almeida-Leñero, L., 2015. “We are the city lungs”: Payments for ecosystem services in the outskirts of Mexico City. *Land use policy* 43, 138–148. doi:10.1016/j.landusepol.2014.11.008
- Castillo, A., Magaña, A., Pujadas, A., Martínez, L., Godínez, C., 2005. Understanding the interaction of rural people with ecosystems: a case study in a tropical dry forest of Mexico. *Ecosystems* 2005, 630–643.
- CONAFOR, 2012. *Servicios Ambientales y Cambio Climático*. CONAFOR, Guadalajara, Mexico.
- Corbera, E., Soberanis, C.G., Brown, K., 2009. Institutional dimensions of Payments for Ecosystem Services: An analysis of Mexico’s carbon forestry programme. *Ecol. Econ.* 68, 743–761. doi:10.1016/j.ecolecon.2008.06.008
- Costedoat, S., Corbera, E., Ezzine-de-Blas, D., Honey-Rosés, J., Baylis, K., Castillo-Santiago, M.A., 2015. How effective are biodiversity conservation payments in Mexico? *PLoS One* 10, e0119881. doi:10.1371/journal.pone.0119881
- Dawelbait, M., Morari, F., 2012. Monitoring desertification in a Savannah region in Sudan using Landsat images and spectral mixture analysis. *J. Arid Environ.* 80, 45–55. doi:10.1016/j.jaridenv.2011.12.011

Farley, J., Costanza, R., 2010. Payments for ecosystem services: From local to global.

Spec. Sect. - Payments Ecosyst. Serv. From Local to Glob. 69, 2060–2068.

doi:10.1016/j.ecolecon.2010.06.010

Foley, J.A., Defries, R., Asner, G.P., Barford, C., Bonan, G., Carpenter, S.R., Chapin,

F.S., Coe, M.T., Daily, G.C., Gibbs, H.K., Helkowski, J.H., Holloway, T.,

Howard, E.A., Kucharik, C.J., Monfreda, C., Patz, J.A., Prentice, I.C.,

Ramankutty, N., Snyder, P.K., 2005. Global consequences of land use. *Science*

309, 570–4. doi:10.1126/science.1111772

Gao, F., Masek, J., Schwaller, M., Hall, F., 2006. On the blending of the Landsat and

MODIS surface reflectance: predicting daily Landsat surface reflectance. *IEEE*

Trans. Geosci. Remote Sens. 44, 2207–2218. doi:10.1109/TGRS.2006.872081

Geist, H.J., Lambin, E.F., 2002. Proximate causes and underlying driving forces of

tropical deforestation. *Bioscience* 52, 143–150.

Haddad, N.M., Brudvig, L.A., Clobert, J., Davies, K.F., Gonzalez, A., Holt, R.D.,

Lovejoy, T.E., Sexton, J.O., Austin, M.P., Collins, C.D., King, A.J., Laurance,

W.F., Levey, D.J., 2015. Habitat fragmentation and its lasting impact on Earth's

ecosystems. *Sci. Adv.* doi:10.1126/sciadv.1500052

Hansen, M.C., Loveland, T.R., 2012. A review of large area monitoring of land cover

change using Landsat data. *Remote Sens. Environ.* 122, 66–74.

doi:10.1016/j.rse.2011.08.024

- Hansen, M.C., Potapov, P. V, Moore, R., Hancher, M., Turubanova, S.A., Tyukavina, A., Thau, D., Stehman, S. V, Goetz, S.J., Loveland, T.R., Kommareddy, A., Egorov, A., Chini, L., Justice, C.O., Townshend, J.R.G., 2013. High-resolution global maps of 21st-century forest cover change. *Science* 342, 850–3. doi:10.1126/science.1244693
- Harper, K. a., Macdonald, E., Burton, P., Chen, J., Brosofske, K.D., Saunders, S.C., Euskirchen, E.S., Roberts, D., Jaiteh, M.S., Esseen, P.-A., 2005. Edge influence on forest structure and composition in fragmented landscapes. *Conserv. Biol.* 19, 768–782. doi:10.1111/j.1523-1739.2005.00045.x
- Hilker, T., Wulder, M.A., Coops, N.C., Seitz, N., White, J.C., Gao, F., Masek, J.G., Stenhouse, G., 2009. Generation of dense time series synthetic Landsat data through data blending with MODIS using a spatial and temporal adaptive reflectance fusion model. *Remote Sens. Environ.* 113, 1988–1999. doi:10.1016/j.rse.2009.05.011
- Huppe, H., 2008. The Forests of Mexico: Sustaining Mexico’s Cultural, Biological and Economic Values for the Future [WWW Document].
- Jia, K., Liang, S., Zhang, L., Wei, X., Yao, Y., Xie, X., 2014. Forest cover classification using Landsat ETM+ data and time series MODIS NDVI data. *Int. J. Appl. Earth Obs. Geoinf.* 33, 32–38. doi:10.1016/j.jag.2014.04.015

- Kim, D.-H., Sexton, J.O., Townshend, J.R., 2015. Accelerated deforestation in the humid tropics from the 1990s to the 2000s. *Geophys. Res. Lett.* 42, 3495–3501.
doi:10.1002/2014GL062777
- Kosoy, N., Corbera, E., Brown, K., 2008. Participation in payments for ecosystem services: Case studies from the Lacandon rainforest, Mexico. *Placing Splintering Urban.* 39, 2073–2083. doi:10.1016/j.geoforum.2008.08.007
- Le Velly, G., Dutilly, C., de Blas, E., Fernandez, C., 2015. PES as compensation ? Redistribution of payments for forest conservation in Mexican common forests. *Études Doc. CERDI* 28, 1–25.
- Lindenmayer, D.B., Fischer, J., 2013. *Habitat Fragmentation and Landscape Change: An Ecological and Conservation Synthesis.* Island Press.
- Manzo-Delgado, L., López-García, J., Alcántara-Ayala, I., 2014. Role of forest conservation in lessening land degradation in a temperate region: The Monarch Butterfly Biosphere Reserve, Mexico. *J. Environ. Manage.* 138, 55–66.
doi:10.1016/j.jenvman.2013.11.017
- Martínez, M.L., Pérez-Maqueo, O., Vázquez, G., Castillo-Campos, G., García-Franco, J., Mehlreter, K., Equihua, M., Landgrave, R., 2009. Effects of land use change on biodiversity and ecosystem services in tropical montane cloud forests of Mexico. *For. Ecol. Manage.* 258, 1856–1863. doi:10.1016/j.foreco.2009.02.023

- Matricardi, E.A.T., Skole, D.L., Pedlowski, M.A., Chomentowski, W., Fernandes, L.C., 2010. Assessment of tropical forest degradation by selective logging and fire using Landsat imagery. *Remote Sens. Environ.* 114, 1117–1129. doi:10.1016/j.rse.2010.01.001
- Metzger, M.J., Rounsevell, M.D.A., Acosta-Michlik, L., Leemans, R., Schröter, D., 2006. The vulnerability of ecosystem services to land use change. *Scenar. Stud. Futur. L. Use Eur.* 114, 69–85. doi:10.1016/j.agee.2005.11.025
- Pagiola, S., Arcenas, A., Platais, G., 2005. Can Payments for Environmental Services Help Reduce Poverty? An Exploration of the Issues and the Evidence to Date from Latin America. *Institutional Arrange. Rural poverty Reduct. Resour. Conserv.* 33, 237–253. doi:10.1016/j.worlddev.2004.07.011
- Rico García-Amado, L., Ruiz Pérez, M., Barrasa García, S., 2013. Motivation for conservation: Assessing integrated conservation and development projects and payments for environmental services in La Sepultura Biosphere Reserve, Chiapas, Mexico. *Ecol. Econ.* 89, 92–100. doi:10.1016/j.ecolecon.2013.02.002
- Sims, K.R., Alix-Garcia, J.M., 2015. It's complicated: Direct vs. incentive-based land conservation in Mexico. *Work. Pap.*
- Tabarelli, M., Peres, C.A., Melo, F.P.L., 2012. The “few winners and many losers” paradigm revisited: Emerging prospects for tropical forest biodiversity. *Biol. Conserv.* 155, 136–140. doi:10.1016/j.biocon.2012.06.020

Yang, J., Weisberg, P.J., Bristow, N.A., 2012. Landsat remote sensing approaches for monitoring long-term tree cover dynamics in semi-arid woodlands: Comparison of vegetation indices and spectral mixture analysis. *Remote Sens. Environ.* 119, 62–71. doi:10.1016/j.rse.2011.12.004

Chapter 1: Payments for ecosystem services in Mexico

reduced forest fragmentation

Contributors: Ramirez-Reyes, C.¹, Radeloff, Volker. C.¹, and Sims, Katherine R. E.²

¹ SILVIS Lab, Department of Forest and Wildlife Ecology, University of Wisconsin-Madison, 1630 Linden Drive, Madison WI 53706, USA.

² Department of Economics, AC 2201, Amherst College, Amherst, MA 01002, USA

1-1 Abstract

Forest fragmentation is a problem because it reduces wildlife habitat, increases forest edges, and exposes forest to disturbances. Different programs aim to protect forests, including programs that offer payment for ecosystem services (PES), and Mexico was one of the first countries to implement a broad-scale PES program enrolling over 2.3 million ha and decreasing deforestation rates. However, it is not clear if this reduction in deforestation also prevented forest fragmentation. Our goal was to determine whether Mexican forests enrolled in the PES program had less forest fragmentation than those who did not participate in the program, and if the PES effects varied among forest types. We analyzed forest cover change maps from 2000 to 2012, applied image morphology, and measured fragmentation to calculate the amount of forest core, edges, number of deforestation patches, and the maximum deforested patch area. We summarized fragmentation according to forest types in four socioeconomic zones. We used matching analysis to investigate the effects of the PES to protect forest across Mexico, and compared the effects of the PES program with that of protected areas. We found that

forest area in Mexico decreased by 3.4% percent from 2000 to 2012, resulting in 9.3% less core areas. Fragmentation rates were highest in the southern part of the country, and high-stature evergreen tropical forest type lost the most core areas (-17%), while oak forest lost the least (-2%). The PES program limited forest loss and forest fragmentation. Edge, forest islets, and maximum deforested patch area increased only half as much in areas enrolled in the PES program compared to non-enrolled areas. Compared to the National Protected Areas System in Mexico, PES areas performed similarly in preventing fragmentation, but not as well as biosphere reserve core areas. We concluded that the PES was successful in limiting forest fragmentation at the regional and country level. However, the program could be improved by targeting areas where forest changes are more frequent, especially in southern Mexico. Fragmentation analysis like ours should be implemented in other areas to monitor the outcomes of protection programs such as REDD+ and PES.

Keywords: Deforestation, land use change, MSPA, image morphology, protected areas

1-2 Introduction

One common consequence of deforestation is the increasing fragmentation of forest ecosystems, which results from reducing forest area, increasing forest edges, and increasing smaller noncontiguous fragments (Broadbent et al., 2008; Laurance, 2000). Forest fragmentation has many negative effects, such as loss of biodiversity (Butchart et al., 2010), changes in species composition (Laurance et al., 2007), reduced habitat connectivity (Dixo et al., 2009) and promotion of non-native species (With, 2004). Furthermore, fragmentation is difficult to reverse after it has occurred, making it a long-lasting problem (Ferraz et al., 2003; Gibson et al., 2013; Vellend et al., 2006). In order to prevent these negative effects, multiple conservation efforts have been promoted, including the creation of protected areas. However, despite a growing number of protected areas, deforestation rates are still high in many forests, resulting in more fragmentation (DeFries et al., 2005).

Global deforestation assessments indicate that although deforestation has slowed overall, there are still hotspots of forest loss (Hansen et al., 2013; Keenan et al., 2015), and this is where fragmentation rates are also most likely high (Wade et al., 2003). Indeed, while only 3.2% of all forests were lost globally between 2000 and 2012, a full 9.9% of interior forests were lost (Riitters et al., 2016). This highlights why fragmentation analyses are crucial in order to identify whether deforestation is affecting forest core areas, which are ecologically most valuable (Vogt et al., 2007a), or areas along forest edges (Harper et al., 2005).

Among all forest types, tropical forests have the highest rates of deforestation, while other forests are most stable (Hansen et al., 2013). This has been the case for several decades, and particularly in the last 20 years, when tropical forest increased their deforestation rates (Kim et al., 2015). Tropical deforestation is partly due to an increasing demand for wood, and also due to the conversion of forests to agricultural and pasture lands (Geist and Lambin, 2002; Gibbs et al., 2010). However, it is in the tropics where species richness is highest (Myers et al., 2000). Moreover, preventing forest loss in the tropics could inhibit changes in the hydrological regime and emission of green houses to the atmosphere (Fearnside, 2005; Geissen et al., 2009).

Several protection programs have been proposed to limit tropical deforestation outside of protected areas. Examples of these efforts are the payment for ecosystems services (PES), and more recently, reducing emissions from deforestation and forest degradation, and foster conservation, sustainable management of forests, and enhancement of forest carbon stocks, REDD+ (Hosonuma et al., 2012). Mexico, which has experienced high deforestation rates (Mas et al., 2004; Velazquez et al., 2002) has initiated a major PES program in 2003, being one of the first of its kind. By the year 2010 over 3,300 properties were enrolled in the program, covering >2.3 million ha. This PES program is managed by Mexico's National Forest Commission, CONAFOR, and pays rural landowners in high-deforestation-risk areas to not deforest and to improve their livelihoods. Local studies that evaluated this PES program reported a range of outcomes, including non-compliance with PES rules (Costedoat et al., 2015; Le Velly et al., 2015), but also successes and positive perception of the PES program (Caro-Borrero et al., 2015;

Manzo-Delgado et al., 2014; Rico García-Amado et al., 2013). Recent nation-wide assessments showed that the PES program successfully reduced deforestation, and provided economic benefits for landowners (Alix-Garcia et al., 2015; Sims et al., 2014), but it is not yet known whether the program is also preventing forest fragmentation.

Our goal was to determine whether areas enrolled in Mexico's PES program had lower forest fragmentation than non-enrolled areas. Our objectives were to a) calculate the differences in forest fragmentation in Mexico between 2000 and 2012, b) identify the forest types that were most affected by fragmentation, c) assess the performance of the PES to prevent fragmentation, and d) compare the performance of the PES program with that of protected areas to diminish forest fragmentation.

1-3 Methods

1-3.1 STUDY AREA

We studied forest fragmentation in Mexico, which is varied in topography, influenced by two oceans, and located in the transition zone of the neotropical and neoartic realms. These environmental conditions result in multiple vegetation types across the country, including evergreen tropical forest, deciduous forest, temperate forest, and deserts (Rzedowski, 2006). We divided the country in four regions, i.e., north, central, southwest and southeast, based on their socioeconomic and vegetation similarities, in order to detect regional variation in the fragmentation..

1-3.2 DATA

Forest cover

We analyzed forest fragmentation from 2000 to 2012 based on the Global Forest Change dataset, GFC, which provides wall-to-wall forest cover, forest loss, and forest gain based on Landsat satellite images (Hansen et al., 2013). We analyzed the 30-m resolution forest cover layer for 2000 as the baseline for our analysis. In order to define a forest-non forest binary map, we considered any pixel with >30% tree cover as forested. We chose this threshold because previous forest fragmentation studies used the same value, thereby ensuring comparability of our results (Haddad et al., 2015; Lira et al., 2012). In order to obtain net forest cover in 2012, we added the 2000-12 forest gain to the 2000 forest cover, and then subtracted 2000-12 forest loss.

PES properties

We analyzed all the properties that were enrolled in the PES between 2003 and 2010 according to a CONAFOR dataset. This dataset included 6297 polygons of enrolled properties ranging in size from 2 to 7287 ha with a mean of 362 ha.

1-3.3 FOREST MORPHOLOGY

In order to quantify forest patterns, we used the Morphological Spatial Pattern Analysis software ‘MSPA’ (Soille and Vogt, 2009). This tool has been previously used to analyze forest fragmentation (e.g., Estreguil and Mouton, 2009; Vogt et al., 2007b) and lauded as a cost-effective tool to monitor forest change (Bucki et al., 2012). With MSPA, we calculated several forest morphology classes, including core (interior area), islets (forest area too small to be considered core), perforation (holes in core area), edge

(external perimeter), bridge (corridor connecting core areas), loop (habitat corridor ending in same core area), and branch (small area connected to core) (Figure 2). We obtained forest morphology for the forest present in both 2000 and 2012, and applied the 8 neighbor rule, in which a forest cell is connected if any of their sides or corners is in contact with another forest cell, and a one-pixel edge. This neighbor rule and edge width has been used previously to calculate forest patches and their connectivity (Locke and Rissman, 2012; Sorte et al., 2004). We also calculated the number of deforested patches and area of the largest deforested patch using the R package *SDMTools* (VanDerWal et al., 2014).

1-3.4 *MICROLANDSCAPES*

Because the PES properties are very different in size, we defined a constant unit of analysis in order to compare enrolled and non-enrolled forests based on the microlandscape approach (Sims, 2014). Specifically, we divided the country into a continuous grid of 1.98 km x 1.98 km microlandscapes. We chose this grid cell size for two reasons, first because this resolution is biologically relevant for large carnivores (Ramirez-Reyes et al., 2016), and second, because the mean size of PES enrolled areas is 362 ha (roughly 1.9 km by 1.9 km). In order to ensure that the forest cover pixels (30 m) were nested within our microlandscapes, we used a 1980 m x 1980 m (67 by 67 pixels in our forest cover data) for the grid cell size.

We differentiated the microlandscape cells according to their protection level. We considered as PES microlandscapes all grid cells with >50% of their area (majority) enrolled in the PES program. The microlandscapes with <5 0% of PES enrolled area

where treated as non-PES microlandscapes. Similarly, we considered as protected areas all the microlandscapes with >50% of their area within the boundaries of the Mexico's National Protected Areas System (CONANP, 2016). Last but not least, we wanted to identify those microlandscapes within core areas in the Biosphere Reserves in Mexico, which have the highest level of protection since human activities are restricted to research and conservation. For that reason we performed another filter for the microlandscapes, in which we selected those with >80% within the Biosphere Reserves' core areas. This threshold was applied to ensure that most of the pixel was within the core area.

1-3.5 *MATCHING MICROLANDSCAPES*

We selected a set of microlandscapes that did not participate in PES as a control group, to be compared to areas that received PES incentives using the R package *MatchIt* (Ho et al., 2013). In order to identify microlandscapes that were comparable, we identified covariates that might influence both deforestation and the protection status of a property enrolled the PES, such as the distance to roads and cities, and slope (full set of covariates in Table 1). Based on these covariates, we selected microlandscapes that did not participate in the PES but have similar geographic characteristics (Randolph et al., 2014; Stuart and Rubin, 2008). We did the matching separately for each of the four zones in the country and only considered microlandscapes with >50% forest cover in 2000 using Mahalanobis distance with replacement following prior studies (Sims, 2014). We also performed a similar process to match microlandscapes enrolled in the PES, with microlandscapes within protected areas.

We summarized forest morphology transitions between 2000 and 2012 for the whole country, and also for each forest type according to a vegetation map for Mexico (CONABIO, 1998), using the percent change formula: $(\% \text{ forest MSPA class}_{2012} * 100) / (\% \text{ forest MSPA class}_{2000}) - 100$. At the regional level, we calculated the percent change of forests for each of the main forest morphology classes (core, islets, perforation, and edge), the number of deforested patches, and the maximum deforested patch area. We performed t-test on the matched sets of microlandscapes in order to test for significant differences between: a) PES enrolled areas vs non-PES areas, b) PES areas vs protected areas and c) PES areas vs core protected areas.

1-4 Results

1-4.1 FOREST MORPHOLOGY IN MEXICO

According to our morphology analysis for 2012, forests in Mexico were mainly core areas (67%) or edges (11%), while the other forest categories ranged between 3 and 5%. Between 2000 and 2012, there were substantial changes in the proportion of the different forest morphology classes, with most of the fragmentation effects happening in the east, central and southern parts of the country (Figure 3). Core areas were lost at particularly high rates in the Yucatan peninsula and along the Gulf of Mexico, while higher changes in forest perforation were also observed in the Yucatan peninsula. We found a total of 21,700 km² that were deforested, which accounted 3.4% of the forest present in year 2000. The majority of what was deforested were core forest areas (69%), while edges and branches contributed with 9% and 5% respectively. As a consequence of

this deforestation, forest core areas diminished by 9.3%. More than half of the forest core that was lost transitioned to other forest categories, such as perforation (24%) and edges (11%), while 40% became non-forest. In case of forest islets, 90% of their surface remained, while 7% became deforested and the rest transitioned to other category such as branches (1%). From the total forest classified as perforation in year 2000, 76.2% remained until 2012, and the rest of forest in that category was either lost (4.1%), or transitioned to forest edge (7.5%), core (5.7), or to other categories in smaller proportion. In the case of forest edges, 90.9% of their surface remained, while 3.2% transitioned to non-forest, 1.7% to bridge, 1.4% to branch, 1.1% to core, and the rest to other categories.

1-4.2 FRAGMENTATION ACCORDING THE FOREST TYPES

Forest fragmentation had different intensities depending on the forest type. The forest that experienced the most deforestation were the mid and high-stature evergreen and semi-evergreen tropical forests, which lost 7.4 and 7.3% of forest cover respectively, followed by mid-stature deciduous and semi-deciduous tropical forest, which each lost 6.3%. This deforestation caused a core forest reduction of 17% for high-stature evergreen and semi-evergreen tropical forests, 13% for mid-stature evergreen and semi-evergreen tropical forests and 8% for cloud forest. Some of this loss of core forest transitioned to another more edge-sensitive forest category, such as islets, perforation, and edges, which increased between 20 and 94% in the same period (Figure 4). The forests types that experienced the least deforestation were oak (-0.7%), conifers other than pine (-0.7%), mangrove (-1%), and pine (-1%). These forest types also presented the least reduction in

core forest (between -2 and -4%), and the least increase of islets, perforation and edge (<7%).

1-4.3 FRAGMENTATION IN PES AREAS

At the national level, the microlandscapes that were enrolled in the PES program had lower fragmentation compared to those that were not enrolled. On average, forest core in PES areas decreased by 2.3%, while areas without protection decreased 3.5%. For other forest categories, forest changes were almost twice as high in areas that were not enrolled in the PES. For instance, forest islets increased on average by 14.4% for PES and 38.4% for non-PES, while edge increased by 44.5% in PES areas, but 87.7 % in non-PES areas. The maximum deforested patch area was also smaller for PES areas (1.87 ha), and higher in non-PES areas (3.4 ha). The number of deforestation patches was 9.5 for PES and 12.9 for non-PES areas (Table 3).

At the regional level, the effects of the PES program to prevent fragmentation were most clearly evident in the southwest and southeast (Figure 5). For instance, in the southeast forest core changed about twice as much in non-PES (-8.1%) compared to PES (-4%). Edges also changed twice as much in non-PES areas (106.4%) compared to PES (236.1%), while islets increased three times more (122.1 and 44.1% respectively). There was a similar trend in for the maximum deforested patch area, where non-PES areas deforested 4.9 ha, while non-PES averaged 11.1 ha. Nevertheless, there were no significant differences between PES and non-PES areas in the central and north regions.

1-4.4 FRAGMENTATION IN PROTECTED AREAS

Areas that were protected in the National Protected Areas System in Mexico had similar outcome as those that were enrolled in the PES in terms of protecting forest core areas, which changed 2.1 and 2% respectively (Fig 6.). However, the PES properties had higher increase in forest perforation (117%) compared to protected areas (62.7%). We also found a significant difference between the maximum area of the largest deforested patch, which was 8.38 ha in the PES areas, and 7.15 ha in the protected areas. Forest islets, edge, and maximum patch area were not significantly different. Similarly, there were no significant differences in change of forest core, edge, and islets, between the PES and the core areas of Biosphere reserves. However, core areas had less increase in perforation (61.3%), in the number of deforested patches (7.1%) and in the maximum area of deforested patch (1 ha). In the case of PES areas, the same categories changed 125%, 8.56% and 1.5 ha respectively.

1-5 Discussion

Our analysis found that forest became more fragmented in Mexico, and especially in tropical forest which are losing core areas, and increasing their edges. However, properties enrolled in the PES program had lower rates of forest fragmentation, particularly in the south, where most of the deforestation occurred. Compared to protected areas, the PES performed similarly well in preventing forest fragmentation. However, when compared to core areas of biosphere reserves, the PES performed less well, and did not match the effectiveness of protection of these most-strictly protected areas.

Deforestation is one of the main causes of forest disturbance in Mexico, as there is constant pressure for new agriculture, and housing development (Calderon-Aguilera et al., 2012). Despite that, deforestation rates have decreased in Mexico (Roth et al., 2016). We found that the majority of forests in Mexico are within core areas (69%), which is also where the majority of deforestation happened (69.2% of the total deforested area). Hence, deforestation in the country occurred both in forest interior and along their edges. We found that the net forest loss was 3.4%, and the loss of core forest was 9.32%. These results are similar to the global fragmentation trends reported for the same period, in which the net forest loss was 3.2% and the forest interior was reduced in 9.9% (Riitters et al., 2016). This highlights that even when deforestation rates are low, fragmentation may proceed rapidly. In our analysis half of the forest core that was lost transitioned to non-forest, while the other half transitioned to another forest category. In consequence, forest categories that are typical for fragmented forests, such as perforation, loop, bridge, and edge increased 16-17% across the country. Although forest edges could provide some benefits such as increasing habitat for certain generalist species (Carrara et al., 2015), they have overall negative effects (Haddad et al., 2015), and edge effects can penetrate into core areas (Laurance, 2000).

Among forest types, tropical forests experienced the most forest changes in Mexico. High- and mid-stature tropical forest had the highest rates of loss of core forest (17 and 13% respectively) and also the highest edge gain (47 and 62%). These high fragmentation rates are likely due to the close proximity of tropical forest to human disturbances in Mexico, where only 12 % of its forests are isolated enough to avoid such

influences (Moreno-Sanchez et al., 2012). The high fragmentation rates that we found are a concern because tropical forest provides multiple ecosystem services, and therefore are of priority for protection (Myers et al., 2000). Some of the effects that fragmentation have in tropical forest are a decrease in primary forest species including insectivores and canopy frugivores (Barlow et al., 2007), decrease bat populations (Arroyo-Rodríguez et al., 2016), and changes in forest composition (Herrerías-Diego et al., 2008). Cloud forest is another forest type that lost forest core areas rapidly (11%). Despite that cloud forest represents only a small proportion of the total forest in Mexico (3.5%), it is a conservation priority because it is high in biodiversity and provides important ecosystem services such as water catchment (Martínez et al., 2009). On the opposite side of the spectrum, forest types that are fairly widespread, such as pine forest (20%), low-stature deciduous forest (15%), and oak forest (13%), had the least forest core loss (4, 4, and 2% respectively). These forest types are relatively resilient to fragmentation, because they harbor more edge-adapted species, but they can still be affected by invasives (Harper et al., 2005). Our observed forest fragmentation in temperate forest is consistent with trends seen in other countries, where these forest types had lower forest loss, or even gained extension (Chazdon, 2008). In Mexico, a large proportion of pine forest (23%) is isolated from human influences and thus preventing its deforestation (Moreno-Sanchez et al., 2012).

The PES program in Mexico has reduced the risk of deforestation between 40–51% (Alix-Garcia et al., 2015), and we found a concomitant reduction in fragmentation within PES areas. However, the PES program had only minor effects in protecting forest

in the north, perhaps because of low access and low population density near forest, which resulted in low rates of fragmentation regardless of whether forests were enrolled in the PES program or not. On the contrary, the PES areas have performed well to prevent fragmentation in the southern parts of the country, particularly in the southeast zone. Part of this reduction in fragmentation is because the Mexican authorities have increased the scope of the PES program, and are targeting high-risk deforestation areas (Sims et al., 2014). It was not surprising that the south exhibited higher rates of fragmentation, given the high deforestation risk due to physical geographic conditions, high population density, and history, particularly along the gulf of Mexico (González-Abraham et al., 2015).

Protected areas are generally effective in terms of preventing deforestation across the world (Naughton-Treves et al., 2005), and we found also positive effects in Mexico, similar to other studies (Sims and Alix-Garcia, 2015). Part of the success of the protected areas is because they have lower human pressures than their surroundings (Gonzalez-Abraham et al., 2016). Another reason is because protected areas can have mixed use management, and funding that facilitates monitoring, enforcement, and planning (Blackman et al., 2015). In our analysis, the PES program performed similarly well as protected areas in terms of preventing forest fragmentation. The effects of protection of the PES program, however, were lower compared to core areas of biosphere reserves. This is possibly because core areas have restricted human activities for longer time, while PES areas could have deforestation inertia. Since human activities are restricted in core areas of biosphere reserves, these areas can be used as a proxy to differentiate natural

(e.g. hurricanes and fires) vs human forest disturbances (e.g. logging and agriculture expansion). We could thus assume that the fragmentation rates observed in core areas are mostly due of natural disturbances and higher rates elsewhere would be due to human disturbances. As most of the forest fragmentation changes in PES are higher than in core areas, we can assume that PES protection decreased human disturbances, but did not stop them entirely.

1-6 Conclusions

We found that Mexico's PES program works well to limit forest fragmentation, particularly in the southwest and southeast parts of the country, where forest edges have doubled or tripled in areas that were not enrolled, and where tropical forests were lost and fragmented. Mexico's deforestation affected especially forest core areas, which either transitioned to edge or to non-forest. Compared to other protection schemes, the PES program performs similar to protected areas in limiting forest fragmentation. This is encouraging, because many countries have implemented PES programs in recent years. The data that we used, i.e., the global analysis for deforestation is available worldwide (Hansen et al., 2013), forest fragmentation assessments using MSPA could, and possibly should, be conducted elsewhere in order to monitor the effects of programs that prevent deforestation.

1-7 Literature cited

- Alix-Garcia, J.M., Sims, K.R.E., Yañez-Pagans, P., 2015. Only one tree from each seed? Environmental effectiveness and poverty alleviation in Mexico's payments for ecosystem services program. *Am. Econ. J. Econ. Policy* 7, 1–40.
doi:10.1257/pol.20130139
- Arroyo-Rodríguez, V., Rojas, C., Saldaña-Vázquez, R.A., Stoner, K.E., 2016. Landscape composition is more important than landscape configuration for phyllostomid bat assemblages in a fragmented biodiversity hotspot. *Biol. Conserv.* 198, 84–92.
doi:10.1016/j.biocon.2016.03.026
- Barlow, J., Mestre, L.A.M., Gardner, T.A., Peres, C.A., 2007. The value of primary, secondary and plantation forests for Amazonian birds. *Biol. Conserv.* 136, 212–231. doi:10.1016/j.biocon.2006.11.021
- Blackman, A., Pfaff, A., Robalino, J., 2015. Paper park performance: Mexico's natural protected areas in the 1990s. *Glob. Environ. Chang.* 31, 50–61.
doi:10.1016/j.gloenvcha.2014.12.004
- Broadbent, E.N., Asner, G.P., Keller, M., Knapp, D.E., Oliveira, P.J.C., Silva, J.N., 2008. Forest fragmentation and edge effects from deforestation and selective logging in the Brazilian Amazon. *Biol. Conserv.* 141, 1745–1757.
doi:10.1016/j.biocon.2008.04.024

Bucki, M., Cuypers, D., Mayaux, P., Achard, F., Estreguil, C., Grassi, G., 2012.

Assessing REDD+ performance of countries with low monitoring capacities: the matrix approach. *Environ. Res. Lett.* 7, 014031. doi:10.1088/1748-9326/7/1/014031

Butchart, S.H.M., Walpole, M., Collen, B., van Strien, A., Scharlemann, J.P.W., Almond, R.E.A., Baillie, J.E.M., Bomhard, B., Brown, C., Bruno, J., Carpenter, K.E., Carr, G.M., Chanson, J., Chenery, A.M., Csirke, J., Davidson, N.C., Dentener, F., Foster, M., Galli, A., Galloway, J.N., Genovesi, P., Gregory, R.D., Hockings, M., Kapos, V., Lamarque, J.-F., Leverington, F., Loh, J., McGeoch, M.A., McRae, L., Minasyan, A., Hernández Morcillo, M., Oldfield, T.E.E., Pauly, D., Quader, S., Revenga, C., Sauer, J.R., Skolnik, B., Spear, D., Stanwell-Smith, D., Stuart, S.N., Symes, A., Tierney, M., Tyrrell, T.D., Vié, J.-C., Watson, R., 2010. Global biodiversity: indicators of recent declines. *Science* 328, 1164–8. doi:10.1126/science.1187512

Calderon-Aguilera, L.E., Rivera-Monroy, V.H., Porter-Bolland, L., Martínez-Yrizar, A., Ladah, L.B., Martínez-Ramos, M., Alcocer, J., Santiago-Pérez, A.L., Hernandez-Arana, H.A., Reyes-Gómez, V.M., Pérez-Salicrup, D.R., Díaz-Núñez, V., Sosa-Ramírez, J., Herrera-Silveira, J., Búrquez, A., 2012. An assessment of natural and human disturbance effects on Mexican ecosystems: current trends and research gaps. *Biodivers. Conserv.* 21, 589–617. doi:10.1007/s10531-011-0218-6

- Caro-Borrero, A., Corbera, E., Neitzel, K.C., Almeida-Leñero, L., 2015. “We are the city lungs”: Payments for ecosystem services in the outskirts of Mexico City. *Land use policy* 43, 138–148. doi:10.1016/j.landusepol.2014.11.008
- Carrara, E., Arroyo-Rodríguez, V., Vega-Rivera, J.H., Schondube, J.E., de Freitas, S.M., Fahrig, L., 2015. Impact of landscape composition and configuration on forest specialist and generalist bird species in the fragmented Lacandona rainforest, Mexico. *Biol. Conserv.* 184, 117–126. doi:10.1016/j.biocon.2015.01.014
- Chazdon, R.L., 2008. Beyond deforestation: restoring forests and ecosystem services on degraded lands. *Science* 320, 1458–60. doi:10.1126/science.1155365
- CONABIO, 1998. *Uso de suelo y vegetación de INEGI agrupado por CONABIO*. Comisión Nacional para el Conocimiento y Uso de la Biodiversidad, Mexico City.
- CONANP, 2016. *Áreas Naturales Protegidas Federales de la República Mexicana*. Mexico City.
- Costedoat, S., Corbera, E., Ezzine-de-Blas, D., Honey-Rosés, J., Baylis, K., Castillo-Santiago, M.A., 2015. How effective are biodiversity conservation payments in Mexico? *PLoS One* 10, e0119881. doi:10.1371/journal.pone.0119881
- DeFries, R., Hansen, A., Newton, A.C., Hansen, M.C., 2005. Increasing isolation of protected areas in tropical forests over the past twenty years. *Ecol. Appl.* 15, 19–26. doi:10.1890/03-5258

- Dixo, M., Metzger, J.P., Morgante, J.S., Zamudio, K.R., 2009. Habitat fragmentation reduces genetic diversity and connectivity among toad populations in the Brazilian Atlantic Coastal Forest. *Biol. Conserv.* 142, 1560–1569.
doi:10.1016/j.biocon.2008.11.016
- Estreguil, C., Mouton, C., 2009. Measuring and reporting on forest landscape pattern, fragmentation and connectivity in Europe: methods and indicators. Varese.
- Fearnside, P.M., 2005. Deforestation in Brazilian Amazonia: History, rates, and consequences. *Conserv. Biol.* 19, 680–688. doi:10.1111/j.1523-1739.2005.00697.x
- Ferraz, G., Russell, G.J., Stouffer, P.C., Bierregaard, R.O., Pimm, S.L., Lovejoy, T.E., 2003. Rates of species loss from Amazonian forest fragments. *Proc. Natl. Acad. Sci.* 100, 14069–14073. doi:10.1073/pnas.2336195100
- Geissen, V., Sánchez-Hernández, R., Kampichler, C., Ramos-Reyes, R., Sepulveda-Lozada, A., Ochoa-Goana, S., de Jong, B.H.J., Huerta-Lwanga, E., Hernández-Daumas, S., 2009. Effects of land-use change on some properties of tropical soils — An example from Southeast Mexico. *Geoderma* 151, 87–97.
doi:10.1016/j.geoderma.2009.03.011
- Geist, H.J., Lambin, E.F., 2002. Proximate causes and underlying driving forces of tropical deforestation. *Bioscience* 52, 143–150.

- Gibbs, H.K., Ruesch, A.S., Achard, F., Clayton, M.K., Holmgren, P., Ramankutty, N., Foley, J.A., 2010. Tropical forests were the primary sources of new agricultural land in the 1980s and 1990s. *Proc. Natl. Acad. Sci.* 107, 16732–16737.
doi:10.1073/pnas.0910275107
- Gibson, L., Lynam, A.J., Bradshaw, C.J.A., He, F., Bickford, D.P., Woodruff, D.S., Bumrungsri, S., Laurance, W.F., 2013. Near-complete extinction of native small mammal fauna 25 years after forest fragmentation. *Science* 341, 1508–10.
doi:10.1126/science.1240495
- González-Abraham, C., Ezcurra, E., Garcillán, P.P., Ortega-Rubio, A., Kolb, M., Bezaury Creel, J.E., 2015. The human footprint in Mexico: Physical geography and historical legacies. *PLoS One* 10, e0121203. doi:10.1371/journal.pone.0121203
- Gonzalez-Abraham, C., Garcillan, P., Ortega-Rubio, A., Ezcurra, E., 2016. Paper parks or effective conservation? The natural protected areas in Mexico., in: *North America Congress for Conservation Biology*. Madison, WI.
- Haddad, N.M., Brudvig, L.A., Clobert, J., Davies, K.F., Gonzalez, A., Holt, R.D., Lovejoy, T.E., Sexton, J.O., Austin, M.P., Collins, C.D., King, A.J., Laurance, W.F., Levey, D.J., 2015. Habitat fragmentation and its lasting impact on Earth's ecosystems. *Sci. Adv.* doi:10.1126/sciadv.1500052
- Hansen, M.C., Potapov, P. V, Moore, R., Hancher, M., Turubanova, S.A., Tyukavina, A., Thau, D., Stehman, S. V, Goetz, S.J., Loveland, T.R., Kommareddy, A., Egorov,

- A., Chini, L., Justice, C.O., Townshend, J.R.G., 2013. High-resolution global maps of 21st-century forest cover change. *Science* 342, 850–3.
doi:10.1126/science.1244693
- Harper, K. a., Macdonald, E., Burton, P., Chen, J., Brososke, K.D., Saunders, S.C., Euskirchen, E.S., Roberts, D., Jaiteh, M.S., Esseen, P.-A., 2005. Edge influence on forest structure and composition in fragmented landscapes. *Conserv. Biol.* 19, 768–782. doi:10.1111/j.1523-1739.2005.00045.x
- Herrerías-Diego, Y., Quesada, M., Stoner, K.E., Lobo, J.A., Hernández-Flores, Y., Sanchez Montoya, G., 2008. Effect of forest fragmentation on fruit and seed predation of the tropical dry forest tree *Ceiba aesculifolia*. *Biol. Conserv.* 141, 241–248. doi:10.1016/j.biocon.2007.09.017
- Ho, D., Imai, K., King, G., Stuart, E., 2013. MatchIt: Nonparametric preprocessing for parametric casual inference.
- Hosonuma, N., Herold, M., De Sy, V., De Fries, R.S., Brockhaus, M., Verchot, L., Angelsen, A., Romijn, E., 2012. An assessment of deforestation and forest degradation drivers in developing countries. *Environ. Res. Lett.* 7, 044009. doi:10.1088/1748-9326/7/4/044009
- Keenan, R.J., Reams, G.A., Achard, F., De Freitas, J. V, Grainger, A., Lindquist, E., 2015. Dynamics of global forest area: Results from the FAO Global Forest Resources Assessment 2015. doi:10.1016/j.foreco.2015.06.014

- Kim, D.-H., Sexton, J.O., Townshend, J.R., 2015. Accelerated deforestation in the humid tropics from the 1990s to the 2000s. *Geophys. Res. Lett.* 42, 3495–3501.
doi:10.1002/2014GL062777
- Laurance, W.F., 2000. Do edge effects occur over large spatial scales? *Trends Ecol. Evol.* 15, 134–135. doi:10.1016/S0169-5347(00)01838-3
- Laurance, W.F., Nascimento, H.E.M., Laurance, S.G., Andrade, A., Ewers, R.M., Harms, K.E., Luizão, R.C.C., Ribeiro, J.E., 2007. Habitat fragmentation, variable edge effects, and the landscape-divergence hypothesis. *PLoS One* 2, e1017.
doi:10.1371/journal.pone.0001017
- Le Velly, G., Dutilly, C., de Blas, E., Fernandez, C., 2015. PES as compensation ? Redistribution of payments for forest conservation in Mexican common forests. *Études Doc. CERDI* 28, 1–25.
- Lira, P.K., Tambosi, L.R., Ewers, R.M., Metzger, J.P., 2012. Land-use and land-cover change in Atlantic Forest landscapes. *For. Ecol. Manage.* 278, 80–89.
doi:10.1016/j.foreco.2012.05.008
- Locke, C.M., Rissman, A.R., 2012. Unexpected co-benefits: Forest connectivity and property tax incentives. *Landsc. Urban Plan.* 104, 418–425.
doi:10.1016/j.landurbplan.2011.11.022
- Manzo-Delgado, L., López-García, J., Alcántara-Ayala, I., 2014. Role of forest conservation in lessening land degradation in a temperate region: The Monarch

- Butterfly Biosphere Reserve, Mexico. *J. Environ. Manage.* 138, 55–66.
doi:10.1016/j.jenvman.2013.11.017
- Martínez, M.L., Pérez-Maqueo, O., Vázquez, G., Castillo-Campos, G., García-Franco, J., Mehlreter, K., Equihua, M., Landgrave, R., 2009. Effects of land use change on biodiversity and ecosystem services in tropical montane cloud forests of Mexico. *For. Ecol. Manage.* 258, 1856–1863. doi:10.1016/j.foreco.2009.02.023
- Mas, J.-F., Velázquez, A., Díaz-Gallegos, J.R., Mayorga-Saucedo, R., Alcántara, C., Bocco, G., Castro, R., Fernández, T., Pérez-Vega, A., 2004. Assessing land use/cover changes: a nationwide multirate spatial database for Mexico. *Int. J. Appl. Earth Obs. Geoinf.* 5, 249–261. doi:10.1016/j.jag.2004.06.002
- Moreno-Sanchez, R., Torres-Rojo, J.M., Moreno-Sanchez, F., Hawkins, S., Little, J., Mcpartland, S., Ruihai, C., 2012. National assessment of the fragmentation, accessibility and anthropogenic pressure on the forests in Mexico. *J. For. Res.* 23, 529–541. doi:10.1007/s11676-012-0293-x
- Myers, N., Mittermeier, R.A., Mittermeier, C.G., Da Fonseca, G.A., Kent, J., 2000. Biodiversity hotspots for conservation priorities. *Nature* 403, 853–858.
- Naughton-Treves, L., Holland, M.B., Brandon, K., 2005. The role of protected areas in conserving biodiversity and sustaining local livelihoods. *Annu. Rev. Environ. Resour* 30, 219–52. doi:10.1146/annurev.energy.30.050504.164507

- Ramirez-Reyes, C., Bateman, B.L., Radeloff, V.C., 2016. Effects of habitat suitability and minimum patch size thresholds on the assessment of landscape connectivity for Jaguars in the Sierra Gorda, Mexico. *Biol. Conserv.* In review.
- Randolph, J.J., Falbe, K., Kureethara Manuel, A., Balloun, J.L., 2014. A step-by-step guide to propensity score matching in R. *Pract. Assessment, Res. Eval.* 19, 1–6.
- Rico García-Amado, L., Ruiz Pérez, M., Barrasa García, S., 2013. Motivation for conservation: Assessing integrated conservation and development projects and payments for environmental services in La Sepultura Biosphere Reserve, Chiapas, Mexico. *Ecol. Econ.* 89, 92–100. doi:10.1016/j.ecolecon.2013.02.002
- Riitters, K., Wickham, J., Costanza, J.K., Vogt, P., 2016. A global evaluation of forest interior area dynamics using tree cover data from 2000 to 2012. *Landsc. Ecol.* 31, 137–148. doi:10.1007/s10980-015-0270-9
- Roth, D., Moreno-Sanchez, R., Torres-Rojo, J.M., Moreno-Sanchez, F., 2016. Estimation of human induced disturbance of the environment associated with 2002, 2008 and 2013 land use/cover patterns in Mexico. *Appl. Geogr.* 66, 22–34. doi:10.1016/j.apgeog.2015.11.009
- Rzedowski, J., 2006. *Vegetacion de Mexico*, Limusa. ed. Comision Nacional para el Conocimiento y Uso de la Biodiversidad, Mexico City.
- Sims, K.R., Alix-Garcia, J.M., 2015. It's complicated: Direct vs. incentive-based land conservation in Mexico. *Work. Pap.*

- Sims, K.R.E., 2014. Do protected areas reduce forest fragmentation? A microlandscapes approach. *Environ. Resour. Econ.* 58, 303–333. doi:10.1007/s10640-013-9707-2
- Sims, K.R.E., Alix-Garcia, J.M., Shapiro-Garza, E., Fine, L.R., Radeloff, V.C., Aronson, G., Castillo, S., Ramirez-Reyes, C., Yañez-Pagans, P., 2014. Improving environmental and social targeting through adaptive management in Mexico's payments for hydrological services program. *Conserv. Biol.* 28, 1151–1159. doi:10.1111/cobi.12318
- Soille, P., Vogt, P., 2009. Morphological segmentation of binary patterns. *Pattern Recognit. Lett.* 30, 456–459. doi:10.1016/j.patrec.2008.10.015
- Sorte, F.A. La, Mannan, R.W., Reynolds, R.T., Grubb, T.G., 2004. Habitat associations of sympatric red-tailed hawks and northern goshawks on the kaibab plateau. *J. Wildl. Manag.* 68, 307–317.
- Stuart, E.A., Rubin, D.B., 2008. Best practices in quasi-experimental designs: Matching methods for causal inference, in: Osborne, J. (Ed.), *Best Practices in Quantitative Methods*. SAGE Publications, pp. 155–176. doi:10.4135/9781412995627
- VanDerWal, J., Falconi, L., Januchowski, S., Shoo, L., Storlie, C., 2014. Package “SDMTools.”
- Velazquez, A., Mas, J.-F., Palacio-Prieto, J.L., Bocco, G., 2002. Land cover mapping to obtain a current profile of deforestation in Mexico. *Unasylva* 53, 37–40.

- Vellend, M., Verheyen, K., Jacquemyn, H., Kolb, A., Van Calster, H., Peterken, G., Hermy, M., 2006. Extinction debt of forest plants persists for more than a century following habitat fragmentation. *Ecology* 87, 542–548. doi:10.1890/05-1182
- Vogt, P., Riitters, K., Estreguil, C., Kozak, J., Wade, T., Wickham, J., 2007a. Mapping spatial patterns with morphological image processing. *Landsc. Ecol.* 22, 171–177.
- Vogt, P., Riitters, K.H., Iwanowski, M., Estreguil, C., Kozak, J., Soille, P., 2007b. Mapping landscape corridors. *Ecol. Indic.* 7, 481–488. doi:10.1016/j.ecolind.2006.11.001
- Wade, T.G., Riitters, K.H., Wickham, J.D., Jones, K.B., Wade, T.G., Riitters, K.H., Wickham, J.D., Jones, K.B., 2003. Distribution and causes of global forest fragmentation. *Conserv. Ecol.* 7.
- With, K.A., 2004. Assessing the risk of invasive spread in fragmented landscapes. *Risk Anal.* 24, 803–15. doi:10.1111/j.0272-4332.2004.00480.x

1-8 Tables

Table 1-1 Variables used for matching

Variable	Source
Average slope	NASA, Shuttle Radar Topography Mission
Maximum slope	NASA, Shuttle Radar Topography Mission
Average elevation	NASA, Shuttle Radar Topography Mission
Maximum elevation	NASA, Shuttle Radar Topography Mission
Average distance to urban areas	INEGI, Carta de poblaciones
Maximum distance to major road	INEGI, Carta de Carreteras
Maximum distance to any road	INEGI, Carta de Carreteras
Average distance to streams	INEGI, Carta topografica
Average distance to border	ESRI, World border map

Table 1-2 Transition between different forest morphology classes from 2000 to 2012.

a) Transition matrix in percentage

		2012							
		Non forest	Forest						
			Core	Islet	Perforation	Edge	Loop	Bridge	Branch
2000	No forest	99.74	0.12	0.04	0.01	0.04	0.01	0.02	0.03
	Forest								
	Core	4.03	90.68	0.09	2.34	1.16	0.68	0.65	0.37
	Islet	7.02	0.32	90.79	0.04	0.49	0.15	0.21	0.98
	Perforation	4.18	5.70	0.25	76.22	7.58	2.59	1.99	1.49
	Edge	3.25	1.16	0.48	0.26	90.89	0.76	1.71	1.49
	Loop	5.24	4.02	0.74	1.37	2.21	77.77	6.58	2.07
	Bridge	4.37	1.81	0.59	0.27	1.99	1.47	87.35	2.15
	Branch	4.66	0.75	2.23	0.18	1.01	0.46	0.84	89.89

b) Transition matrix in area (km2)

		2012							
		Non forest	Forest						
			Core	Islet	Perforation	Edge	Loop	Bridge	Branch
2000	No forest	1416297	1651	521	175	508	174	300	402
	Forest								
	Core	15028	338028	325	8719	4311	2544	2424	1381
	Islet	1042	47	13479	5	73	23	31	146
	Perforation	1049	1431	62	19138	1904	649	500	375
	Edge	1883	674	280	151	52717	443	990	865
	Loop	638	490	90	167	269	9472	801	252
	Bridge	910	377	122	56	414	306	18173	447
	Branch	1150	184	550	44	248	113	207	22195

Table 1-3 Percent change in forest morphology classes

PES vs non-PES							
	Zone	Mean PES	Mean no PES	<i>t</i>	df	p value	Sig. ¹
Δ % Core	Country	-2.34	-3.5	-7.23	4825	5.24E-13	***
	N	-0.85	-1.01	-1.1	1340.8	0.26	
	C	-1.98	-1.76	0.94	1424.9	0.34	
	SW	-2.5	-4.19	-6.05	1220.3	1.86E-09	***
	SE	-4.03	-8.12	-8.62	934.23	2.20E-16	***
Δ % Islet	Country	14.41	38.09	3.48	3754.2	5.02E-04	***
	N	3.08	19.36	1.56	743.9	0.11	
	C	6.74	20.5	1.24	713.82	0.21	
	SW	11.82	26.93	1.19	917.12	0.23	
	SE	41.16	122.1	3.4	827.32	7.04E-04	***
Δ % Perforation	Country	114.2	90.31	-1.73	4896.4	0.08	
	N	14.84	9.25	-1.06	1227.8	0.28	
	C	73.64	19.89	-2.97	879.81	3.63E-05	***
	SW	155.84	120	1.23	955	0.216	
	SE	271.27	296.7	-0.37	972.51	0.71	
Δ % Edge	Country	44.5	87.79	2.08	4737.1	0.03	*
	N	3.78	20.94	2.48	684.62	0.01	*
	C	34.55	43.42	0.48	1388.4	0.62	
	SW	43.65	99.35	1.8	929.89	0.07	
	SE	106.41	236.1	1.86	1047.2	0.06	
Number of patches	Country	9.52	12.92	8.06	5200.6	9.28E-16	***
	N	4.01	4.87	2.07	1249.3	0.03	**
	C	7.99	8.2	0.29	1435.7	0.76	
	SW	11.43	16.77	6.77	1259	1.95E-11	***
	SE	14.57	23.77	8.84	1105.6	2.20E-16	***
Max. Patch area ha	Country	1.87	3.46	6.18	4249.8	6.73E-10	***
	N	0.54	0.71	0.88	1282.9	0.37	
	C	0.98	1.21	0.78	1394.5	0.43	
	SW	1.15	1.87	3.4	1024.8	6.98E-04	***
	SE	4.9	11.13	6.89	903.53	1.20E-11	***
PES vs protected areas							
	Zone	Mean PES	Mean protected area	<i>t</i>	df	p value	
Δ % Core	All protected	-2.04	-2.12	-0.62	3639	0.51	
	Core protected	-2.11	-1.7	1.52	2379.2	0.12	
Δ % Islet	All protected	10.02	14.97	1.25	2771.4	0.2	
	Core protected	9.82	15.18	0.65	2005.5	0.51	
Δ % Perforation	All protected	117.18	62.75	-3.25	1893.6	1.15E-03	**
	Core protected	125.06	61.38	-3.07	2040	2.13E-03	**
Δ % Edge	All protected	41.27	49.53	0.42	2260.4	0.67	
	Core protected	42.91	18.36	-1.12	1848.1	0.26	
Number of patches	All protected	8.38	7.15	-3.68	2468.7	2.38E-04	***
	Core protected	8.56	4.25	-10.15	2832.7	2.20E-16	***
Max. Patch area ha	All protected	1.53	1.4	-0.81	2371.8	0.41	
	Core protected	1.53	1.01	-2.89	2979.4	4.70E-03	**

¹ Significance levels: * p<.05; ** p<.01; *** p<.001

1-9 Figures

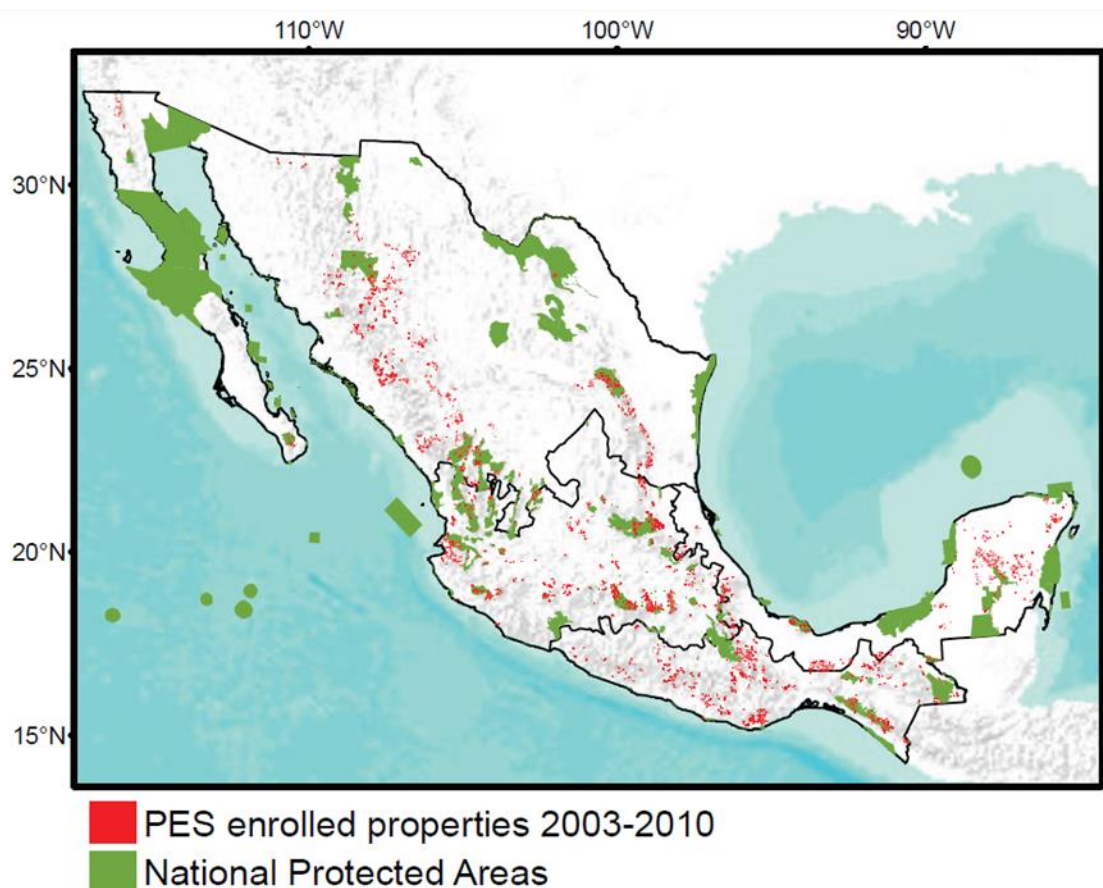


Figure 1-1: Our study area in Mexico, including the properties enrolled in the PES between 2003 and 2010, as well as the north, central, southwest and southeast zones that we used for our analysis.

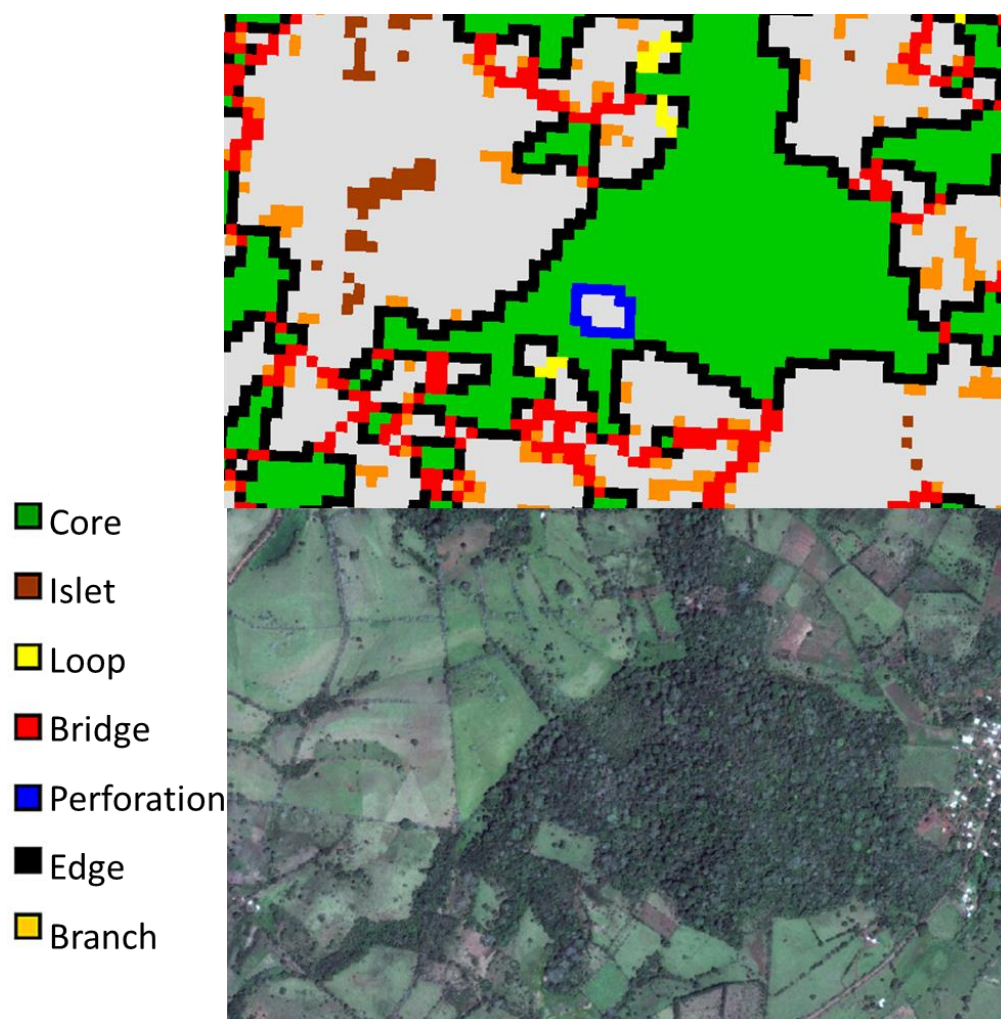


Figure 1-2: Example of forest morphology analysis. Depending on the neighborhood cover type, forested pixels will be assigned to different categories.

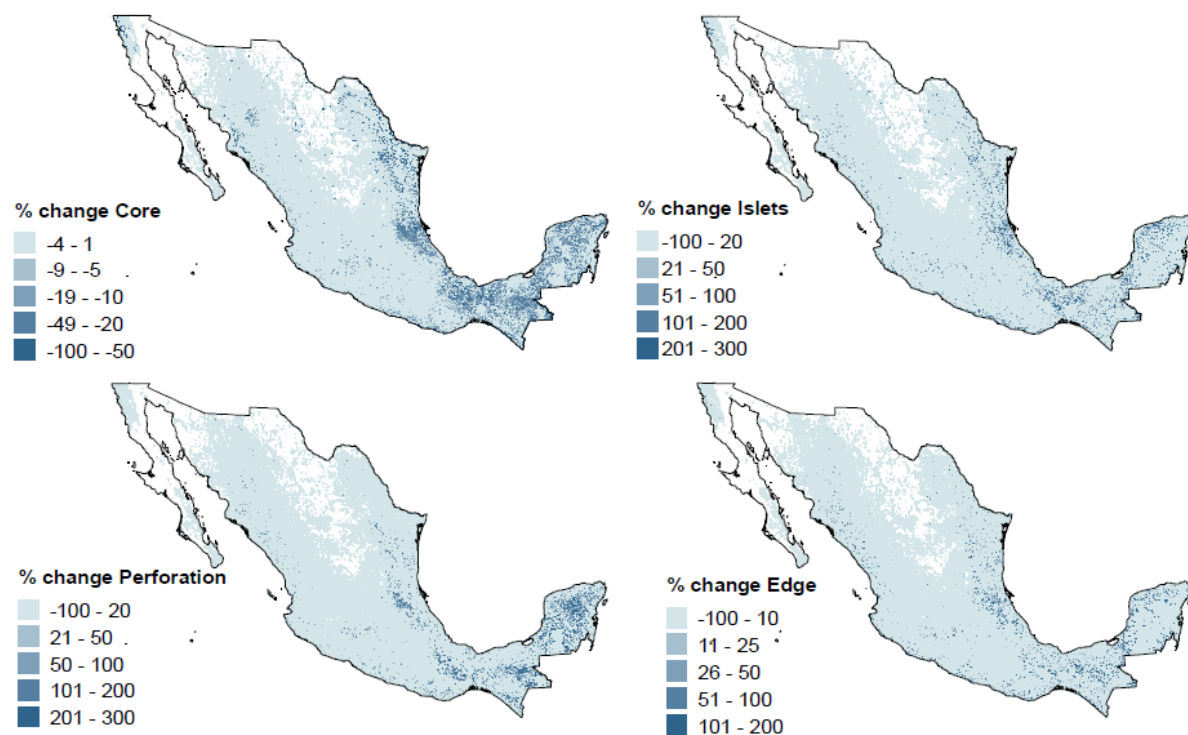


Figure 1-3: Percent change for the main forest morphology categories for all of Mexico.

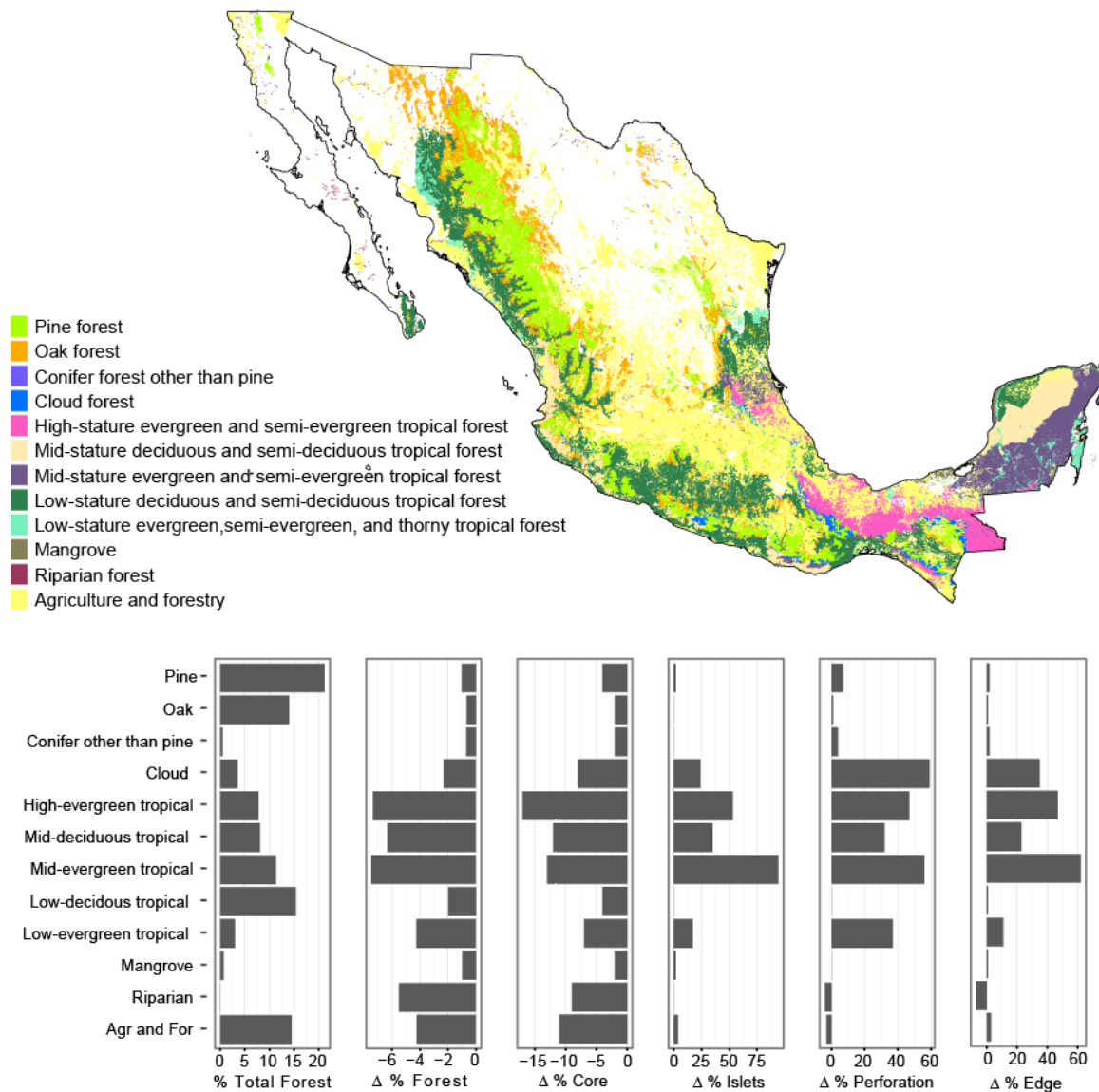


Figure 1-4: Top: Map of vegetation type in Mexico in which we only include forests types. Bottom: Forest morphology changes in each vegetation type (proportion of the total of forest per category in 2000).

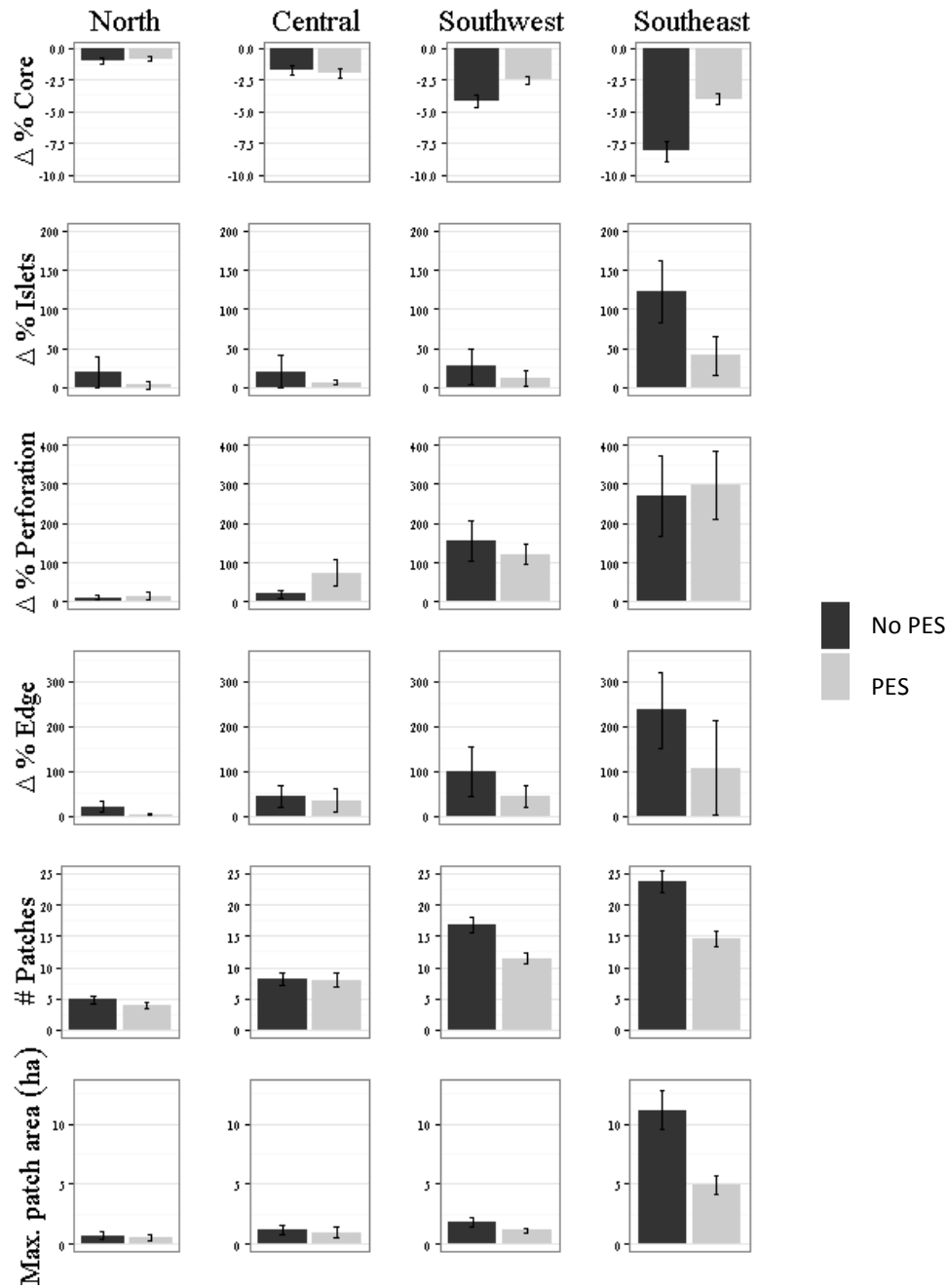


Figure 1-5 Comparison between forest morphology changes in PES and non-PES microlandscapes. We calculated the changes in relation to the total forest area in category in 2000, and conducted the analysis for each zone.

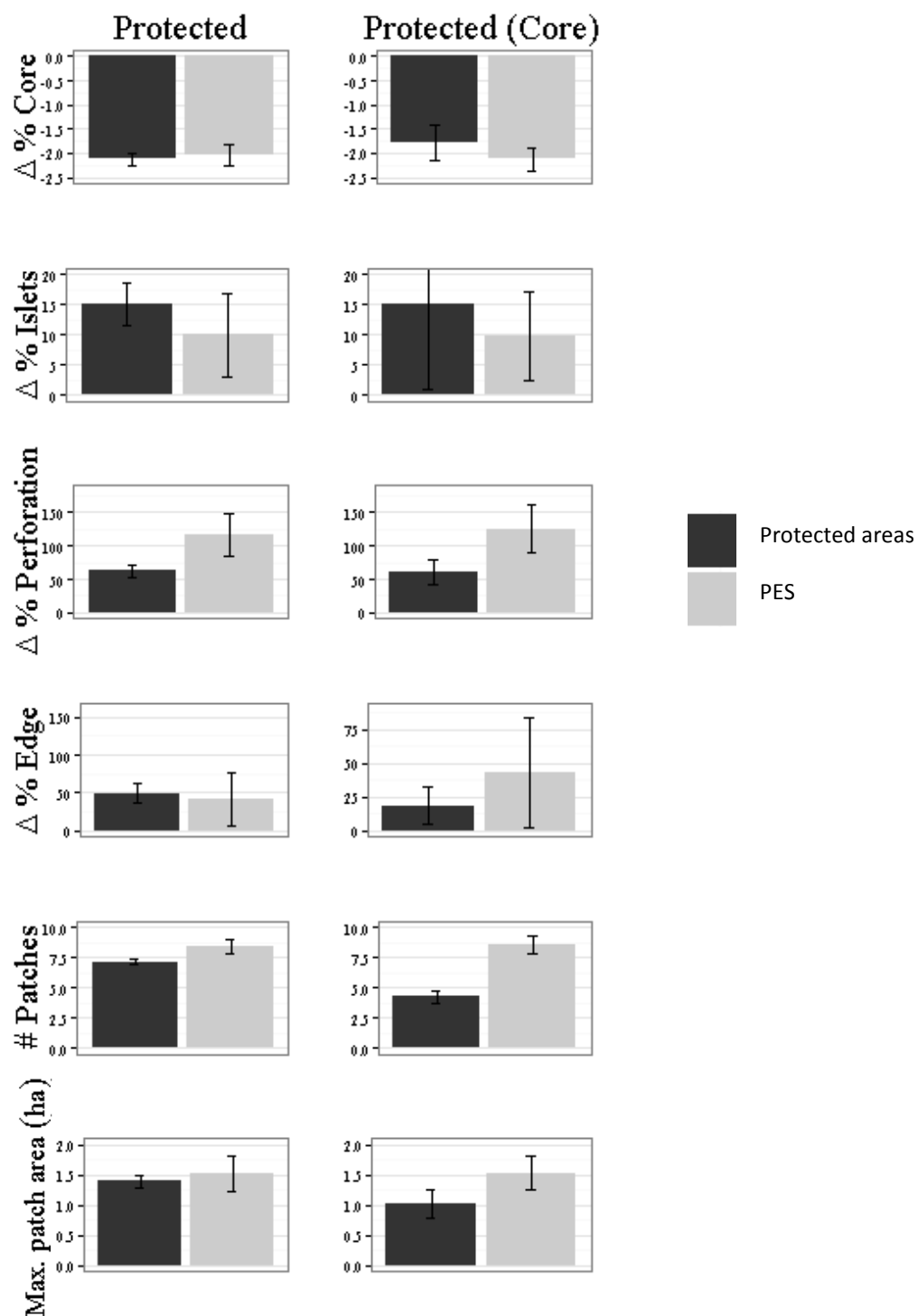


Figure 1-6 Comparison between forest morphology changes in PES areas and the National Protected Areas System. We calculated the changes in relation to the total forest area in category in 2000, and conducted the analysis for each zone.

Chapter 2: Spectral Mixture Analysis of STARFM fusion images improves deforestation assessments of diverse forest types in Mexico

Contributors: Ramirez-Reyes, Carlos¹ and Volker C. Radeloff¹

¹ SILVIS Lab, Department of Forest and Wildlife Ecology, University of Wisconsin-Madison, 1630 Linden Drive, Madison WI 53706, USA

2-1 Abstract

Deforestation greatly diminishes ecosystem services provided by forests and can threaten people's livelihood. The analysis of satellite imagery can reveal deforestation, but requires cloud-free imagery for different phenological stages during the growing season, and that is often not the case. One potential way to obtain the necessary imagery is to combine imagery from Landsat, which at 30-m resolution is well suited to monitor deforestation, but is less frequently available, with that from MODIS, which is more frequently available, but of coarser resolution, and the STARFM algorithm is designed to generate Landsat-like imagery from MODIS data. Our objectives were to a) measure deforestation rates in different areas of Mexico and b) evaluate the usefulness of STARFM-generated Landsat-like imagery and Spectral Mixture Analysis to assess deforestation. We applied Spectral Mixture Analysis, and calculated vegetation fraction maps for three Landsat footprints in Mexico between 2000 and 2010 based on three different types of imagery: a) raw surface reflectance images, b) radiometrically

normalized images, and c) STARFM fusion images. Based on these fraction maps, we calculated change in the vegetation fractions over time, conducted a sensitivity analysis of the resulting maps of forest change, and assessed their accuracy. We found generally high rates of deforestation, but a strong north-south gradient with much higher deforestation rates in the south. In our southeastern Landsat footprint, a full 6.8% of the forest cover was lost from 2000 to 2010, compared with 5.2% in the central footprint and only 1.2% in the northern-most one. Deforestation maps based on the STARFM-generated images outperformed those based on radiometrically normalized imagery, and the raw Landsat reflectance images in areas with high phenology. The average increase in accuracy when using the STARFM-generated images was 8 percentage points in the areas with stronger phenology. We conclude that STARFM can improve forest change analysis by reducing the classification errors caused by comparing images from different phenological stages. More broadly speaking, remote sensing can provide essential information for deforestation monitoring, but data from multiple sensors may be required to capture deforestation rates accurately.

Keywords: Radiometric normalization, phenology, degradation

2-2 Introduction

Deforestation is a major threat to forest ecosystems and the services they provide such as sustaining food production, maintaining freshwater and forest resources, as well as climate and air quality regulation (Foley et al., 2005). Deforestation has accelerated in recent decades, due to direct human pressures such as logging, grazing, and development (Yang et al., 2012). Accurate monitoring of deforestation can help to understand changes in wildlife habitat, water filtration, soil nutrients and human livelihoods (Hansen et al., 2013; Lawley et al., 2015). Because deforestation has the most dramatic environmental effects on a per-area basis, compared to forest degradation, most assessments of deforestation evaluate forest loss as a binary variable where forests are either present or absent (Putz and Redford, 2010). However, forest degradation can also have major environmental effects (Anderson et al. 2011) even though it may not cause a reduction of the forest area but rather a decrease in its quality (Davidson et al., 2008). Furthermore, the threshold at which a certain amount of canopy loss, and hence forest degradation, can be considered deforestation is not clear.

In general, mapping degradation is more difficult than mapping deforestation. However, even when the goal is to demarcate deforestation, it can be beneficial to measure first the loss of forest cover as a continuous variable, and assess deforestation based on that. Such a forest degradation assessment can be done via a Spectral Mixture Analysis, SMA (Adams et al., 1986), which estimates the fraction of different cover types for each pixel (Veraverbeke et al., 2012). SMA has been applied to detect degradation processes in tropical forests, such as selective logging in the Amazon (Adams et al.,

1995; Matricardi et al., 2010; Souza Jr. et al., 2003). SMA is also useful for assessments of sparse vegetation in semiarid areas (Smith et al., 1990), degradation of semi-arid woodlands (Yang et al., 2012), grazing impacts (Röder et al., 2008), and desertification rates (Dawelbait and Morari, 2012).

Measuring deforestation via SMA, however, requires to compare images that capture similar phenological stages, particularly when assessing deciduous forests (Adams and Gillespie, 2006). While Landsat TM, ETM+, and OLI data has the best spatial resolution to monitor deforestation (30 m), data are often not available for required dates because of its limited temporal resolution of 16 days, the Scan Line Correction error for Landsat 7, and persistent cloud cover in some areas (Wulder et al., 2008). Other types of satellite data have the advantage of a much higher temporal resolution. For instance, MODIS has a temporal resolution of one day. However, MODIS' lower spatial resolution (250 – 1000 m, depending on the spectral bands of interest) means that it does not capture small deforestation events.

One way to overcome the problem of limited Landsat data is to fuse Landsat and MODIS imagery. Image fusion can be done using the Spatial and Temporal Adaptive Reflectance Fusion Model algorithm, STARFM (Gao et al., 2006). STARFM has been successfully used to classify landcover (Xu and Huang, 2014), it also improves detection of land cover changes in agricultural areas (Chen et al., 2014; Watts et al., 2011; Zhu et al., 2015) and land cover classifications in forest ecosystems (Hilker et al., 2009; Jia et al., 2014; Watts et al., 2011). STARFM produces Landsat-like reflectance images using a pair of MODIS and Landsat images for a day for which cloud-free imagery is available,

and then predicting 30-m reflectance values for any date for which only a MODIS image is available. Thus, STARFM may be useful for obtaining imagery for a specific phenological stage when Landsat data are lacking, and hence to improve deforestation assessment. However, the utility of STARFM for detecting forest degradation via SMA has yet to be tested. If successful, SMA of STARFM fusion images would be particularly valuable to assess forest degradation in areas with limited image availability.

One place where the availability of Landsat imagery is limited is Mexico, where there is constant cloud cover over most the country during the growing season, and strong phenology in many of its dry forests. Further, Mexico's forest ecosystems are highly diverse, ranging from dense vegetation in evergreen rainforest to forests where tree cover is sparse, and shrubs and grasses are intermixed with trees such as the pine-oak forest (Rzedowski, 2006). Despite great advances in deforestation monitoring with MODIS (Aide et al., 2013) and Landsat (Hansen et al., 2013), deforestation monitoring in dry tropical forest continues to be challenging (Barreda-Bautista et al., 2011; Martinez Morales et al., 2008; Mitchard et al., 2013). Especially, small scale deforestation remains difficult to detect (Lippitt et al., 2008).

Forests in Mexico are also experiencing high deforestation rates that threaten the provision of ecosystem services (Trejo and Dirzo, 2000). Because of these high deforestation rates, Mexico implemented a payment for ecosystem services program (PES) in 2003, which aims to prevent deforestation within the REDD framework. For PES programs, it is very important to accurately measure deforestation in order to enforce compliance and assess effectiveness. Unfortunately, despite efforts to monitor

deforestation at the global level (Hansen et al., 2013), the available data about small-scale deforestation is still limited, because it is difficult to detect deforestation in dry forests using binary forest-no-forest classifications, especially when cuts are smaller than single pixels. Thus, data fusion with STARFM and MODIS to overcome the limited availability of Landsat data, and analyzing the resulting images with SMA, may be particularly useful for analyzing forest change in Mexico and other places with similar vegetation.

Our major goal was to evaluate the performance of STARFM fusion images in Spectral Mixture Analysis to improve deforestation detection in Mexico. Our objectives were to: 1. Measure deforestation rates in different forest types of Mexico, and 2. evaluate the potential use of STARFM-generated imagery as the basis for Spectral Mixture Analysis, which we assessed by comparing a) surface reflectance images, b) radiometric normalized images, and c) STARFM fusion images.

2-3 Methods

2-3.1 STUDY AREA

We performed our analysis in three Landsat footprints in Mexico (Figure 1). These footprints are located in northern, central and southeastern Mexico, capturing a variety of different forest types. In the northern footprint, forest vegetation includes oak forest, pine forest, and tropical deciduous forest. In the central footprint, there are tropical deciduous forest, cloud forest, pine forest, and oak forest. In the southern footprint, forest vegetation includes tropical deciduous forest and evergreen tropical forest. In addition, the three footprints capture a topographic gradient, ranging from flat wetlands in the

southern footprint, to mountainous in the other two, and large differences in terms of socioeconomic activities and population densities among the three footprints, resulting in different land use patterns.

2-3.2 Image Preprocessing

Landsat

We assessed deforestation from 2000 to 2010 in each of the three footprints. We analyzed Landsat 7 ETM+ images from the peak growing season in Mexico (July-September) in order to minimize errors due to differences in phenology (Hesketh and Sánchez-Azofeifa, 2012). In order to also minimize the effects of clouds present in the imagery, we selected the least cloudy images available in the LANDSAT archives within a two year window around 2000 (T_0) and 2010 (T_1) (Table 1). To account for atmospheric variation between years, we calibrated all the images to surface reflectance units using the LEDAPS radiometric correction tool (Masek et al., 2013). However, because cloud cover is persistent during the growing season for most of the country, the majority of the images contained some clouds. We masked the remaining clouds in each image using the cloud-masking algorithm F-mask (Zhu and Woodcock 2012).

MODIS

As input for STARFM, we used the MODIS 500-m resolution surface reflectance product MOD09A1, which is an 8-day image composite, because it minimizes the amount of clouds (Table 1). Each of the MODIS images was cropped, resampled to 30 m, and projected to WGS84/UTM zones 13, 14 and 16 for the northern, central, and south

eastern imagery, respectively, using the MODIS Reprojection Tool (NASA Land Processes Distributed Active Archive Center) in order to match the corresponding Landsat scenes.

2-3.3 *RELATIVE RADIOMETRIC NORMALIZATION.*

In order to further minimize phenological and radiometric differences, we performed a relative radiometric normalization (RRN). This technique assures that two images represent comparable atmospheric conditions (Hall et al., 1991). In the northern footprint, the image with the least clouds was T_0 , which is why we used it as a reference to normalize the later T_1 scene. For the central and southeastern footprints the least cloudy image was the T_1 image, and we normalized the T_0 images. For the normalization, we sampled 100 random points in each image and visually verified that their land cover did not change between the two dates using the Landsat imagery. We considered these non-changing points as the pseudo invariant features (PIF) needed for the radiometric normalization. Based on these points, we parameterized linear regressions for each of the image bands and applied the regression equations to the corresponding band of the image that needed to be normalized.

2-3.4 *STARFM*

We ran the STARFM algorithm (Gao et al. 2006) for our three footprints to create Landsat-like images using the MODIS-Landsat pair images in Table 1. STARFM makes a prediction of the T_1 Landsat image based on the T_1 MODIS image and the spatial and spectral differences observed in the T_0 Landsat and MODIS calibration pair. In order to

improve the accuracy of our predictions, we only predicted areas without clouds in both T_0 and T_1 Landsat images. The result from this analysis was a synthetic T_1 image that was as close as possible to the calendar date of the T_0 image.

2-3.5 *SPECTRAL MIXTURE ANALYSIS*

Once we obtained all the surface reflectance images with the three approaches: raw surface reflectance, normalized surface reflectance, and STARFM predicted surface reflectance, we calculated vegetation fraction maps using linear SMA, which estimates the proportion of vegetation of each pixel. For the SMA, we identified the spectral response of pure features in the landscape, known as endmembers, using a combination of reference endmembers from the USGS spectral library (Clark et al., 1993) (i.e., GDS91-green vegetation, CDE059 -dry vegetation) and image endmembers collected from the satellite images themselves (i.e., agriculture soil and sand). We used the same endmembers for all three footprints, because the endmembers were distinct from each other and we focused only on the green vegetation endmember to describe changes in vegetation (Figure 2). With this set of endmembers, we generated vegetation fraction maps for T_0 and T_1 for the three footprints for a) the raw Landsat surface reflectance images, b) radiometric normalized images, and c) STARFM fusion images.

2-3.6 *DEFORESTATION ESTIMATION*

In order to assess deforestation, we calculated the difference between the T_0 and T_1 vegetation fraction maps for each footprint. Based on the resulting difference map, we conducted a sensitivity analysis in which we used different thresholds ($T_0 - T_1 > 0.1$; $T_0 -$

$T_1 > 0.2$, and $T_0 - T_1 > 0.3$) to find the optimal cutoff value at which to designate deforestation. Second, in order to corroborate our choice of threshold, we applied a logistic regression in which we created deforestation models based on the vegetation difference in fraction maps and whether that point was deforested or not. Third, we parameterized multivariate deforestation models in which we described the observed deforestation, or absence of it, in our verification dataset in relation with the change in vegetation fraction plus the initial vegetation proportion, to see if this additional information could improve the deforestation estimates.

2-3.7 *ACCURACY ASSESSMENT*

We evaluated the accuracy of each of the resulting deforestation maps focusing on cloud-free areas considered as forested in a base vegetation map available for Mexico (CONABIO, 1998). As our reference dataset, we digitized a set of deforestation polygons using high resolution imagery available in Google Earth in our study areas. To find these deforestation polygons, we created a systematic sampling grid that covered about 20 percent of each Landsat footprint. In each of the quadrants of the grid we looked for all available high resolution imagery and digitized deforestation between 2000 and 2010. Within the deforestation areas, we sampled 100 random points in the areas that remained intact forest and 100 random points within the polygons that we identified as deforested. We visually verified that the land cover of these verification points did not change prior or after the high-resolution images were captured by inspecting our Landsat imagery. This step was necessary because the dates of the Google Earth imagery did not always include the full 2000 to 2010 time period, and we needed to ensure that the points that we

mapped in the reference dataset as intact were not deforested after the last date for which high-resolution Google Earth imagery was available. We calculated the accuracy of each of the deforestation maps produced at different thresholds based on their ability to detect the deforestation we observed in our verification dataset.

Finally, we calculated the deforestation rates for each of the footprints with the most accurate deforestation maps based on the formula $FCC(\%) = (1/T_2 - T_1) \times \ln(A_2/A_1) \times 100$; where $(T_2 - T_1)$ is the period analyzed, and A_1 and A_2 the forest cover at time T_1 and T_2 , respectively (Puyravaud, 2003).

2-4 Results

We estimated vegetation fraction maps for the three types of input imagery: a) original surface reflectance, b) radiometric normalized images, and c) STARFM fusion images for each footprint the initial T_0 and final T_1 . We found considerable differences in the range of vegetation fractions among the three footprints. For instance, in the northern footprint the vegetation fraction values ranged largely from 0.1-0.7, for the central footprint from 0.2-0.6, and in the southeastern footprint from 0.4-0.6, which is a consequence of the vegetation types present on each footprint, with denser forests in the south and more open forests in the north. In general, we found a positive correlation between the initial and later vegetation fraction maps, but the strength of the correlations varied (Figure 3). We expected a strong correlation between the fraction maps of the two dates, because the majority of the forest cover remained between the two dates. However, we were interested to see if the strength of the correlations varied systematically depending on the type of input data. If the correlations between vegetation fraction maps

were similar among the three types of input data, that would indicate that STARFM or RRN performed similarly to raw surface reflectance in describing the forest cover. For the northern footprint, we obtained the strongest correlation between the vegetation fraction maps obtained with the raw T_0 surface reflectance values and the fraction map of the original surface reflectance values of T_1 ($r^2=0.75$). For the central footprint, the strongest correlation occurred for vegetation fraction maps produced with the initial T_0 surface reflectance values and the STARFM fusion image values for T_1 ($r^2=0.53$). In the case of the southeastern footprint we found generally weaker correlations cases (Figure 3), maybe because of clouds that were not successfully masked out by Fmask. Among the three vegetation maps that we tested in this footprint, we found the strongest correlate between the fraction maps based on raw reflectance values, but even for these the correlation was weak ($r^2=0.24$).

The deforestation regression analysis, based on the T_0 - T_1 difference in vegetation fraction maps, performed well (Figure 4), and most of the models were significant (Table 3). The exception was the central footprint for the RRN approach. The inclusion of the vegetation proportion at T_0 in addition to the change in vegetation T_0 - T_1 did not contribute to describe deforestation for most of the models. The threshold of the differences in the vegetation fraction map that we selected to identify deforestation, greatly affected both the amount of deforestation that was mapped, as we had expected, and the accuracy of our resulting deforestation maps (Table 2). Interestingly, the thresholds also varied substantially depending on the type of input imagery in some of the footprints. In the northern footprint, the most accurate deforestation maps resulted from a

difference threshold of 0.2 for the surface reflectance image, 0.1 for the atmospheric corrected image, and 0.3 for the STARFM fusion image (Figure 5). For the southeastern footprint we observed better deforestation detection with a threshold difference of 0.1 for the original surface reflectance pixels, 0.1 for the atmospherically corrected image, and 0.1 for the STARFM fusion image. For the southeastern footprint, the original surface reflectance values and the atmospheric corrected values were the most accurate at the 0.1 threshold. For the STARFM fusion image, we obtained the best deforestation estimation for a threshold of 0.2. These thresholds were very approximate to those thresholds suggested in the logistic regression analysis above, at which deforestation events surpassed the inflexion point on the model (Table 3). Also, the addition of the initial vegetation proportion improved the models in half of the cases.

We calculated the deforestation rates based on the optimal threshold for the change in the vegetation fraction (Table 4). In the case of the northern footprint 1.7% of the forest was lost between 2001 and 2010, or 0.19% per year. In the central footprint, 5.2% of the forest has been lost, or 0.48% per year, between 2001 and 2012. In the southeastern footprint, forests were lost at a rate of 6.88% between 2001 and 2008, or 1.1% per year.

The overall accuracy of our deforestation maps was 78%, 79%, and 72% in the central, northern, and southeastern footprints, respectively (Table 2). For comparison, we calculated the accuracy of the Global Forest Change (Hansen et al., 2013) based on our verification dataset, which was lower for the northern and central footprints (62% and 65% respectively), but higher in the southeastern footprint (83%).

275 **2-5 Discussion**

276 Combining radiometric normalization with STARFM improved our ability to
277 detect deforestation in Mexico, and we found widespread deforestation, especially in our
278 southeastern Landsat footprint. Our results indicated that Landsat-style satellite imagery
279 generated with STARFM can improve deforestation estimates in areas where the
280 availability of actual Landsat data is limited. We suggest that our approach is especially
281 useful in areas with constant cloud cover and areas where phenology changes rapidly.

282 The accuracy of our deforestation estimates depended on both forest type and how
283 strong phenology effects were. The available Landsat scenes for the central footprint, in
284 particular, differed somewhat in terms of their phenology. We tried to limit differences as
285 much as possible by finding the best image in the Landsat archives, but image availability
286 was limited, and that is not untypical across the globe (Goward et al., 2006). Our analyses
287 highlighted the extent to which phenological differences due to limited image availability
288 can lower the accuracy of deforestation maps when using raw surface reflectance images.
289 Moreover, even when images from similar dates were available, partial cloud
290 contamination was a problem, and that is not uncommon (Ju and Roy, 2008). In cases
291 where phenology is different between the comparing dates, e.g., in our central footprint,
292 radiometric normalization did result in a decent approximation of the later phenological
293 stage. However, STARFM-generated images presented the biggest improvement and
294 minimized differences the most, compared to our relative normalization and raw surface
295 reflectance approaches. The radiometric normalization process corrected for some
296 differences in vegetation phenology, but mainly for differences in solar angle, azimuth,

and topography (Caselles and Lopez Garcia, 1989). In other words, when two images represented vegetation at different phenological stages, then the radiometric normalization was not able to account for that and the normalized image did not predict different phenological stages (Lunetta et al., 2002). The STARFM fusion images, on the other hand, were able to handle actual difference in phenology, because they incorporated phenology as captured in the MODIS imagery (Walker et al., 2014; Watts et al., 2011).

Interestingly though, while we achieved higher accuracy using the STARFM-generated imagery for the central footprint, this was not the case for the other footprints. Thus, the capabilities of these methods changes according to the study area, forest type, phenology, and the magnitude of difference between phenological stages at the first and the second date of the Landsat images. The radiometric normalization worked better when phenological differences were minor. In our study area, that was the case in the northern and southeastern footprints. In the northern footprint, forests are primarily coniferous, while the southeastern footprint is dominated by tropical forest, and this means that phenology is not strong in either footprint. In the central footprint, forests are primarily deciduous, with a small portion of coniferous forest, and that means that phenological differences are stronger. Also, in the central footprint, the length of time between images was the highest (44 days), and this exacerbated phenological difference so much that the radiometric normalization could not overcome them.

Forests in the southeastern footprint had the highest deforestation rates during our study period (Figure 6). This pattern is consistent with prior decades, when forest in southern Mexico were lost rapidly due to higher population densities, increasing

development, and agriculture expansion (Sohn et al., 1999; Turner et al., 2001). Furthermore, high deforestation rates in Mexico's tropical forests are similar to those in other tropical forests (Kim et al., 2015). In the central footprint, the rates of deforestation were also high, compared to the north. In this footprint large forest areas have already been lost, but pressure for land conversion remains high (Trejo and Dirzo, 2000), and this is why we anticipated large deforestation rates. In the northern footprint, we observed the lowest deforestation rate, and this was also expected because human population densities are lower, topography is more rugged, and the land is less suitable for farming. Given deforestation trends in Mexico (Velazquez et al., 2002a), we believe that most of the forest loss is caused because of human activities rather than natural disturbances.

We found annual deforestation rates for the three footprints of 0.19% in the north, 0.48% for the central and 1.1% in the southeastern footprint. These deforestation rates are similar to those between 1976 and 2000, when the deforestation rates for Mexico were as high as 0.43% per year (Velazquez et al., 2002b), or between 1993 and 2000, when deforestation rates reached 1-2 % per year (Velazquez et al., 2002a). However, we caution that our deforestation rates are for three footprints only, and we cannot extrapolate to other areas of the country. Nevertheless, we suggest that there may have been a reduction in deforestation rates.

While the STARFM generated images resulted in the most accurate deforestation maps when phenology effects were higher, they also exhibited more changes in vegetation that can be confused with deforestation. This situation can be reduced by using a threshold selection like the one we proposed, in which actual deforestation can be

differentiated from changes in vegetation due to phenological stages. Furthermore, by using STARFM images as input for Spectral Mixture Analysis we obtained a continuous measure of reductions in forest canopy density, which may reflect forest degradation. However, we did not have verification data for degradation, which is why we did not analyze the extent of forest degradation explicitly.

2-6 Conclusions

We found that STARFM fusion imagery can improve the accuracy of deforestation estimates, especially in areas where phenological differences are pronounced, and where limited image availability precludes the analysis of Landsat images from similar phenological stages in different years. However, in areas with low phenological variability, and better image availability, radiometric normalization performed better. To our knowledge, our study was one of the first to estimate deforestation based on a combination of Spectral Mixture Analysis and STARFM data fusion images. We explored deforestation mapping in a range of tropical and sub-tropical forest types, which provided some unique challenges because of a wide range of ecological conditions, and relatively minor spectral differences between forest and non-forest lands in the more arid areas of northern Mexico where forests are sparse. We suggest that our findings are valid for similar ecosystems where limited availability of Landsat imagery makes it difficult to capture different phenological stages, and that our approach can be valuable for forest management and monitoring in such settings, because it provides a tool to detect deforestation.

2-7 Literature cited

- Adams, J.B., Gillespie, A.R., 2006. Remote sensing of landscapes with spectral images: A physical modeling approach. Cambridge University Press.
- Adams, J.B., Sabol, D.E., Kapos, V., Almeida Filho, R., Roberts, D.A., Smith, M.O., Gillespie, A.R., 1995. Classification of multispectral images based on fractions of endmembers: Application to land-cover change in the Brazilian Amazon. *Remote Sens. Environ.* 52, 137–154. doi:10.1016/0034-4257(94)00098-8
- Adams, J.B., Smith, M.O., Johnson, P.E., 1986. Spectral mixture modeling: A new analysis of rock and soil types at the Viking Lander 1 Site. *J. Geophys. Res.* 91, 8098–8112. doi:10.1029/JB091iB08p08098
- Aide, T.M., Clark, M.L., Grau, H.R., López-Carr, D., Levy, M.A., Redo, D., Bonilla-Moheno, M., Riner, G., Andrade-Núñez, M.J., Muñiz, M., 2013. Deforestation and Reforestation of Latin America and the Caribbean (2001-2010). *Biotropica* 45, 262–271. doi:10.1111/j.1744-7429.2012.00908.x
- Barreda-Bautista, B., Lopez-Caloca, A., Couturier, S., Silvan-Carnenas, J., 2011. Tropical dry forests in the global picture: The challenge of remote sensing-based change detection in tropical dry environments, in: Carayannis, E. (Ed.), *Planet Earth 2011 - Global Warming Challenges and Opportunities for Policy and Practice*. InTech, NYC, pp. 232–256. doi:10.5772/24283
- Caselles, V., Lopez Garcia, M.J., 1989. An alternative simple approach to estimate

- 382 atmospheric correction in multitemporal studies. *Int. J. Remote Sens.* 10, 1127–
 383 1134. doi:10.1080/01431168908903951
- 384 Chen, C.-R., Chen, C.-F., Son, N.-T., 2014. Rice crop monitoring with multitemporal
 385 MODIS-Landsat data fusion. *EGU Gen. Assem.* 2014.
- 386 Clark, R.N., Swayze, G.A., Gallagher, A.J., King, T.V. V., Calvin, W.M., 1993. The U.
 387 S. Geological Survey, Digital Spectral Library: Version 1: 0.2 to 3.0 microns.
- 388 CONABIO, 1998. Uso de suelo y vegetación de INEGI agrupado por CONABIO.
 389 Comisión Nacional para el Conocimiento y Uso de la Biodiversidad, Mexico
 390 City.
- 391 Davidson, E.A., Asner, G.P., Stone, T.A., Neill, C., Figueiredo, R.O., 2008. Objective
 392 indicators of pasture degradation from spectral mixture analysis of Landsat
 393 imagery. *J. Geophys. Res. Biogeosciences* 113, 1–7. doi:10.1029/2007JG000622
- 394 Dawelbait, M., Morari, F., 2012. Monitoring desertification in a Savannah region in
 395 Sudan using Landsat images and spectral mixture analysis. *J. Arid Environ.* 80,
 396 45–55. doi:10.1016/j.jaridenv.2011.12.011
- 397 Foley, J.A., Defries, R., Asner, G.P., Barford, C., Bonan, G., Carpenter, S.R., Chapin,
 398 F.S., Coe, M.T., Daily, G.C., Gibbs, H.K., Helkowski, J.H., Holloway, T.,
 399 Howard, E.A., Kucharik, C.J., Monfreda, C., Patz, J.A., Prentice, I.C.,
 400 Ramankutty, N., Snyder, P.K., 2005. Global consequences of land use. *Science*
 401 309, 570–4. doi:10.1126/science.1111772

- 402 Gao, F., Masek, J., Schwaller, M., Hall, F., 2006. On the blending of the Landsat and
 403 MODIS surface reflectance: predicting daily Landsat surface reflectance. IEEE
 404 Trans. Geosci. Remote Sens. 44, 2207–2218. doi:10.1109/TGRS.2006.872081
- 405 Goward, S., Arvidson, T., Williams, D., Faundeen, J., Irons, J., Franks, S., 2006.
 406 Historical record of Landsat global coverage. Photogramm. Eng. Remote Sens.
 407 72, 1155–1169. doi:10.14358/PERS.72.10.1155
- 408 Hall, F.G., Strebel, D.E., Nickeson, J.E., Goetz, S.J., 1991. Radiometric rectification:
 409 Toward a common radiometric response among multirate, multisensor images.
 410 Remote Sens. Environ. 35, 11–27. doi:10.1016/0034-4257(91)90062-B
- 411 Hansen, M.C., Potapov, P. V, Moore, R., Hancher, M., Turubanova, S.A., Tyukavina, A.,
 412 Thau, D., Stehman, S. V, Goetz, S.J., Loveland, T.R., Kommareddy, A., Egorov,
 413 A., Chini, L., Justice, C.O., Townshend, J.R.G., 2013. High-resolution global
 414 maps of 21st-century forest cover change. Science (80-.). 342, 850–3.
 415 doi:10.1126/science.1244693
- 416 Hesketh, M., Sánchez-Azofeifa, G.A., 2012. The effect of seasonal spectral variation on
 417 species classification in the Panamanian tropical forest. Remote Sens. Environ.
 418 118, 73–82. doi:10.1016/j.rse.2011.11.005
- 419 Hilker, T., Wulder, M.A., Coops, N.C., Seitz, N., White, J.C., Gao, F., Masek, J.G.,
 420 Stenhouse, G., 2009. Generation of dense time series synthetic Landsat data
 421 through data blending with MODIS using a spatial and temporal adaptive
 422 reflectance fusion model. Remote Sens. Environ. 113, 1988–1999.

- 423 doi:10.1016/j.rse.2009.05.011
- 424 Jia, K., Liang, S., Zhang, L., Wei, X., Yao, Y., Xie, X., 2014. Forest cover classification
425 using Landsat ETM+ data and time series MODIS NDVI data. *Int. J. Appl. Earth*
426 *Obs. Geoinf.* 33, 32–38. doi:10.1016/j.jag.2014.04.015
- 427 Ju, J., Roy, D.P., 2008. The availability of cloud-free Landsat ETM+ data over the
428 conterminous United States and globally. *Remote Sens. Environ.* 112, 1196–1211.
429 doi:10.1016/j.rse.2007.08.011
- 430 Kim, D.-H., Sexton, J.O., Townshend, J.R., 2015. Accelerated deforestation in the humid
431 tropics from the 1990s to the 2000s. *Geophys. Res. Lett.* 42, 3495–3501.
432 doi:10.1002/2014GL062777
- 433 Lawley, V., Lewis, M., Clarke, K., Ostendorf, B., 2015. Site-based and remote sensing
434 methods for monitoring indicators of vegetation condition: An Australian review.
435 *Ecol. Indic.* 60, 1273–1283. doi:10.1016/j.ecolind.2015.03.021
- 436 Lippitt, C.D., Rogan, J., Li, Z., Ronald Eastman, J., Jones, T.G., 2008. Mapping Selective
437 Logging in Mixed Deciduous Forest: A Comparison of Machine Learning
438 Algorithms. *Photogramm. Eng. Remote Sens.* 74, 1201–1211.
- 439 Lunetta, R.S., Ediriwickrema, J., Johnson, D.M., Lyon, J.G., McKerrow, A., 2002.
440 Impacts of vegetation dynamics on the identification of land-cover change in a
441 biologically complex community in North Carolina, USA. *Remote Sens. Environ.*
442 82, 258–270. doi:10.1016/S0034-4257(02)00042-1

- 443 Martinez Morales, R., Miura, T., Idol, T., 2008. An assessment of Hawaiian dry forest
444 condition with fine resolution remote sensing. *For. Ecol. Manage.* 255, 2524–
445 2532. doi:10.1016/j.foreco.2008.01.049
- 446 Masek, J., Vermonte, E., Saleous, N., Wolfer, R., Hall, F., Huemmrich, K., Gao, F.,
447 Kutler, 2013. LEDAPS Calibration, Reflectance, Atmospheric Correction
448 Preprocessing Code, Version 2. doi:10.3334/ORNLDAAAC/1146
- 449 Matricardi, E.A.T., Skole, D.L., Pedlowski, M.A., Chomentowski, W., Fernandes, L.C.,
450 2010. Assessment of tropical forest degradation by selective logging and fire
451 using Landsat imagery. *Remote Sens. Environ.* 114, 1117–1129.
452 doi:10.1016/j.rse.2010.01.001
- 453 Mitchard, E.T., Saatchi, S.S., Baccini, A., Asner, G.P., Goetz, S.J., Harris, N.L., Brown,
454 S., 2013. Uncertainty in the spatial distribution of tropical forest biomass: a
455 comparison of pan-tropical maps. *Carbon Balance Manag.* 8, 10.
456 doi:10.1186/1750-0680-8-10
- 457 Putz, F.E., Redford, K.H., 2010. The Importance of Defining “Forest”: Tropical Forest
458 Degradation, Deforestation, Long-term Phase Shifts, and Further Transitions.
459 *Biotropica* 42, 10–20. doi:10.1111/j.1744-7429.2009.00567.x
- 460 Puyravaud, J.-P., 2003. Standardizing the calculation of the annual rate of deforestation,
461 *Forest Ecology and Management.* doi:10.1016/S0378-1127(02)00335-3
- 462 Röder, A., Udelhoven, T., Hill, J., del Barrio, G., Tsiourlis, G., 2008. Trend analysis of

- 463 Landsat-TM and -ETM+ imagery to monitor grazing impact in a rangeland
464 ecosystem in Northern Greece. *Remote Sens. Environ.* 112, 2863–2875.
465 doi:10.1016/j.rse.2008.01.018
- 466 Rzedowski, J., 2006. *Vegetacion de Mexico*, Limusa. ed. Comision Nacional para el
467 Conocimiento y Uso de la Biodiversidad, Mexico City.
- 468 Smith, M.O., Ustin, S.L., Adams, J.B., Gillespie, A.R., 1990. Vegetation in deserts: A
469 regional measure of abundance from multispectral images. *Remote Sens. Environ.*
470 31, 1–26. doi:10.1016/0034-4257(90)90074-V
- 471 Sohn, Y., Moran, E.F., Gurri, E., 1999. Deforestation in North-Central Yucatan (1985-
472 1995): Mapping secondary succession of forest and agricultural land use in Sotuta
473 using the Cosine of the angle concept. *Photogramm. Eng. Remote Sens.* 65, 947–
474 958.
- 475 Souza Jr., C., Firestone, L., Silva, L.M., Roberts, D., 2003. Mapping forest degradation in
476 the Eastern Amazon from SPOT 4 through spectral mixture models. *Large Scale*
477 *Biosph. Atmos. Exp. Amaz.* 87, 494–506. doi:10.1016/j.rse.2002.08.002
- 478 Trejo, I., Dirzo, R., 2000. Deforestation of seasonally dry tropical forest: a national and
479 local analysis in Mexico. *Biol. Conserv.* 94, 133–142. doi:10.1016/S0006-
480 3207(99)00188-3
- 481 Turner, B., Villar, S.C., Foster, D., Geoghegan, J., Keys, E., Klepeis, P., Lawrence, D.,
482 Mendoza, P.M., Manson, S., Ogneva-Himmelberger, Y., Plotkin, A.B., Salicrup,

- 483 D.P., Chowdhury, R.R., Savitsky, B., Schneider, L., Schmook, B., Vance, C.,
 484 2001. Deforestation in the southern Yucatán peninsular region: an integrative
 485 approach. *For. Ecol. Manage.* 154, 353–370. doi:10.1016/S0378-1127(01)00508-
 486 4
- 487 Velazquez, A., Mas, J., Diaz-Gallegos, J., Mayorga Saucedo, R., Alcantara, C., Castro,
 488 R., Fernandez, T., Boco, G., Ezcurra, E., Palacio, J., 2002a. Patrones y Tasas de
 489 Cambio de Uso de Suelo en Mexico. *Gac. Ecol. Inst. Ecol. UNAM* 62, 21–37.
- 490 Velazquez, A., Mas, J.-F., Palacio-Prieto, J.L., Bocco, G., 2002b. Land cover mapping to
 491 obtain a current profile of deforestation in Mexico. *Unasylva* 53, 37–40.
- 492 Veraverbeke, S., Somers, B., Gitas, I., Katagis, T., Polychronaki, A., Goossens, R., 2012.
 493 Spectral mixture analysis to assess post-fire vegetation regeneration using Landsat
 494 Thematic Mapper imagery: Accounting for soil brightness variation. *Int. J. Appl.*
 495 *Earth Obs. Geoinf.* 14, 1–11. doi:10.1016/j.jag.2011.08.004
- 496 Walker, J.J., de Beurs, K.M., Wynne, R.H., 2014. Dryland vegetation phenology across
 497 an elevation gradient in Arizona, USA, investigated with fused MODIS and
 498 Landsat data. *Remote Sens. Environ.* 144, 85–97. doi:10.1016/j.rse.2014.01.007
- 499 Watts, J.D., Powell, S.L., Lawrence, R.L., Hilker, T., 2011. Improved classification of
 500 conservation tillage adoption using high temporal and synthetic satellite imagery.
 501 *Remote Sens. Environ.* 115, 66–75. doi:10.1016/j.rse.2010.08.005
- 502 Wulder, M.A., White, J.C., Goward, S.N., Masek, J.G., Irons, J.R., Herold, M., Cohen,

- 503 W.B., Loveland, T.R., Woodcock, C.E., 2008. Landsat continuity: Issues and
504 opportunities for land cover monitoring. *Remote Sens. Environ.* 112, 955–969.
505 doi:10.1016/j.rse.2007.07.004
- 506 Xu, Y., Huang, B., 2014. Spatial and temporal classification of synthetic satellite
507 imagery: land cover mapping and accuracy validation. *Geo-spatial Inf. Sci.* 17, 1–
508 7. doi:10.1080/10095020.2014.881959
- 509 Yang, J., Weisberg, P.J., Bristow, N.A., 2012. Landsat remote sensing approaches for
510 monitoring long-term tree cover dynamics in semi-arid woodlands: Comparison
511 of vegetation indices and spectral mixture analysis. *Remote Sens. Environ.* 119,
512 62–71. doi:10.1016/j.rse.2011.12.004
- 513 Zhu, L., Radeloff, V.C., Ives, A., Barton, B., 2015. Mapping Crop Patterns in Central US
514 Agricultural Systems from 2000 to 2014 Based on Landsat Data: To What Degree
515 Does Fusing MODIS Data Improve Classification Accuracies?, in: 2015 AGU
516 Fall Meeting.
- 517 Zhu, Z., Woodcock, C.E., 2012. Object-based cloud and cloud shadow detection in
518 Landsat imagery. *Remote Sens. Environ.* 118, 83–94.
519 doi:10.1016/j.rse.2011.10.028

520 **2-8 Tables**

521 Table 2-1: Modis and Landsat image datasets used in the study

Region	Landsat 7 Path/Row	Landsat start date	Landsat final date	MODIS MOD09A1 path row	Modis calibration date ¹	Modis predicted date
Northern	33/41	9/17/2001	8/9/2010	h08 v06	7/28/2010	9/30/2010
Central	27/45	7/21/2001	9/5/2012	h08 v06	7/20/2001	9/14/2001
Southeastern	20/46	7/20/2001	8/24/2008	h09 v06	7/20/2001	8/13/2001

522 ¹ 8-day composite start date

523 Table 2-2: Accuracy of the detected deforestation using different thresholds.

		Raw Surface Reflectance			Radiometric Normalized			STARFM		
		0.1	0.2	0.3	0.1	0.2	0.3	0.1	0.2	0.3
Northern	Overall accuracy	0.73	0.66	0.62	0.74	0.68	0.62	0.77	0.75	0.66
	Deforestation user accuracy	0.94	1.00	1.00	0.83	0.95	1.00	0.73	0.85	1.00
	Deforestation producer accuracy	0.40	0.21	0.11	0.48	0.25	0.11	0.73	0.48	0.21
	No deforestation user accuracy	0.69	0.63	0.61	0.71	0.64	0.61	0.80	0.71	0.63
	No deforestation producer accuracy	0.98	1.00	1.00	0.93	0.99	1.00	0.80	0.94	1.00
Central	Overall accuracy	0.70	0.66	0.59	0.63	0.55	0.52	0.79	0.71	0.64
	Deforestation user accuracy	0.92	0.96	1.00	0.77	0.88	0.00	0.85	0.91	0.92
	Deforestation producer accuracy	0.40	0.30	0.13	0.33	0.08	0.00	0.67	0.44	0.26
	No deforestation user accuracy	0.64	0.61	0.56	0.60	0.54	0.52	0.75	0.65	0.59
	No deforestation producer accuracy	0.97	0.99	1.00	0.91	0.99	1.00	0.89	0.96	0.98
Southern	Overall accuracy	0.72	0.75	0.65	0.74	0.64	0.58	0.64	0.72	0.69
	Deforestation user accuracy	0.72	0.94	1.00	0.91	1.00	1.00	0.59	0.77	0.95
	Deforestation producer accuracy	0.72	0.52	0.28	0.53	0.27	0.15	0.82	0.63	0.40
	No deforestation user accuracy	0.73	0.68	0.59	0.68	0.59	0.55	0.73	0.69	0.63
	No deforestation producer accuracy	0.73	0.97	1.00	0.95	1.00	1.00	0.46	0.82	0.98

525 Table 2-3: Regression model coefficients for the models with one and with two terms.

		Model [†]	Term	Estimate	S.E.	Statistic	p value	Sig	AIC	Intercept at 0.5*
NORTH	Raw	1	$\Delta\%Veg$	9.64	1.97	4.90	9.80E-07	***	200.12	0.04
		2	$Vegt_0$	3.85	1.18	3.27	1.08E-03	**	190.9	0.45
			$\Delta\%Veg$	11.33	2.09	5.43	5.67E-08	***		
	Normalized	1	$\Delta\%Veg$	11.10	2.04	5.44	5.30E-08	***	192.78	0.07
		2	$Vegt_0$	1.31	1.58	0.83	4.06E-01		194.1	0.92
			$\Delta\%Veg$	10.74	2.02	5.32	1.06E-07	***		
	STARFM	1	$\Delta\%Veg$	11.05	1.84	6.01	1.81E-09	***	182.15	0.13
		2	$Vegt_0$	0.95	1.48	0.64	5.23E-01		183.75	0.15
			$\Delta\%Veg$	11.03	1.82	6.07	1.27E-09	***		
CENTRAL	Raw	1	$\Delta\%Veg$	12.87	2.12	6.08	1.21E-09	***	184.95	0
		2	$Vegt_0$	2.56	0.98	2.62	8.84E-03	**	179.81	0.23
			$\Delta\%Veg$	10.63	2.23	4.77	1.81E-06	***		
	Normalized	1	$\Delta\%Veg$	0.26	0.93	0.28	7.80E-01		265.5	0.31
		2	$Vegt_0$	17.37	2.70	6.43	1.25E-10	***	176.47	0.25
			$\Delta\%Veg$	10.67	2.18	4.90	9.77E-07	***		
	STARFM	1	$\Delta\%Veg$	7.28	1.26	5.77	7.72E-09	***	213.94	0.08
		2	$Vegt_0$	4.83	1.10	4.38	1.17E-05	***	193.7	0.36
			$\Delta\%Veg$	4.87	1.37	3.55	3.87E-04	***		
SOUTH	Raw	1	$\Delta\%Veg$	9.60	1.67	5.74	9.63E-09	***	210.49	0.13
		2	$Vegt_0$	-3.63	3.13	-1.16	2.46E-01		211.2	0.14
			$\Delta\%Veg$	10.49	1.88	5.57	2.58E-08	***		
	Normalized	1	$\Delta\%Veg$	10.50	1.86	5.65	1.64E-08	***	213.65	0.06
		2	$Vegt_0$	-0.40	6.92	-0.06	9.54E-01		215.65	-1.12
			$\Delta\%Veg$	10.51	1.86	5.64	1.67E-08	***		
	STARFM	1	$\Delta\%Veg$	7.98	1.39	5.76	8.57E-09	***	215.11	0.19
		2	$Vegt_0$	-5.66	2.49	-2.28	2.29E-02	*	211.59	0.24
			$\Delta\%Veg$	10.17	1.80	5.66	1.51E-08	***		

526 † 1= Def~($\Delta\%Veg$); 2= Def~($\Delta\%Veg, Vegt_0$)

527 * Intercept at the 0.5 value, which reference the inflexion point.

528 Sig. *** 0.001 , ** 0.01, * 0.05

529

530 Table 2-4: Deforestation in the study areas

	Initial forest (ha)	Final forest (ha)	Deforested area (ha)	Deforestation rate (%/year)	Forest loss (percentage points)
Northern	2,251,710	2,213,019	38,691	-0.19	1.72
Central	694,980	658,723	36,257	-0.48	5.22
Southeastern	1,757,040	1,636,085	120,955	-1.01	6.88

531

2-9 Figures

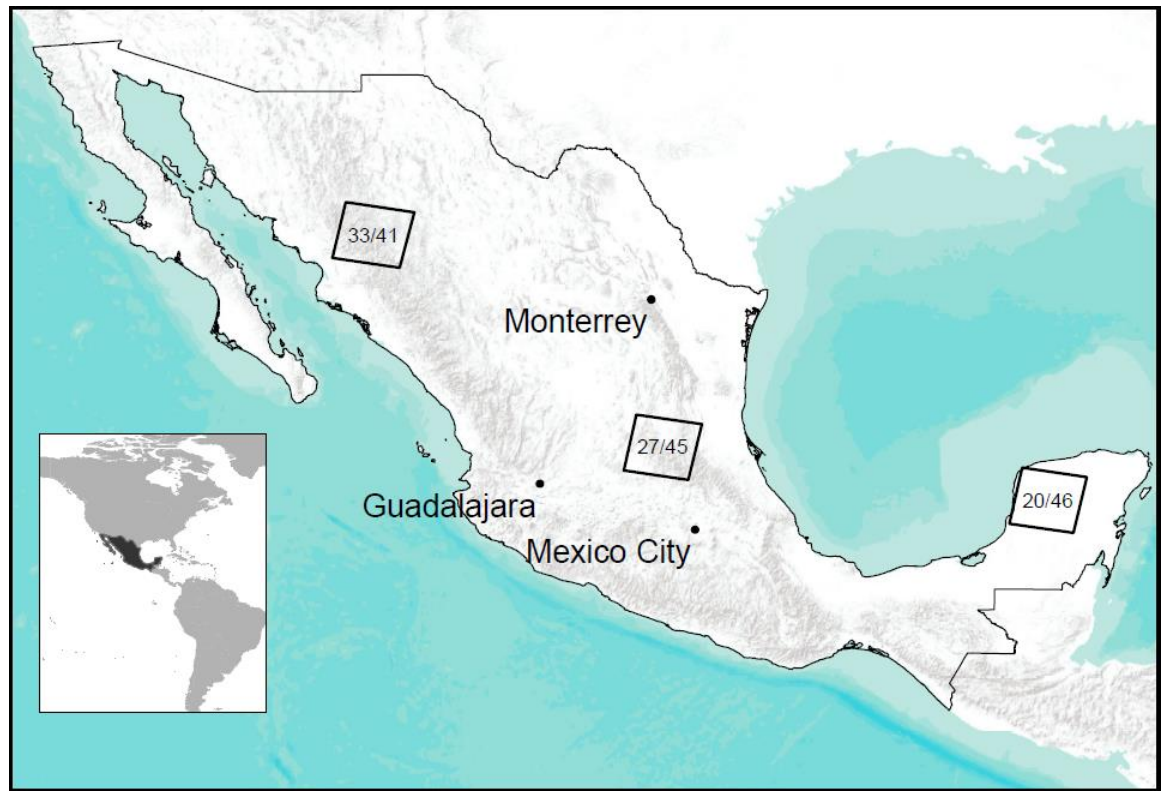


Figure 2-1: Study area. The three squares represent the northern, central and southeastern Landsat footprints that we analyzed in Mexico. We include the path and row for each of the footprints.

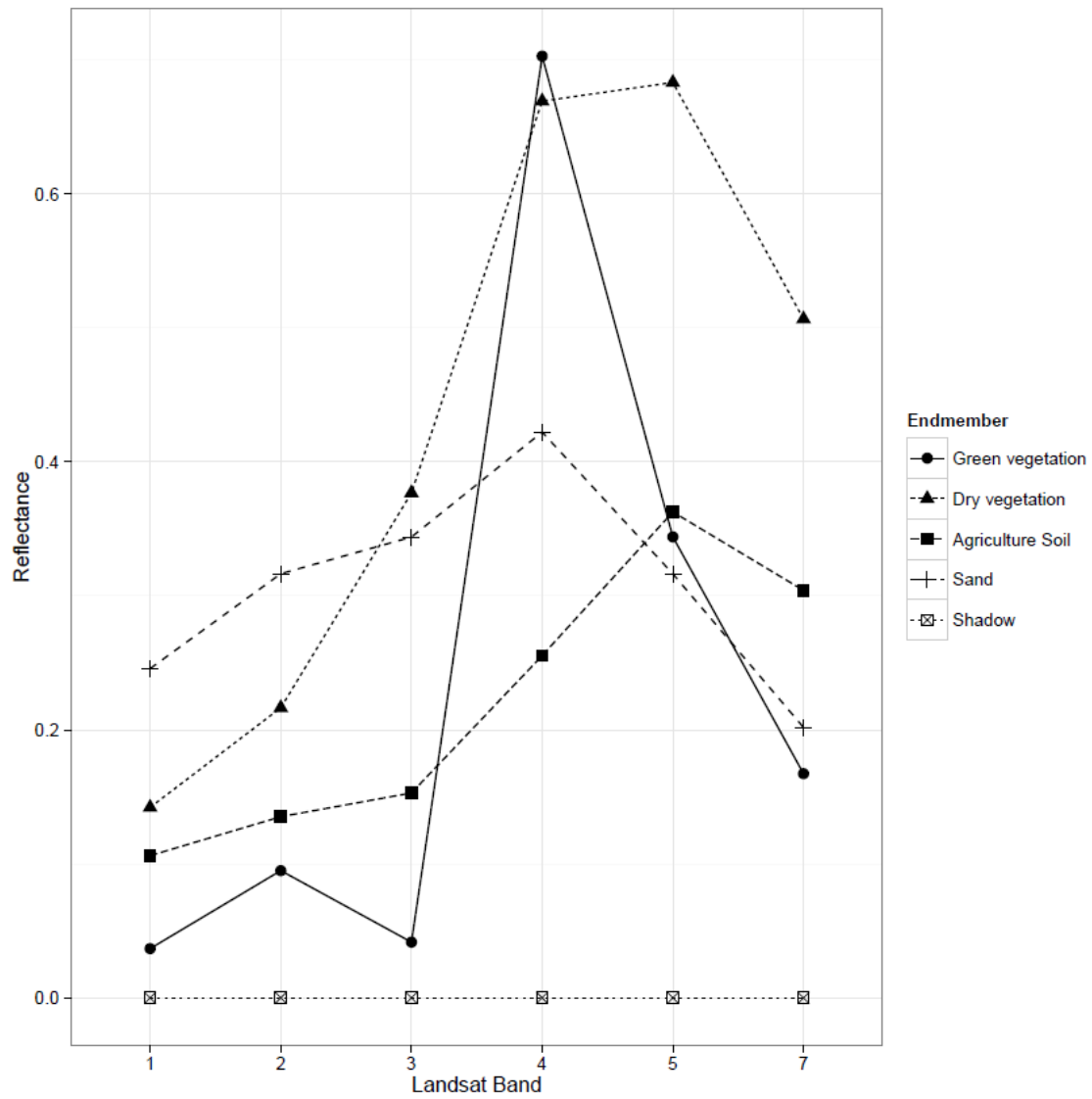


Figure 2-2: Endmembers used in the spectral unmixing process.

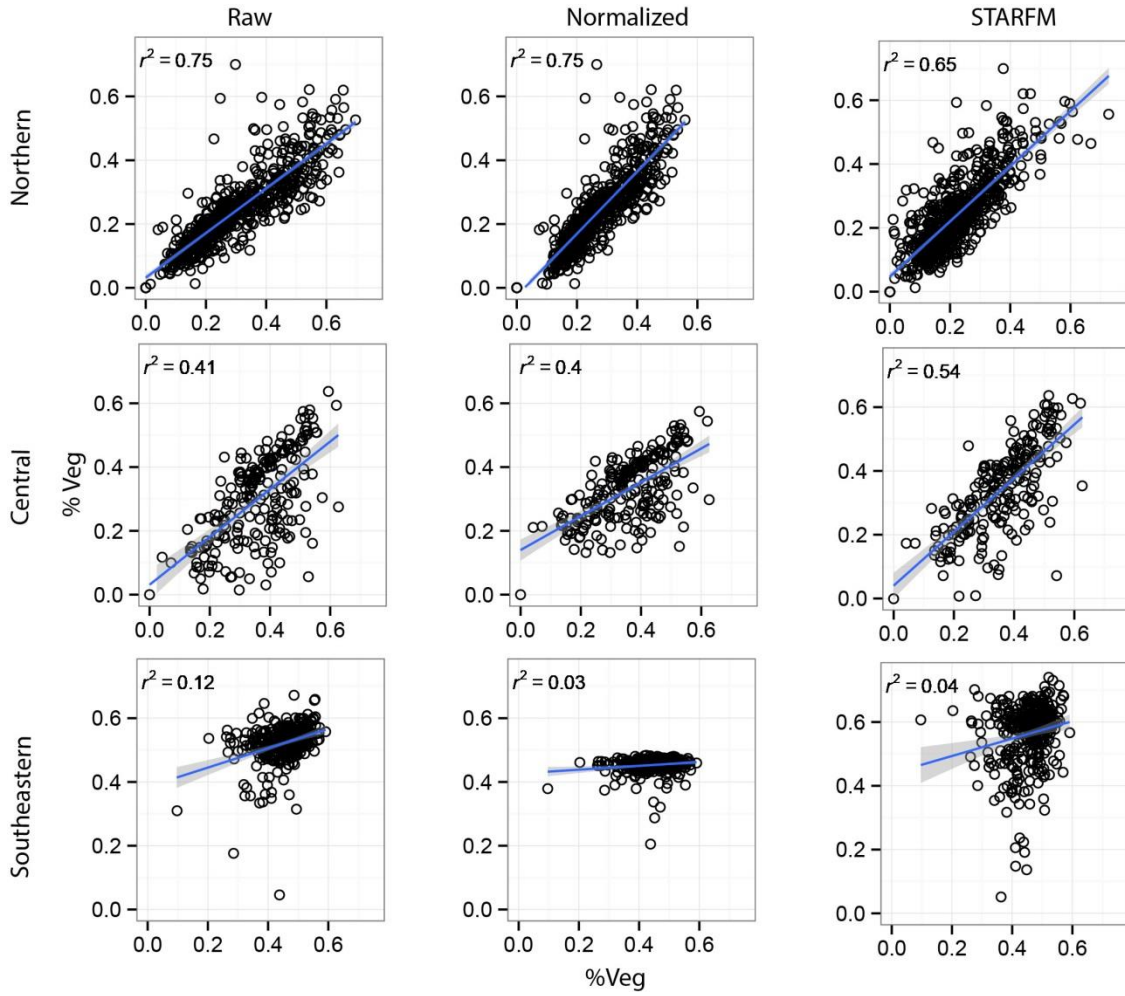


Figure 2-3: Correlation between the vegetation fraction maps produced with T_0 raw surface reflectance values of the T_1 fraction maps produced with a) raw surface reflectance, b) radiometric normalization and c) STARFM fusion image. We show the r^2 value of the regression lines. The grey area represents a confidence interval for the fitted values of the model.

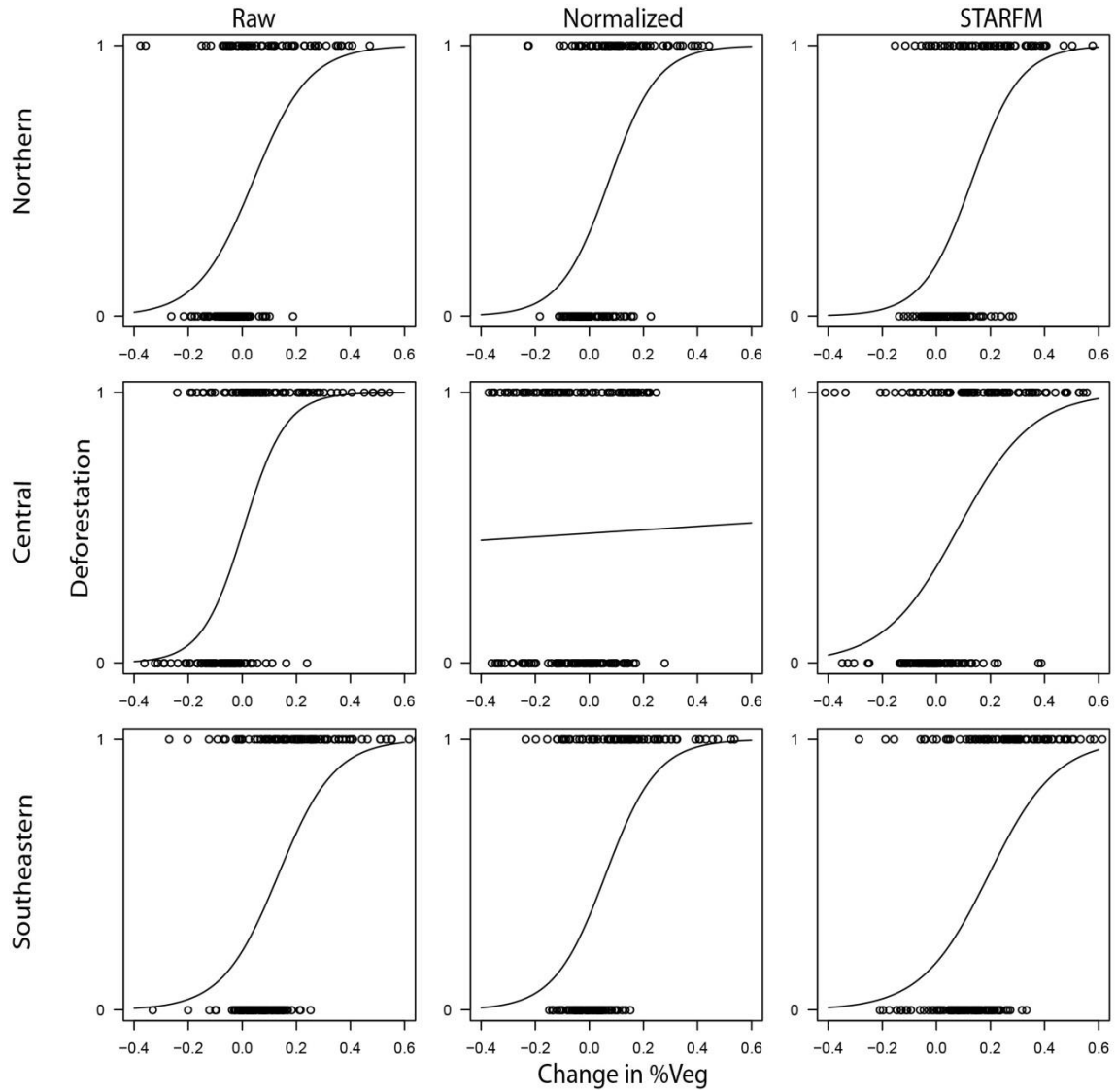


Figure 2-4: Changes between vegetation fraction maps T_1 and T_0 and the corresponding deforestation validation points, where 1 corresponds to a deforested pixel and 0 to an intact forest pixel.

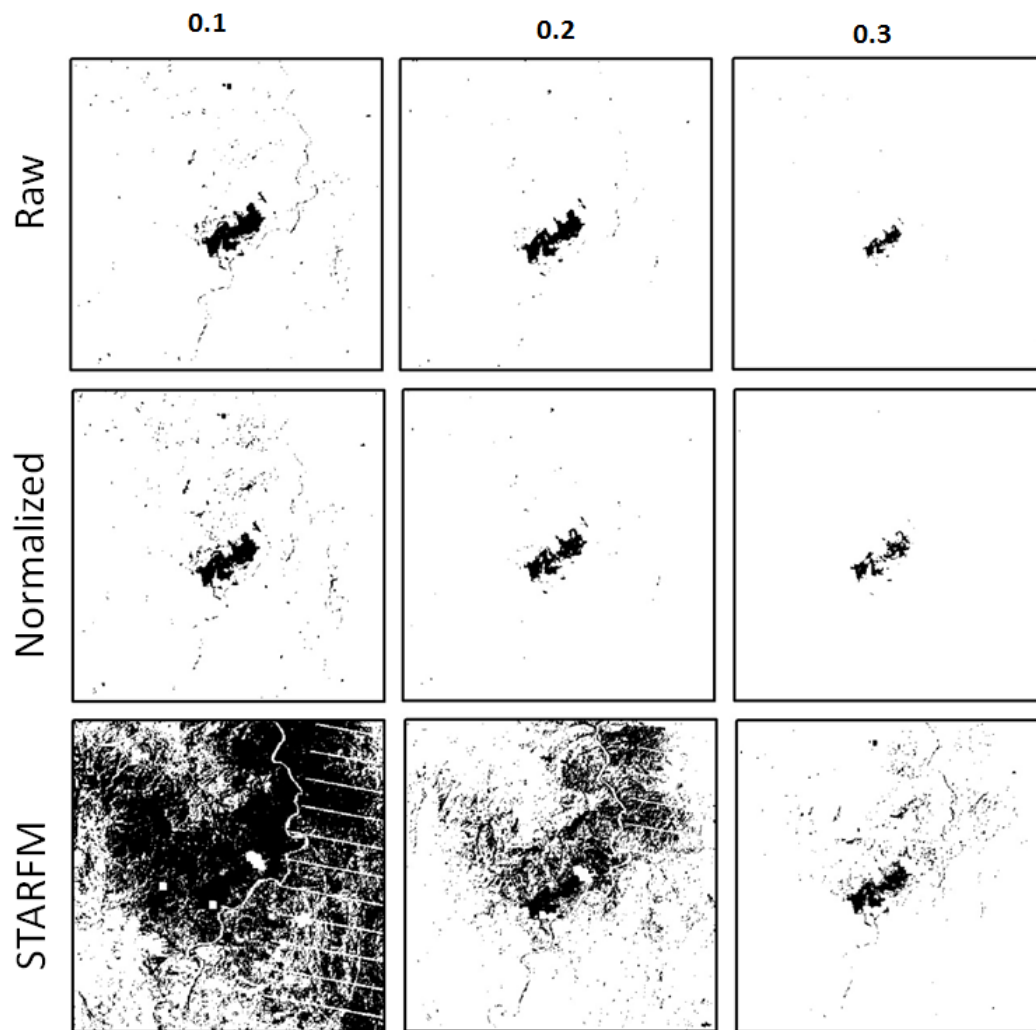


Figure 2-5: Example of the deforestation found using 0.1, 0.2 and 0.3 threshold values for the difference in vegetation fraction maps. This area corresponds to a large deforested area in the northern footprint.



Figure 2-6: Example of the deforestation detected using a STARFM fusion image. The images correspond to a) the surface reflectance in 2001, b) surface reflectance in 2012, and c) surface reflectance in 2012, with the mapped deforestation in orange.

Chapter 3: Effects of habitat suitability and minimum patch size thresholds on the assessment of landscape connectivity for jaguars in the Sierra Gorda, Mexico

Contributors: Ramirez-Reyes, C.¹, Bateman, Brooke L.¹, Radeloff, Volker C.¹

¹ SILVIS Lab, Department of Forest and Wildlife Ecology, University of Wisconsin-Madison, 1630 Linden Drive, Madison WI 53706, USA.

3-1 Abstract

Maintaining habitat and its connectivity is a major conservation goal, especially for large carnivores. Assessments of habitat connectivity are typically based on the output of habitat suitability models to first map potential habitat, and then identify where corridors exist. This requires separating habitat from non-habitat, thus one must choose specific thresholds for both habitat suitability and the minimum patch size that can be occupied. The selection of these thresholds is often arbitrary, and the effects of threshold choice on assessments of connectivity are largely unknown. We sought to quantify how habitat-suitability and patch-size thresholds influence connectivity assessments for jaguars (*Panthera onca*) in the Sierra Gorda Biosphere Reserve in central Mexico. We modeled potential habitat for jaguars using the species distribution modelling algorithm Maxent, and assessed potential habitat connectivity with the landscape connectivity software Conefor Sensinode. We repeated these analyses for 45 combinations of habitat suitability based thresholds and minimum patch sizes. Our results indicated that the

thresholds influenced connectivity assessments greatly, and different combinations of the two thresholds yielded vastly different map configurations of suitable habitat for jaguars. We developed an approach to identify the pair of thresholds that best matched the jaguar occurrence points based on the connectivity scores. Among the combinations that we tested, a threshold of 0.3 for habitat suitability and 2 km² for minimum patch size produced the best fit (AUC = 0.9). Surprisingly, in our best potential habitat model we found low suitable habitat for jaguars in most of the core areas of the reserve, and highly suitable areas in the buffer zones and just outside of the reserve. We conclude that the best and most connected potential areas for jaguar habitat are in the central eastern part of the Sierra Gorda. More broadly, landscape connectivity analyses appears to be highly sensitive to the thresholds used to identify suitable habitat, and we recommend conducting sensitivity analyses as introduced here to identify the optimal combination of thresholds.

Keywords: Maxent, Conefor Sensinode, species distribution modeling, *Panthera onca*

3-2 Introduction

Wildlife habitat and species' ranges are diminishing rapidly due to landscape modification (Lindenmayer and Fischer, 2013; Newbold et al., 2015), and human activities such as agriculture, livestock, mining, and the expansion of urban areas (Wood et al., 2013). In addition to the loss of habitat, changes in habitat configuration can diminish the connectivity among areas occupied by different populations of a given species (Tischendorf and Fahrig, 2000). This could reduce the ability of species to survive extreme events such as fires, diseases, and predation (Clark et al., 2011), thereby increasing the risk of extinction (Reed, 2004). Changes in landscape connectivity are particularly detrimental to apex predators that require large areas of suitable habitat, and securing habitat corridors for these species is critical for their long-term conservation (Soisalo and Cavalcanti, 2006). Thus, it is important to both preserve the remaining habitat available for species and to maintain or enhance habitat connectivity (Peterson, 2011; Sanderson et al., 2002).

Mapping species distributions is the first step when developing conservation management strategies that account for population and habitat patterns at local and landscape scales (Cavalcanti & Gese, 2009; Turner et al., 2001). Often, obtaining the actual species distribution is not possible because of time constraints or incomplete data. This is why presence-only models are often used to estimate potential habitat based on occurrences and predictor variables that are biologically meaningful for the species (Bradley et al., 2012). The resulting models can then be used to identify additional areas with similar environmental conditions that could potentially serve as habitat for the

species of interest. Once these potential habitat areas are identified, they can be analyzed in terms of their spatial configuration and connectivity.

Connectivity can be measured in many different way, either focusing only on patches of suitable habitat, or on the entire landscape (Calabrese and Fagan, 2004). However, connectivity assessments based on the graph theory, which quantify the arrangement of habitat patches, have become popular for conservation purposes (Correa Ayram et al., 2015). In the graph theory framework (Bunn et al., 2000), a potential habitat network is organized in patches of potential habitat (nodes) that are connected via edges (Urban and Keitt, 2001). In this context, there are several challenges associated with the assessment of habitat connectivity. First, because the output of potential distribution models is a continuum of suitability values, it is necessary to choose a threshold to differentiate habitat from non-habitat. Different techniques have been proposed to define suitable habitat areas, such as using an arbitrary threshold (Manel et al., 1999) or to determine the threshold that minimizes the error rate for positive and negative observations in a potential habitat model (Jiménez-Valverde & Lobo, 2007; Liu et al., 2013). A second challenge is that any threshold of habitat suitability will result in patches that are highly variable in size, but many species can only occur in patches of a certain minimum patch size (Schutltz and Crone, 2005). Ultimately, the selection of both the suitable habitat and the minimum patch size thresholds may greatly affect the configuration of potential habitat patches (Saura and Martinez-Mlian, 2001; Turner, 1989; Wu, 2004) and therefore affect subsequent habitat connectivity analysis.

Analyses of habitat connectivity are inherently place and species specific, but case studies are valuable, especially in areas with high biodiversity and when the results can be translated to other ecosystems. One such area is Mexico, which has a high diversity of mammals, including several species of felines (CONABIO, 2008). Felines are considered a keystone species because they can control herbivore populations (Miller et al., 2001; Terborgh et al., 2001). Furthermore, felines are an important target for conservation plans, and their presence can indicate healthy ecosystems (Sanchez et al., 2002; Terborgh et al., 2001). However, populations of many felines, including jaguar (*Panthera onca*), have decreased in Mexico, and their habitats have become increasingly fragmented (Polisar et al., 2003). Prior studies have analyzed the potential habitat distribution of jaguars throughout Mexico (Cevallos et al., 2007; Rodríguez-Soto et al., 2011). There are also some local studies of jaguar habitat in southern (Figel et al., 2009), central (Monroy-Vilchis et al., 2008), and northern Mexico (Navarro-Serment et al., 2005), and jaguar habitat connectivity at local level in the north east of Puebla state (Petracca et al., 2014). However, there is still uncertainty about landscape-scale jaguar habitat patterns, i.e., the scales where most conservation decisions are made. In terms of management, understanding habitat connectivity is important for the prioritization of conservation efforts, and to promote the effective allocation of conservation resources (Moilanen et al., 2009). Furthermore, studies on habitat connectivity are missing, despite their importance for the long-term conservation of wide-ranging species such as jaguar (Soisalo and Cavalcanti, 2006).

In this study, our goals were to a) assess potential habitat for jaguars and its connectivity in the Sierra Gorda reserve in Central Mexico, b) examine in detail the effects of different thresholds of habitat suitability and minimum patch size on the resulting connectivity, and c) develop a new approach to identify the optimal combination of these thresholds. Our hypothesis is that larger habitat patches obtained with lower thresholds will promote better landscape connectivity within the landscape for jaguars. With the integration of potential habitat and connectivity, we hope to develop a new approach that can be used to better understand the landscape and habitat use by jaguars in the area, and to assess habitat connectivity for other species and in other areas more accurately.

3-3 Methods

3-3.1 STUDY AREA

We conducted our study in the Sierra Gorda Biosphere Reserve (Sierra Gorda) in central Mexico, and all areas within 20 km of its border (11,548 km², Figure 1). The Sierra Gorda is situated in the Sierra Madre mountain range and contains many vegetation types, including semi-deserts, evergreen and deciduous tropical forest, oak, pine and cloud forests. Elevation ranges from 300-3160 m above sea level. Because of this variety of conditions, the reserve hosts a diversity of wildlife species and is one of the last refuges for jaguars in central western Mexico. The reserve contains a buffer zone, in which some human activities are allowed including agriculture and forestry in temperate areas and grazing on drier lands (INE, 1999). There are also eleven core zones

within the Sierra Gorda reserve, in which human use is limited to conservation and research-related activities. All of the core areas are located at the edge of the reserve, which is different from the more typical pattern, where core areas are near the center of the reserves (Figure 1).

3-3.2 *INPUT DATA: JAGUAR OCCURRENCES AND ENVIRONMENTAL DATA*

We obtained a digital georeferenced database of 117 jaguar occurrence points in the Sierra Gorda. The database was collected by the conservation group Grupo Ecologico Sierra Gorda between 2006 and 2009. The database includes direct animal observations (i.e., visual observations, camera trap photos), and indirect observations (i.e., footprints, droppings, reported cattle attacks). We assumed the database was accurate, as jaguars have a distinct appearance that is not easily confused with other species in the area. Although this database has not been updated since 2009, jaguars have been reported in the area since then (GESG, 2014). For the training and testing of our model, we divided the jaguar occurrence points into two sets. For model testing, we randomly selected 26 points (22% of total) that were at least 2 km apart from each other. For the remaining 91 occurrence points we conducted spatial filtering to eliminate points based on climatic heterogeneity using the SDM toolbox (Brown, 2014). The spatial filtering used the first three principal components of the environmental variables to find areas with low or high climate heterogeneity. Based on this assessment, we reduced the number of presence points in areas with similar climatic conditions to one point location for every 5 km², which is the minimum home range for female jaguars (Rodríguez-Soto et al., 2011). We applied this filtering to prevent the over-fitting of our model to environmental conditions

present in clusters of points with low variability (Boria et al., 2014). The final training point database included 26 occurrence points. This number is low, but working with a limited number of points is common and when working with a rare species such as jaguar as it is preferable to have fewer number of training data rather than spatially autocorrelated points (Bean et al., 2012; Hernandez et al., 2006; van Proosdij et al., 2016). For the purpose of comparison, we also generated a model including the whole 117 points dataset and split it into two parts for training: 91 for training and 26 for testing.

We included six environmental predictor variables from multiple sources (Table 1) associated with the presence of jaguars (Spangle et al., 2014; Valera-Aguilar, 2010). These variables were temperature, precipitation, land cover, ecoregions, elevation and slope. We retained all of these environmental variables after confirming that there was no strong correlation among them (Table A.1). All the environmental information was converted and scaled into raster format with 30-m resolution.

3-3.3 *POTENTIAL HABITAT MODELING*

We performed a series of analyses to determine jaguars' potential habitat and connectivity for the Sierra Gorda (Figure 2). To identify the areas of potential habitat for jaguars, we used the maximum entropy algorithm Maxent (Phillips et al., 2006). This machine-learning method uses species occurrence and environmental constraints from the study area, or background data, to estimate the probability of occurrence of the species based on the principle of maximum entropy. We restricted the calibration of our Maxent model to the areas within the Sierra Gorda found as suitable jaguar habitat in a previous

coarse-scale analysis for jaguars in Mexico, which used a different jaguar dataset and a coarser resolution (Rodríguez-Soto et al., 2011). We did this to ensure that the background points were not taken at places that are widely afar from our occurrence data (Van Der Wal et al., 2009). We ran Maxent with the default settings (Phillips and Dudík, 2008), i.e., with a regularization multiplier of 1; and a maximum number of background points of 10,000, and we ran 10 replicates with cross-validation. We then extrapolated the model to the rest of the study area to map potential habitat of jaguars within the entire Sierra Gorda.

3-3.4 *CONNECTIVITY ANALYSIS*

In order to calculate habitat connectivity, we had to differentiate areas of habitat from non-habitat. We identified two types of thresholds to separate the areas suitable for jaguars from areas that are not suitable. The first threshold is based on Maxent's habitat suitability index, a continuous value ranging from zero to one across the study area, with values below the selected cutoff deemed to be non-habitat. The second threshold was based on the minimum patch size, with values below the selected cutoff deemed to be unsuitable, even if the habitat suitability value indicated the patch to be suitable. We performed 45 analyses using different values for our two thresholds to test how different combinations affected the subsequent connectivity assessment (Figure 2). We first constructed multiple habitat suitability maps, where suitable habitat was defined as values greater than or equal to 0.1, 0.2, 0.3,..., 0.9 in Maxent's habitat suitability index, increasing in steps of 0.1 units. We then eliminated potential jaguar habitat patches smaller than 2, 5, 10, 15, and 20 km² in each of the previous habitat suitability maps, for

a total of 45 different potential habitat maps. We selected this range of minimum patch values because jaguars generally prefer large habitat patches of at least 20 km² (Núñez et al., 2002) but can temporarily occupy areas as small as 2 km² (Chavez and Cevallos, 2007). We measured the effects on landscape configuration caused by varying the thresholds in the resulting potential habitat maps. For this reason we calculated four landscape fragmentation metrics (number of patches, total patch area, mean patch area, and edge density) for each of the potential habitat networks obtained by each threshold combination using the software Fragstats (McGarigal et al., 2012).

We used Conefor Sensinode (Saura and Pascual-Hortal, 2007) to assess the patch connectivity within each potential habitat map obtained with a particular combination of thresholds. Conefor Sensinode is a decision-support tool that complements habitat analyses by quantifying the importance of specific habitat patches for overall landscape habitat connectivity (Ziółkowska et al., 2012). Conefor Sensinode calculates several connectivity indices, and we report here the delta of the Integrated Index of Connectivity (dIIC) because it has been proposed as ideal for connectivity analysis (Pascual-Hortal and Saura, 2007). The dIIC ranges from 0-100 and assigns a value to each habitat patch, where small values indicate low importance for the overall connectivity of the habitat patch network and large values indicate high importance.

3-3.5 IDENTIFICATION OF THE OPTIMAL COMBINATION OF THRESHOLDS

In order to identify the optimal combination of thresholds for habitat suitability index and minimum patch size that describe our data best we performed a sensibility analysis. For this we created 45 potential habitat maps using the connectivity scores as

the only environmental input for habitat modeling and evaluated the performance of the model to describe our jaguar presence dataset (Figure 2). We started with the maps obtained from the connectivity analysis, which contain the dIIC values obtained, and transformed it into a raster format. We then used Maxent with each of these maps with dIIC values as the only predictor variable for our jaguar presence points. Finally, we ranked the performance of each of the new runs using the area under the curve (AUC) for both the training and testing presence points. AUC scores above 0.5 are considered better than random predictions and values above 0.9 considered highly accurate (Bateman et al., 2012; Guisan et al., 2007). In this way we could identify which model combination of thresholds best described the relationship between the connectivity values obtained and the occurrence points.

3-4 Results

We obtained a potential habitat model based on the spatially filtered jaguar occurrences ($n = 26$). The model had an AUC of 0.91 for the training data and an AUC of 0.83 for the testing data. For comparison purposes, we obtained a model using all 117 occurrence data that resulted in an AUC of 0.92 for training and 0.86 for testing. The model results based on all occurrence points were overall very similar, but predicted a smaller area as highly suitable habitat than the model with the subset of points (Appendix 1). The model we used for subsequent analysis was the one produced with the subset of presence points because of the potential autocorrelation of the training points in the model produced with the full dataset of points.

We found that two of the eleven core zones of the reserve contained highly suitable habitat for jaguars (Figure 3). Most of the potential habitat was located in the central eastern part of the reserve in areas that are formally designated as buffer zones. No areas were identified with a habitat suitability index greater than 0.87. Among the environmental predictor variables, ecoregions, land cover, and slope were the main explanatory variables, contributing 91% of the model's explanatory power, while precipitation, temperature and elevation contributed only 9% (See appendix). The most important ecoregions for jaguar habitat were the Sierra Madre Oriental pine and oak forest and the Planicie Costera Tamaulipeca dry forest. The vegetation types with higher likelihood for jaguar occurrences were tropical deciduous forest and temperate forest, and areas with precipitation of 1000-2000 mm/year. There was minimal potential jaguar habitat in the desert and semi-desert regions within the study area. The habitat model also indicated that occurrence points were primarily located on slopes less than 40 degrees.

3-4.1 *THRESHOLD SELECTION*

The 45 binary maps of potential habitat versus non-habitat generated with different combinations of habitat suitability index and minimum patch size thresholds resulted in vastly different total areas and spatial configurations of remaining habitat patches (Figure 4). As expected, when selecting smaller habitat suitability index values, we obtained relatively few, large and continuous suitable patches across our study area (Figure 5). In contrast, with higher habitat suitability index thresholds, only small patches remained, which were concentrated in the north eastern part of the reserve. We also observed our expected changes in the configuration of suitable habitat patches when

applying different minimum patch size thresholds. Small thresholds ($<10 \text{ km}^2$) resulted in numerous patches located across the reserve. In contrast, higher thresholds ($>10 \text{ km}^2$) led to a smaller number of patches located towards the central and eastern part of the reserve (Figure 4). The mean patch area decreased proportionally to minimum patch size, and the edge density increased as we restricted the habitat suitability threshold. Large thresholds on both of the variables reduced the total area of the potential habitat patches.

3-4.2 *HABITAT CONNECTIVITY*

Different combinations of our two thresholds resulted in vastly different connectivity dIIC values, which changed according to the number and size of the habitat patches. The dIIC connectivity values ranged from one, for patches that contributed little for the connectivity of the patch system, to 100, for those patches that contributed the most. Among the different sets of patches obtained with different threshold combinations, the dIIC values ranged from 0-6 in landscapes comprised on numerous patches, and 0-95 for a habitat landscape with fewer patches (Figure 4). As anticipated, the patches that were most important for maintaining connectivity were generally the larger ones, and the most important patches for connectivity were located towards the center and eastern part of study area. However, the potential habitat patch configuration resulting from lower threshold combinations indicated that patches located in the central area of the reserve had the highest dIIC values.

3-4.3 *THE OPTIMAL COMBINATION OF THRESHOLDS*

When we used the potential habitat patches and their respective connectivity values as the only explanatory variable for Maxent, we obtained different model performances and AUCs ranging from 0.49 to 0.90 for the training data (Figure 6). Based on these results, we selected the best performing model, which was based on a habitat suitability index threshold of 0.3 and minimum patch size of 2 km². This model had a performance an AUC of 0.90 for the training data and 0.78 for the testing one. From the two variables, changes in habitat suitability index resulted in a larger variation in the AUC compared to changes in the minimum patch size.

3-5 Discussion

Potential habitat mapping is a tool that is widely used in conservation science and conservation planning (Elith and Leathwick, 2009; Guisan and Thuiller, 2005), and forms the basis for most habitat connectivity analyses. Here we mapped the potential habitat for jaguars in the Sierra Gorda reserve and explored its connectivity. We found that connectivity was highly sensitive to the thresholds used to delimit potential habitat. Based on our novel approach to identify the optimal threshold values, we found that a threshold for the habitat suitability index of 0.3 and for minimum patch size of 2 km² produced the optimal potential habitat assessment, because it resulted in the connectivity assessment that best matched our jaguar observations.

The potential habitat map for jaguars that resulted from our analysis captured jaguar occurrences in the Sierra Gorda well, as evidenced by the high AUC of 0.91. The predicted areas of high habitat suitability also coincided with the vegetation types reported as habitat for jaguars in other studies such as temperate, deciduous and

tropical forest (Navarro-Serment et al., 2005; Zarco-González et al., 2009), and oak-pine forest (Figel et al., 2009; Monroy-Vilchis et al., 2008). Drier vegetation types in the western parts of the study area were not detected as potential habitat for jaguars, although xeric vegetation is occupied by jaguars in other parts of Mexico (Sanderson et al., 2002; Valera-Aguilar, 2010). Not including xeric vegetation as habitat in our map may be a consequence of not having presence points on such dry land. However, our map is consistent with a nationwide analysis of jaguar habitat in the area, which found low habitat suitability in the dry land of the reserve (Rodríguez-Soto et al., 2011). Also, our model showed more limited potential habitat areas for our study area compared with the previous national model, possibly because we had a local dataset and incorporated a sensitivity analysis on both thresholds. In the future, given the opportunistic nature of our presence data, there are opportunities to incorporate a more systematic data sample via GPS or camera traps, which could improve model outputs by capturing a larger variability of conditions in which the species occurs (Tobler et al., 2008). This highlights the need for local and regional analyses of habitat suitability even for wide-ranging species, such as jaguars, because their habitat-use can differ within larger areas.

Selecting thresholds correctly is crucial when using the output from a potential habitat model for further analyses such as connectivity assessments (Liu et al., 2005). Several threshold selection criteria have been proposed to delimit suitable habitat (Freeman and Moisen, 2008; Jiménez-Valverde and Lobo, 2007; Liu et al., 2013; Norris, 2014), but none of these took into account how the thresholds may affect connectivity. In our analysis, we produced numerous connectivity assessments, and these assessments

varied greatly in their ability to explain jaguar presence data. While changing the habitat suitability thresholds, we observed a tradeoff of either being very restrictive in our analysis (with higher habitat suitability index thresholds) or too permissive (using lower habitat suitability index scores). When using large thresholds, only few areas remained as potential habitat and many of our presence points were outside of those areas.

From our analysis of 45 combinations of thresholds, we found that the best connectivity assessment was the one resulting from a habitat suitability index threshold of 0.3. This number is consistent with the habitat suitability threshold values obtained using two of Maxent's calculated logistic thresholds: the 10th percentile training presence (0.36) and the maximum training sensitivity plus specificity thresholds (0.32). Maxent's thresholds are calculated by evaluating model performance based on omission rate (number of training/test presences that fall into unsuitable pixels) and the proportional predicted area (the proportion of all pixels that are predicted suitable for a species), (Phillips et al., 2006). The 10th percentile threshold corresponds to the predicted habitat suitability value with a 10% omission rate on occurrence points, which has been suggested as an ideal threshold in similar studies (Escalante et al., 2013; McFarland et al., 2013). The maximum training sensitivity plus specificity threshold balances the chance of correctly identifying suitable areas (sensitivity) with the change of correctly assigning unsuitable areas (specificity). By maximizing specificity plus sensitivity we delimit the best areas within our landscape that can host jaguars, and eliminate areas with lower habitat potential (being more specific). A higher threshold value can be used to target the best areas able to host jaguars by reducing the risk of choosing low quality sites but with

the risk of eliminating some locations with actual jaguar observations (being less sensitive), (Pearce and Ferrier, 2000; Pearson, 2007).

Minimum patch size had previously been identified as important for landscape connectivity (Pascual-Hortal and Saura, 2007), and for the delineation of potential habitat (Olson et al., 2014), and our results highlighted the extent to which connectivity depended on minimum patch size. However, the effects of minimum patch size on connectivity were smaller than those of the habitat suitability index threshold. The AUC changed much more when varying the cutoff value of habitat suitability index and less when varying the minimum patch size cutoff value. We detected that the best performance in predicting our jaguar occurrence points was with a minimum potential habitat patch size of 2 km². Jaguars have a large range and they have been reported to prefer large habitat patches of 20 km² or more (Núñez et al., 2002; Valera-Aguilar, 2010). However, jaguars may also explore areas as small as 2 km² when dispersing to other territories or for hunting (Cavalcanti and Gese, 2009). In our study, larger patch size thresholds (>15 km²) reduced the number of potential habitat patches to a level where they no longer captured the presence points. This may indicate that jaguars, although prefer large habitat patches, are forced to use relatively small patches of fragmented potential habitat in Sierra Gorda, such as farm areas, where prey might also be available including livestock.

The most important potential habitat patches for overall connectivity were generally the largest patches. This is partly a function of the dICC metric which weighs the area of each of the potential habitat patches, giving priority to larger patches.

Ecologically though, these large patches are also very important for jaguars because their home range is large (typically more than 20 km²) and the remaining large potential habitat patches should be a priority for conservation. The dIIC has been used previously to identify the most important patches for maintaining and prioritize forest protection (García-Feced et al., 2010; Pascual-Hortal and Saura, 2007; Shanthala Devi et al., 2013), as well as providing habitat for other large mammals such as tapir (García and Leonardo, 2016). Therefore, we suggest that based on our analysis, the best connected areas located in the central eastern part of the reserve deserve particular conservation attention (Figure 7), because they have vegetation types that are highly suitable for jaguars and these areas are part of the proposed jaguar corridor for central Mexico (Rabinowitz and Zeller, 2010).

The current designation of core and buffer areas in the Sierra Gorda reserve neither captures the highest quality habitat for jaguars nor the most important patches for connectivity very well. In our potential habitat map, a small percentage of the core area of the reserve was suitable for jaguars. When created in 1997, the Sierra Gorda reserve included eleven core zones to preserve forests located at the edges of the reserve, with the purpose of having multiple ecosystems represented and to have more conserved lands with restricted access (INE, 1999). However, most of these areas have little potential for hosting jaguars according to our results, whereas the central buffer zone has higher likelihood for jaguar presence. We also detected areas outside of the reserve that are suitable for jaguars. Our finding parallels that of another study, which found that the current core areas of the reserve have also lower potential for providing bird habitat in the

region, compared to central regions of the reserve (Almazán-Núñez, et al. 2013) and we suggest that additional core areas in the center of the Sierra Gorda reserve could be highly valuable for conservation.

In summary, we were successful in mapping potential jaguar habitat and its connectivity in the Sierra Gorda reserve. In our analyses, we focused in particular on the effects of thresholds for habitat suitability and minimum patch size, showed that these two thresholds have large effects on subsequent connectivity assessments, and developed a new method to identify the optimal combination of these thresholds. This approach for assessing landscape connectivity can easily be transferred to other ecosystems and different species. In terms of conservation we identified the areas more suitable to provide habitat for jaguars in the Sierra Gorda reserve, and those that contribute most to their connectivity. Unfortunately, many of these areas are not currently designated as core zones of the reserve. These areas could host jaguars and other species that may well be using the landscape regardless of current protection status. Therefore local-scale studies such as our one might highlight the opportunities for reaching larger and integrated conservation goals. Managers and stakeholders may want to use our findings in combination to other local studies to improve their conservation efforts.

3-6 Literature cited

- Almazán-Núñez, R.C., Aquino, S.L. De, Ríos-Muñoz, C.A., Navarro-Sigüenza, A.G., 2013. Áreas potenciales de riqueza, endemismo y conservación de las aves del estado de Querétaro, México. *Interciencia* 38, 26–34.
- Bateman, B.L., VanDerWal, J., Johnson, C.N., 2012. Nice weather for bettongs: using weather events, not climate means, in species distribution models. *Ecography (Cop.)*. 35, 306–314. doi:10.1111/j.1600-0587.2011.06871.x
- Bean, W.T., Stafford, R., Brashares, J.S., 2012. The effects of small sample size and sample bias on threshold selection and accuracy assessment of species distribution models. *Ecography (Cop.)*. 35, 250–258. doi:10.1111/j.1600-0587.2011.06545.x
- Boria, R.A., Olson, L.E., Goodman, S.M., Anderson, R.P., 2014. Spatial filtering to reduce sampling bias can improve the performance of ecological niche models. *Ecol. Modell.* 275, 73–77. doi:10.1016/j.ecolmodel.2013.12.012
- Bradley, B.A., Olsson, A.D., Wang, O., Dickson, B.G., Pelech, L., Sesnie, S.E., Zachmann, L.J., 2012. Species detection vs. habitat suitability: Are we biasing habitat suitability models with remotely sensed data? *Ecol. Modell.* 244, 57–64. doi:10.1016/j.ecolmodel.2012.06.019
- Brown, J.L., 2014. SDMtoolbox: a python-based GIS toolkit for landscape genetic, biogeographic and species distribution model analyses. *Methods Ecol. Evol.* 5, 694–700. doi:10.1111/2041-210X.12200

- Bunn, A.G., Urban, D.L., Keitt, T.H., 2000. Landscape connectivity: A conservation application of graph theory. *J. Environ. Manage.* 59, 265–278. doi:10.1006
- Calabrese, J.M., Fagan, W.F., 2004. A comparison-shopper's guide to connectivity metrics. *Front. Ecol. Environ.* 2, 529–536. doi:10.1890/1540-9295(2004)002[0529:ACGTCM]2.0.CO;2
- Cavalcanti, S.M.C., Gese, E.M., 2009. Spatial Ecology and Social Interactions of Jaguars (*Panthera Onca*) in the Southern Pantanal, Brazil. *J. Mammal.* 90, 935–945. doi:10.1644/08-MAMM-A-188.1
- Cevallos, G., Chavez, C., List, R., Zarza, H., 2007. Conservación y manejo del jaguar en México: estudios de caso y perspectivas. Universidad Nacional Autónoma de México, Mexico City.
- Chavez, S., Cevallos, G., 2007. El jaguar mexicano en el siglo XXI. Universidad Nacional Autónoma de México, Mexico City.
- Clark, R.W., Marchand, M.N., Clifford, B.J., Stechert, R., Stephens, S., 2011. Decline of an isolated timber rattlesnake (*Crotalus horridus*) population: Interactions between climate change, disease, and loss of genetic diversity. *Biol. Conserv.* 144, 886–891. doi:10.1016/j.biocon.2010.12.001
- CONABIO, 2008. Capital natural de México, vol 1: Conocimiento actual de la biodiversidad. Comisión Nacional para el Conocimiento y Uso de la Biodiversidad, Mexico City.

- Correa Ayram, C.A., Mendoza, M.E., Etter, A., Pérez Salicrup, D.R., 2015. Habitat connectivity in biodiversity conservation: A review of recent studies and applications. *Prog. Phys. Geogr.* 1–32. doi:10.1177/0309133315598713
- Elith, J., Leathwick, J.R., 2009. Species Distribution Models: Ecological Explanation and Prediction Across Space and Time. *Annu. Rev. Ecol. Evol. Syst.* 40, 677–697. doi:10.1146/annurev.ecolsys.110308.120159
- Escalante, T., Rodríguez-Tapia, G., Linaje, M., Illoldi-Rangel, P., González-López, R., 2013. Identification of areas of endemism from species distribution models: threshold selection and Nearctic mammals. *TIP Rev. Espec. en Ciencias Químico-Biológicas* 16, 5–17. doi:10.1016/S1405-888X(13)72073-4
- Figel, J.J., Durán, E., Bray, D.B., Prisciliano-Vázquez, J.-R., 2009. New jaguar records from montane forest at a priority site in southern Mexico. *CATnews* 50.
- Freeman, E.A., Moisen, G.G., 2008. A comparison of the performance of threshold criteria for binary classification in terms of predicted prevalence and kappa. *Ecol. Modell.* 217, 48–58. doi:10.1016/j.ecolmodel.2008.05.015
- García, M.J., Leonardo, R., 2016. Classification of potential habitat of the Central American tapir (*Tapirus bairdii* Gill, 1865) for their conservation in Guatemala. *THERYA* 7, 107–121.

- García-Feced, C., Saura, S., Elena-Rosselló, R., 2010. Improving landscape connectivity in forest districts: A two-stage process for prioritizing agricultural patches for reforestation. *For. Ecol. Manage.* 261, 154–161. doi:10.1016/j.foreco.2010.09.047
- GESG, 2014. Sierra Gorda, Noticias de Julio [WWW Document]. URL <http://sierragorda.net/sierra-gorda-noticias-de-julio/> (accessed 10.19.15).
- Guisan, A., Graham, C.H., Elith, J., Huettmann, F., 2007. Sensitivity of predictive species distribution models to change in grain size. *Divers. Distrib.* 13, 332–340. doi:10.1111/j.1472-4642.2007.00342.x
- Guisan, A., Thuiller, W., 2005. Predicting species distribution: offering more than simple habitat models. *Ecol. Lett.* 8, 993–1009. doi:10.1111/j.1461-0248.2005.00792.x
- Hernandez, P.A., Graham, C.H., Master, L.L., Albert, D.L., 2006. The effect of sample size and species characteristics on performance of different species distribution modeling methods. *Ecography (Cop.)*. 29, 773–785. doi:10.1111/j.0906-7590.2006.04700.x
- INE, 1999. Programa de Manejo de la Reserva de la Biosfera Sierra Gorda. Instituto Nacional de Ecología, Mexico City.
- Jiménez-Valverde, A., Lobo, J.M., 2007. Threshold criteria for conversion of probability of species presence to either–or presence–absence. *Acta Oecologica* 31, 361–369. doi:10.1016/j.actao.2007.02.001

Lindenmayer, D.B., Fischer, J., 2013. *Habitat Fragmentation and Landscape Change: An Ecological and Conservation Synthesis*. Island Press.

Liu, C., Berry, P.M., Dawson, T.P., Pearson, R.G., 2005. Selecting thresholds of occurrence in the prediction of species distributions. *Ecography (Cop.)*. 28, 385–393. doi:10.1111/j.0906-7590.2005.03957.x

Liu, C., White, M., Newell, G., 2013. Selecting thresholds for the prediction of species occurrence with presence-only data. *J. Biogeogr.* 40, 778–789. doi:10.1111/jbi.12058

Manel, S., Dias, J.-M., Ormerod, S.J., 1999. Comparing discriminant analysis, neural networks and logistic regression for predicting species distributions: a case study with a Himalayan river bird. *Ecol. Modell.* 120, 337–347. doi:10.1016/S0304-3800(99)00113-1

McFarland, K.P., Rimmer, C.C., Goetz, J.E., Aubry, Y., Wunderle, J.M., Sutton, A., Townsend, J.M., Sosa, A.L., Kirkconnell, A., 2013. A winter distribution model for Bicknell's Thrush (*Catharus bicknelli*), a conservation tool for a threatened migratory songbird. *PLoS One* 8, e53986. doi:10.1371/journal.pone.0053986

McGarigal, K., Cushman, S.A., Ene, E., 2012. *FRAGSTATS v4: Spatial pattern analysis program for categorical and continuous maps*.

- Miller, B., Dugelby, B., Foreman, D., Martinez Del Río, C., Noss, R., Phillips, M., Reading, R., Soulé, M.E., Terborgh, J., Willcox, L., 2001. The Importance of Large Carnivores to Healthy Ecosystems. *Endanger. Species Updat.* 18.
- Moilanen, A., Wilson, K.A., Possingham, H., 2009. *Spatial Conservation Prioritization: Quantitative Methods and Computational Tools*. Oxford University Press, Oxford.
- Monroy-Vilchis, O., Sánchez, Ó., Aguilera-Reyes, U., Suárez, P., Urios, V., 2008. Jaguar (*Panthera onca*) in the State of Mexico. *Southwest. Nat.* 53, 533–537.
doi:10.1894/CJ-144.1
- Navarro-Serment, C.J., López-González, C.A., Gallo-Reynoso, J.-P., 2005. Occurrence of Jaguar (*Panthera onca*) in Sinaloa Mexico. *Southwest. Nat.* 50, 102–106.
- Newbold, T., Hudson, L.N., Hill, S.L.L., Contu, S., Lysenko, I., Senior, R.A., Börger, L., Bennett, D.J., Choimes, A., Collen, B., Day, J., De Palma, A., Díaz, S., Echeverria-Londoño, S., Edgar, M.J., Feldman, A., Garon, M., Harrison, M.L.K., Alhusseini, T., Ingram, D.J., Itescu, Y., Kattge, J., Kemp, V., Kirkpatrick, L., Kleyer, M., Correia, D.L.P., Martin, C.D., Meiri, S., Novosolov, M., Pan, Y., Phillips, H.R.P., Purves, D.W., Robinson, A., Simpson, J., Tuck, S.L., Weiher, E., White, H.J., Ewers, R.M., Mace, G.M., Scharlemann, J.P.W., Purvis, A., 2015. Global effects of land use on local terrestrial biodiversity. *Nature* 520, 45–50.
doi:10.1038/nature14324

- Norris, D., 2014. Model thresholds are more important than presence location type :
Understanding the distribution of lowland tapir (*Tapirus terrestris*) in a
continuous Atlantic forest of southeast Brazil. *Trop. Conserv. Sci.* 7, 529–547.
- Núñez, R., Miller, B., Lindzey, F., 2002. Ecología del jaguar en la reserva de la biosfera
Chamela-Cuixmala, in: Medellín, R. (Ed.), *El Jaguar En El Nuevo Milenio*.
Fondo de Cultura Económica, pp. 107–126.
- Olson, L.E., Sauder, J.D., Albrecht, N.M., Vinkey, R.S., Cushman, S.A., Schwartz, M.K.,
2014. Modeling the effects of dispersal and patch size on predicted fisher
(*Pekania [Martes] pennanti*) distribution in the U.S. Rocky Mountains. *Biol.*
Conserv. 169, 89–98. doi:10.1016/j.biocon.2013.10.022
- Pascual-Hortal, L., Saura, S., 2007. Impact of spatial scale on the identification of critical
habitat patches for the maintenance of landscape connectivity. *Landsc. Urban*
Plan. 83, 176–186. doi:10.1016/j.landurbplan.2007.04.003
- Pearce, J., Ferrier, S., 2000. Evaluating the predictive performance of habitat models
developed using logistic regression. *Ecol. Modell.* 133, 225–245.
- Pearson, R.G., 2007. Species distribution modeling for conservation educators and
practitioners. *Lessons Conserv.* 3, 54–89.
- Peterson, A.T., 2011. *Ecological Niches and Geographic Distributions* (MPB-49).
Princeton University Press.

- Petracca, L.S., Ramírez-Bravo, O.E., Hernández-Santín, L., 2014. Occupancy estimation of jaguar *Panthera onca* to assess the value of east-central Mexico as a jaguar corridor. *Oryx* 48, 133–140. doi:10.1017/S0030605313000069
- Phillips, S.J., Anderson, R.P., Schapire, R.E., 2006. Maximum entropy modeling of species geographic distributions. *Ecol. Modell.* 190, 231–259. doi:10.1016/j.ecolmodel.2005.03.026
- Phillips, S.J., Dudík, M., 2008. Modeling of species distributions with Maxent: new extensions and a comprehensive evaluation. *Ecography (Cop.)*. 31, 161–175. doi:10.1111/j.0906-7590.2008.5203.x
- Polisar, J., Maxit, I., Scognamillo, D., Farrell, L., Sunkuist, M.E., Eisenberg, J.F., 2003. Jaguars, pumas, their prey base, and cattle ranching: ecological interpretations of a management problem. *Biol. Conserv.* 109, 297–310. doi:10.1016/S0006-3207(02)00157-X
- Rabinowitz, A., Zeller, K.A., 2010. A range-wide model of landscape connectivity and conservation for the jaguar, *Panthera onca*. *Biol. Conserv.* 143, 939–945. doi:10.1016/j.biocon.2010.01.002
- Reed, D.H., 2004. Extinction risk in fragmented habitats. *Anim. Conserv.* 7, 181–191. doi:10.1017/S1367943004001313
- Rodríguez-Soto, C., Monroy-Vilchis, O., Maiorano, L., Boitani, L., Faller, J.C., Briones, M.Á., Núñez, R., Rosas-Rosas, O., Ceballos, G., Falcucci, A., 2011. Predicting

potential distribution of the jaguar (*Panthera onca*) in Mexico: identification of priority areas for conservation. *Divers. Distrib.* 17, 350–361. doi:10.1111/j.1472-4642.2010.00740.x

Sanchez, O., Ramirez-Pulido, J., Aguilera-Reyes, U., Monroy-Vilchis, O., 2002. Felid record from the State of México. *Mammalia* 66, 289–294.

Sanderson, E.W., Redford, K.H., Chetkiewicz, C.-L.B., Medellin, R.A., Rabinowitz, A.R., Robinson, J.G., Taber, A.B., 2002. Planning to Save a Species: the Jaguar as a Model. *Conserv. Biol.* 16, 58–72. doi:10.1046/j.1523-1739.2002.00352.x

Sanderson, E.W., Redford, K.H., Vedder, A., Coppolillo, P.B., Ward, S.E., 2002. A conceptual model for conservation planning based on landscape species requirements. *Landsc. Urban Plan.* 58, 41–56. doi:10.1016/S0169-2046(01)00231-6

Saura, S., Martinez-Milian, J., 2001. Sensitivity of Landscape Pattern Metrics to Map Spatial Extent. *Photogramm. Eng. Remote Sens.* 67, 1027–1036.

Saura, S., Pascual-Hortal, L., 2007. A new habitat availability index to integrate connectivity in landscape conservation planning: Comparison with existing indices and application to a case study. *Landsc. Urban Plan.* 83, 91–103. doi:10.1016/j.landurbplan.2007.03.005

- Schuttlz, C.B., Crone, E.E., 2005. Patch Size and Connectivity Thresholds for Butterfly Habitat Restoration. *Conserv. Biol.* 19, 887–896. doi:10.1111/j.1523-1739.2005.00462.x
- Shanthala Devi, B.S., Murthy, M.S.R., Debnath, B., Jha, C.S., 2013. Forest patch connectivity diagnostics and prioritization using graph theory. *Ecol. Modell.* 251, 279–287. doi:10.1016/j.ecolmodel.2012.12.022
- Soisalo, M.K., Cavalcanti, S.M.C., 2006. Estimating the density of a jaguar population in the Brazilian Pantanal using camera-traps and capture–recapture sampling in combination with GPS radio-telemetry. *Biol. Conserv.* 129, 487–496. doi:10.1016/j.biocon.2005.11.023
- Spangle, S., Humphrey, J., Buckley, T., 2014. Service designates jaguar critical habitat in Arizona and New Mexico. Albuquerque.
- Terborgh, J., Lopez, L., Nuñez, P., Rao, M., Shahabuddin, G., Orihuela, G., Riveros, M., Ascanio, R., Adler, G.H., Lambert, T.D., Balbas, L., Pace, M.L., Cole, J.J., Carpenter, S.R., Kitchell, J.F., Polis, G.A., Hairston, N.G., Smith, F.E., Slobodkin, L.B., Terborgh, J., Polis, G.A., Strong, D.R., Krebs, C.J., Schmitz, O.J., Hambäck, P.A., Beckerman, A.P., Oksanen, L., Oksanen, T., Alvarez, E., Balbas, L., Massa, I., Pacheco, J., Huber, O., Terborgh, J., Lopez, L., Tello, J.S., Rao, M., Persson, L., Leigh, E.G., Wright, S.J., Herre, E.A., Putz, F.E., Rao, M., Terborgh, J., Nuñez, P., Bremen, H., Ellis, J., Galvin, K.A., Alverson, W.S., Waller, D.M., Solheim, S.L., Ickes, K., Dewalt, S.J., Appanah, S., Coley, P.,

- Bryant, J.P., Chapin, F.S., McLaren, B.E., Peterson, R.O., 2001. Ecological meltdown in predator-free forest fragments. *Science* 294, 1923–6. doi:10.1126/science.1064397
- Tischendorf, L., Fahrig, L., 2000. On the usage and measurement of landscape connectivity. *Oikos* 90, 7–19. doi:10.1034/j.1600-0706.2000.900102.x
- Tobler, M.W., Carrillo-Percegué, S.E., Leite Pitman, R., Mares, R., Powell, G., 2008. An evaluation of camera traps for inventorying large- and medium-sized terrestrial rainforest mammals. *Anim. Conserv.* 11, 169–178. doi:10.1111/j.1469-1795.2008.00169.x
- Turner, M., Gardner, R., O'neil, R., 2001. *Landscape ecology in theory and practice*. Springer, USA.
- Turner, M.G., 1989. Landscape Ecology: The Effect of Pattern on Process. *Annu. Rev. Ecol. Syst.* 20, 171–197. doi:10.1146/annurev.es.20.110189.001131
- Urban, D., Keitt, T., 2001. Landscape Connectivity: A Graph-Theoretic Perspective. *Ecology* 82, 1205–1218.
- Valera-Aguilar, D., 2010. *Conectividad de las poblaciones de jaguar en el noroeste de México*. Universidad Autónoma de Querétaro.

- Van Der Wal, J., Shoo, L.P., Graham, C., Williams, S.E., 2009. Selecting pseudo-absence data for presence-only distribution modeling: How far should you stray from what you know? *Ecol. Modell.* 220, 589–594. doi:10.1016/j.ecolmodel.2008.11.010
- van Proosdij, A.S.J., Sosef, M.S.M., Wieringa, J.J., Raes, N., 2016. Minimum required number of specimen records to develop accurate species distribution models. *Ecography (Cop.)*. 39, 542–552. doi:10.1111/ecog.01509
- Wood, A., Stedman-Edwards, P., Mang, J., 2013. *The Root Causes of Biodiversity Loss*. Routledge.
- Wu, J., 2004. Effects of changing scale on landscape pattern analysis: scaling relations. *Landsc. Ecol.* 19, 125–138. doi:10.1023/B:LAND.00000021711.40074.ae
- Zarco-González, M., Rodríguez-Soto, C., Monroy-Vilchis, O., Urios, V., 2009. Cougar and jaguar habitat use and activity patterns in central Mexico. *Anim. Biol.* 59, 145–157. doi:10.1163/157075609X437673
- Ziółkowska, E., Ostapowicz, K., Kuemmerle, T., Perzanowski, K., Radeloff, V.C., Kozak, J., 2012. Potential habitat connectivity of European bison (*Bison bonasus*) in the Carpathians. *Biol. Conserv.* 146, 188–196. doi:10.1016/j.biocon.2011.12.017

3-7 Tables

Table 3-1: Predictor variables used to find potential habitat for jaguar in Sierra Gorda

Variable	Source	Resolution
Temperature	Servicio Meteorológico Nacional, based on meteorological stations	1 km
Precipitation	Servicio Meteorológico Nacional, based on meteorological stations	1 km
Elevation	Shuttle Radar Topography Mission (SRTM)	90 m
Slope	Shuttle Radar Topography Mission (SRTM)	90 m
Ecoregions	Instituto Nacional de Estadística, Geografía e Informática	30 m
Landcover	Instituto Nacional de Estadística, Geografía e Informática. Serie IV. Derived of the classification of Landsat imagery	30 m

3-8 Figures

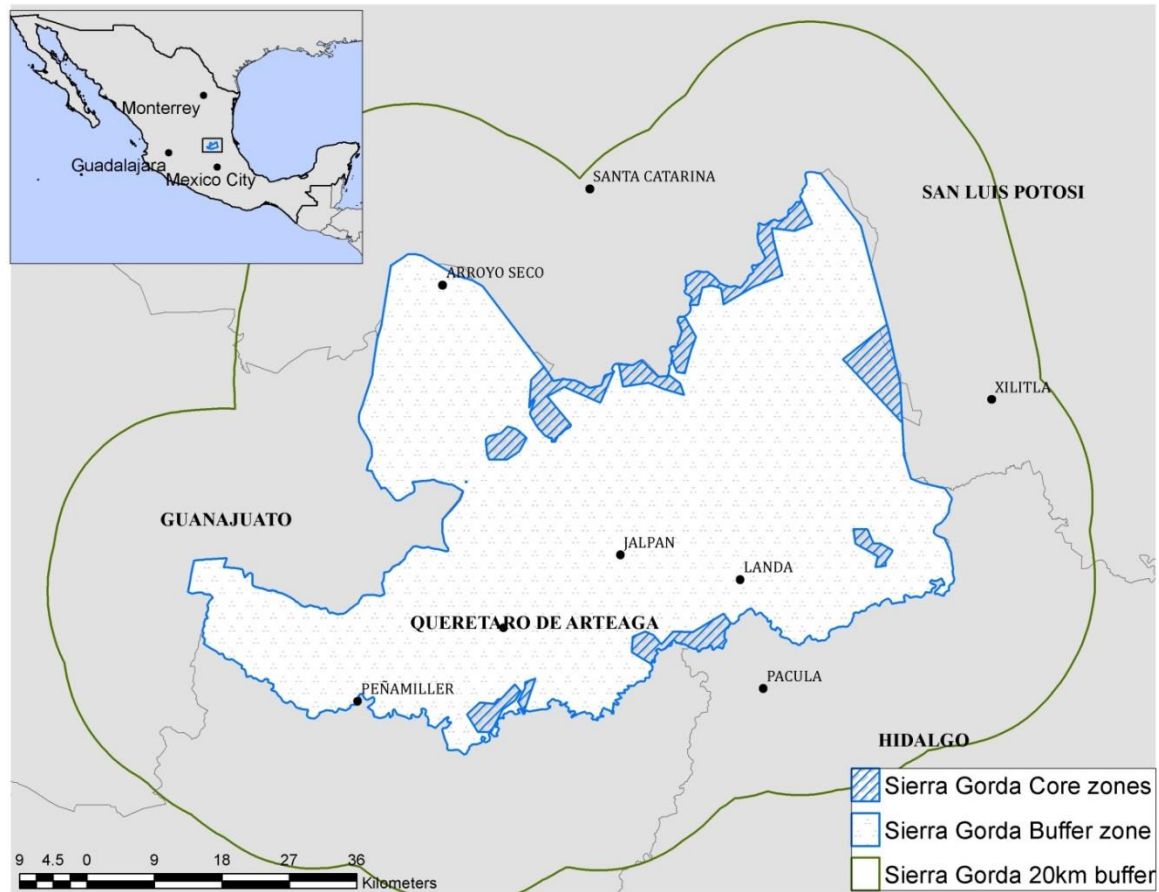


Figure 3-1 Sierra Gorda Biosphere Reserve in Central Mexico. The core zones are located at the margins of the reserve.

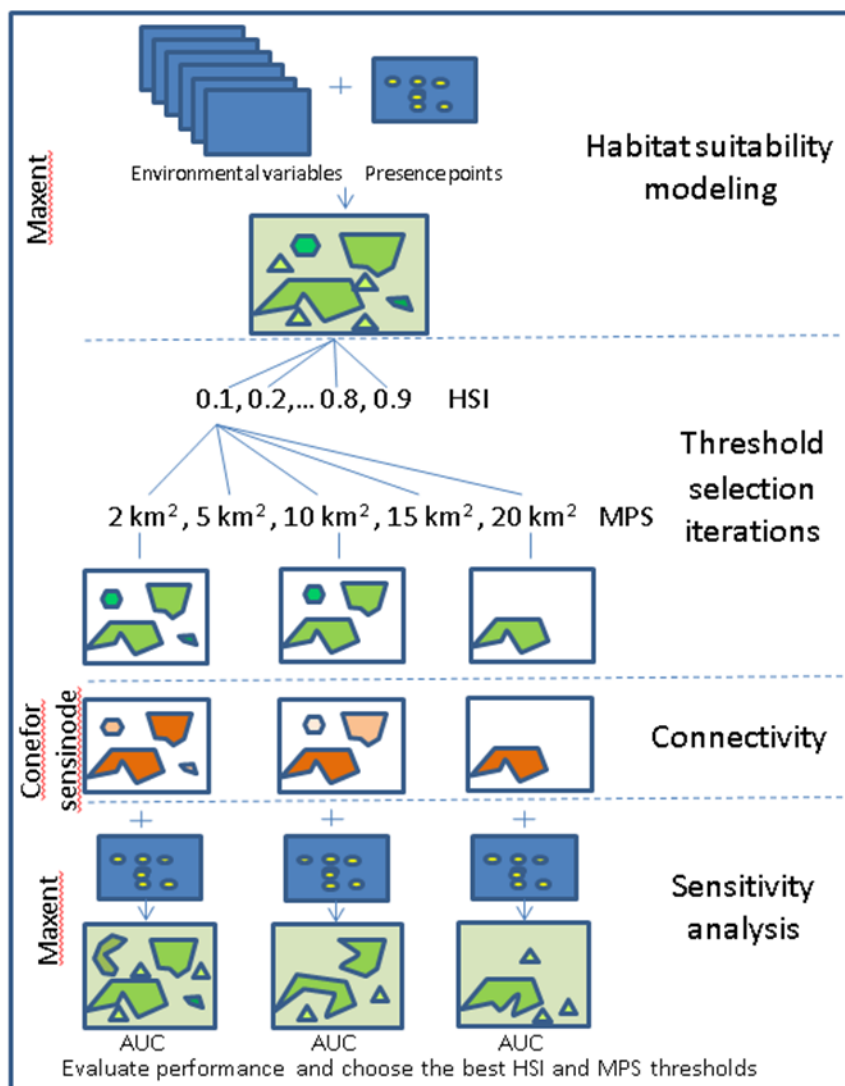


Figure 3-2: Flow diagram of the approach that we developed to identify the best thresholds for habitat suitability index, HSI, and minimum patch size, MPS. We evaluated the performance of each combination of thresholds to describe connectivity based on the area under the curve, AUC. The processes are mentioned on the right while the tools used at each step are mentioned on the left. Only a few examples from the total of 45 combinations that we evaluated are shown here.

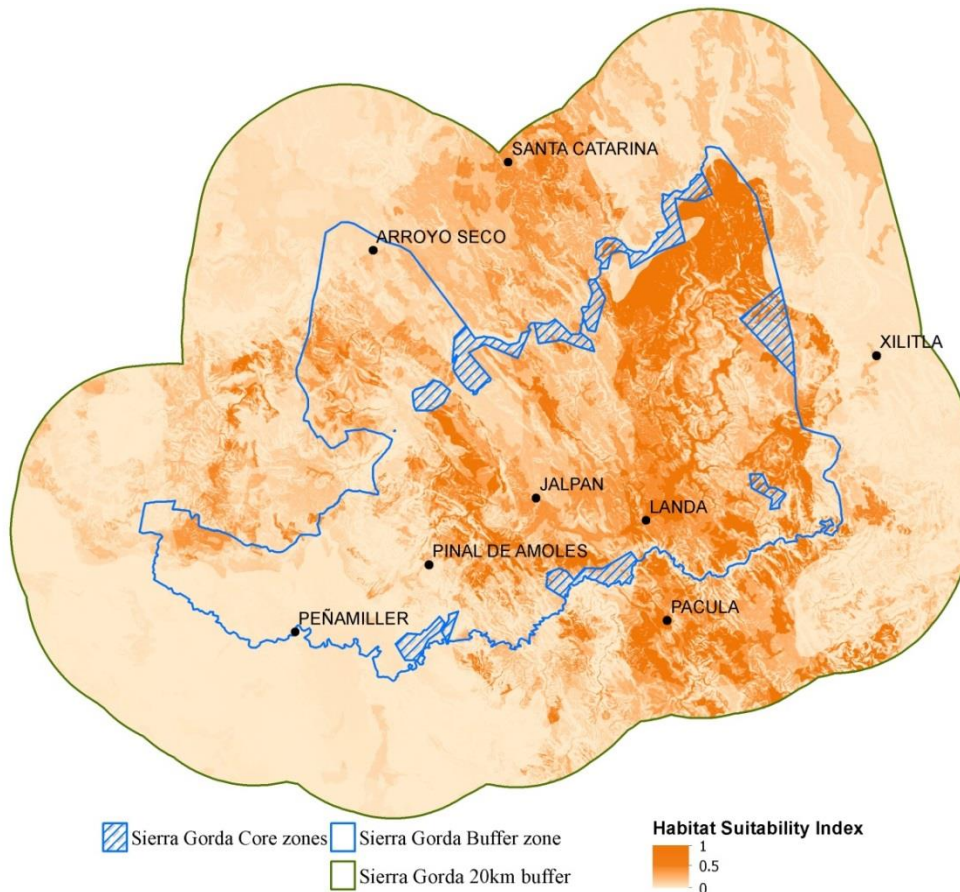


Figure 3-3: Habitat suitability in the study area as determined by our model. The most suitable areas are in the central-eastern part of the reserve and in the south.

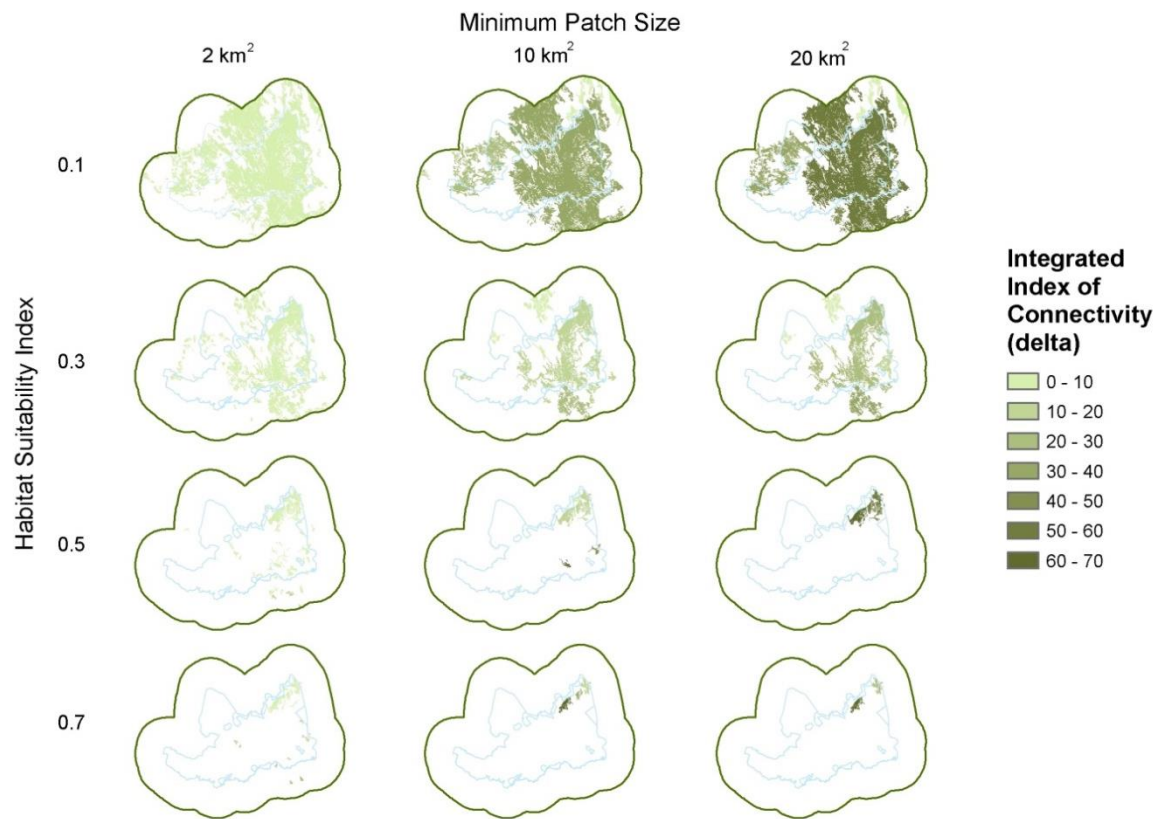


Figure 3-4: Figure 4: Performance of the integral index of connectivity, dIIC, obtained with different habitat suitability thresholds and minimum patch size for the jaguar presence points. Patches with dark colors provide better connectivity for the patch network. For display purposes we do not include all the different combinations tested at different habitat suitability indexes and minimum patch size. No patches remained at a HSI larger than 0.8.

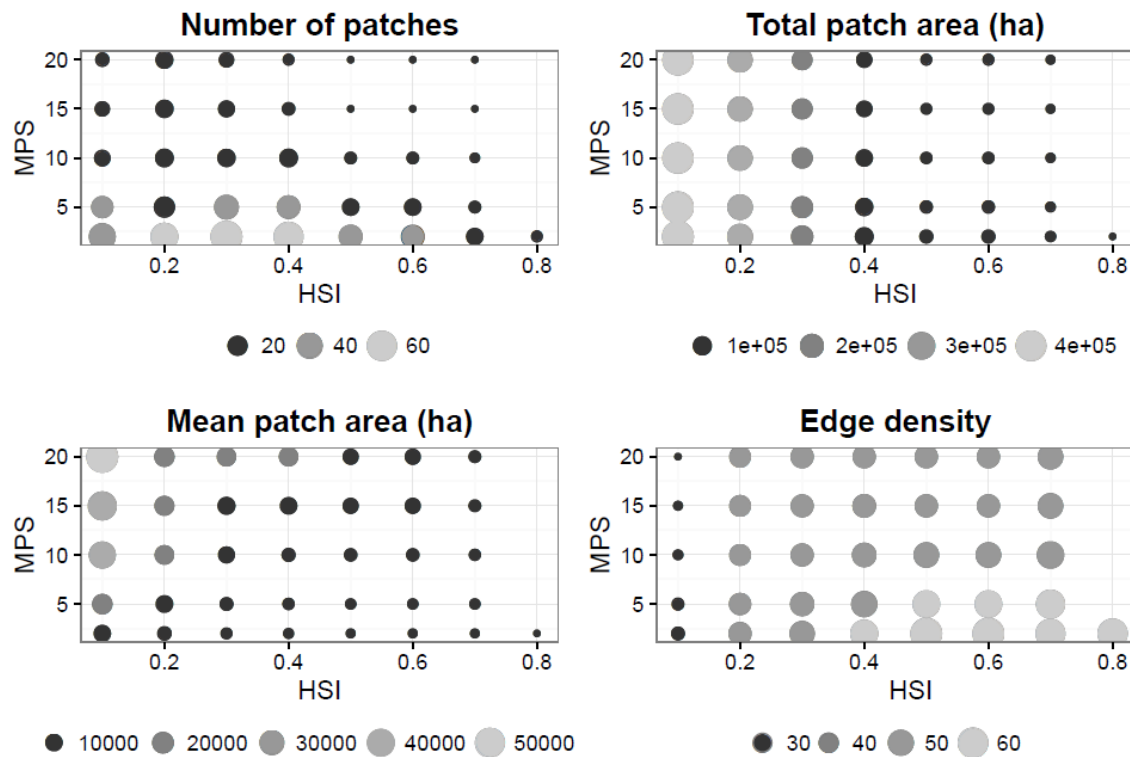


Figure 3-5: Landscape configuration metrics for different habitat suitability index, HSI, and minimum patch size, MPS. Both the color and size of the circles are proportionate to their respective metric score.

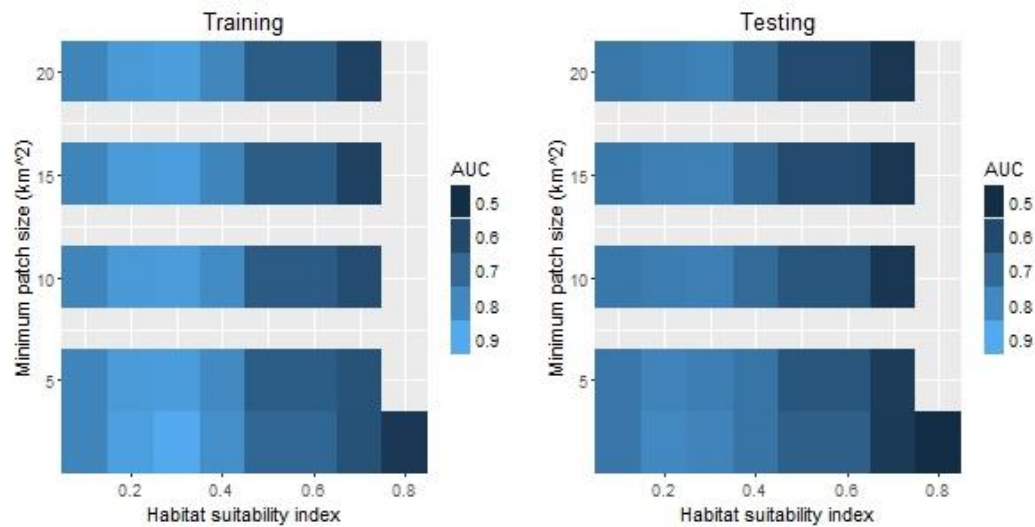


Figure 3-6: Performance of the integral index of connectivity obtained with different habitat suitability thresholds, and minimum patch size for the jaguar presence points. A better model has a higher area under the curve (AUC), and therefore a lighter color. No patches were left with a HSI larger than 0.8.

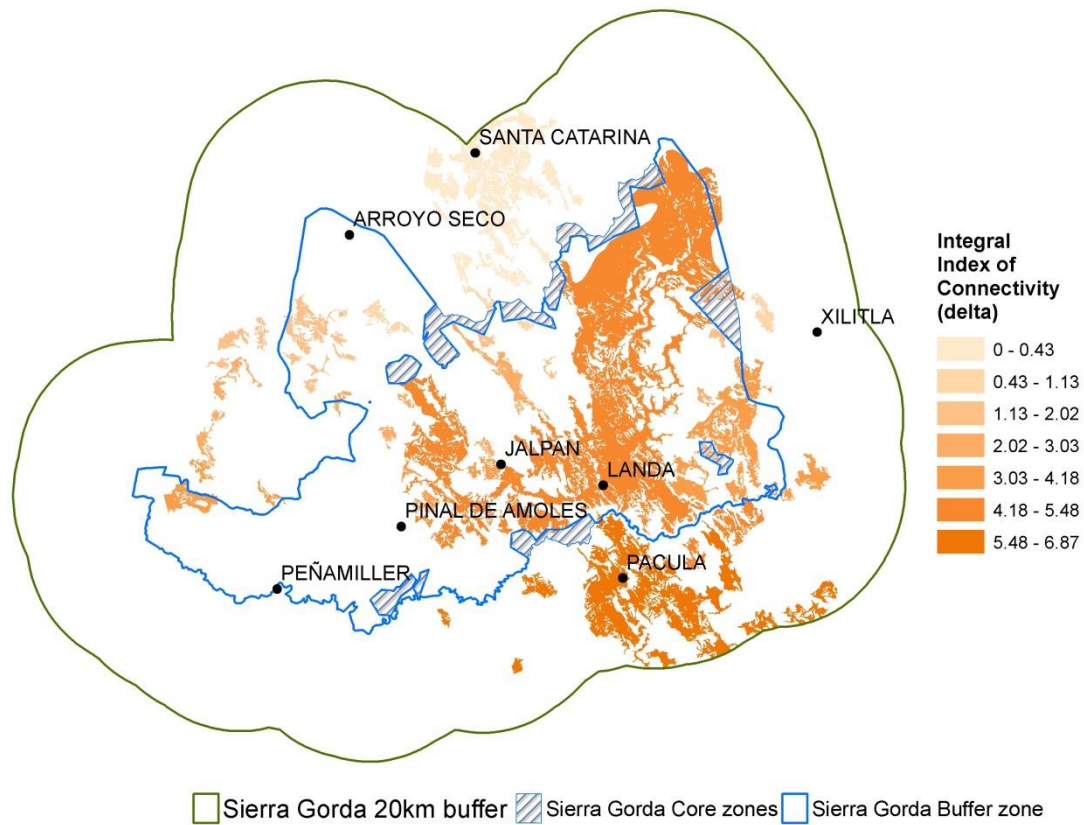


Figure 3-7: Connectivity of the potential habitat for jaguars in the reserve using the combination of thresholds for habitat suitability index 0.3 and a minimum patch size of 2km^2 . The habitat areas that are most important for the connectivity of the area are located in the eastern portion of the reserve

Appendix

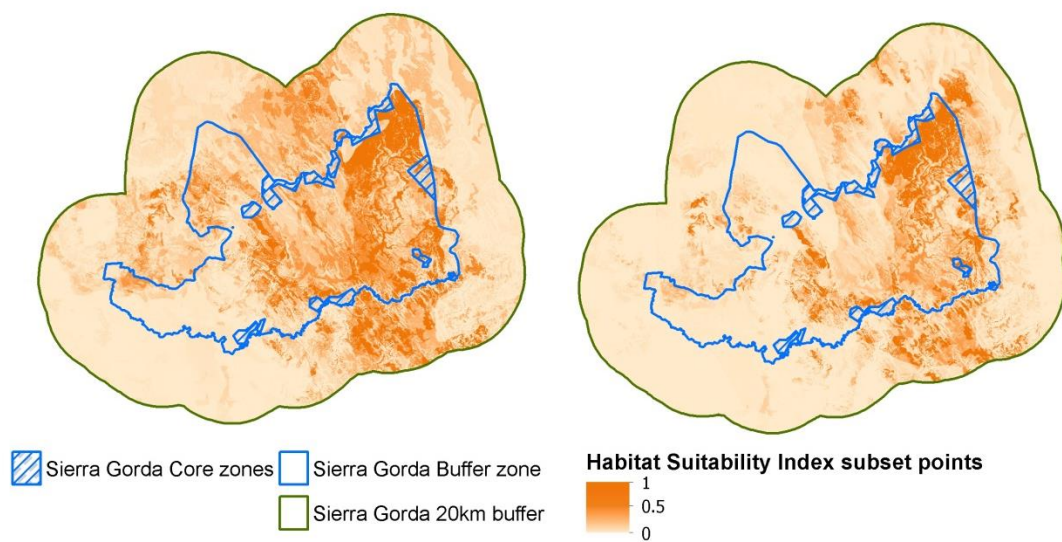


Figure A.1 Habitat suitability index for the study area obtained with 26 spatially filtered subset of training points (left) and with all the 91 training points (right).

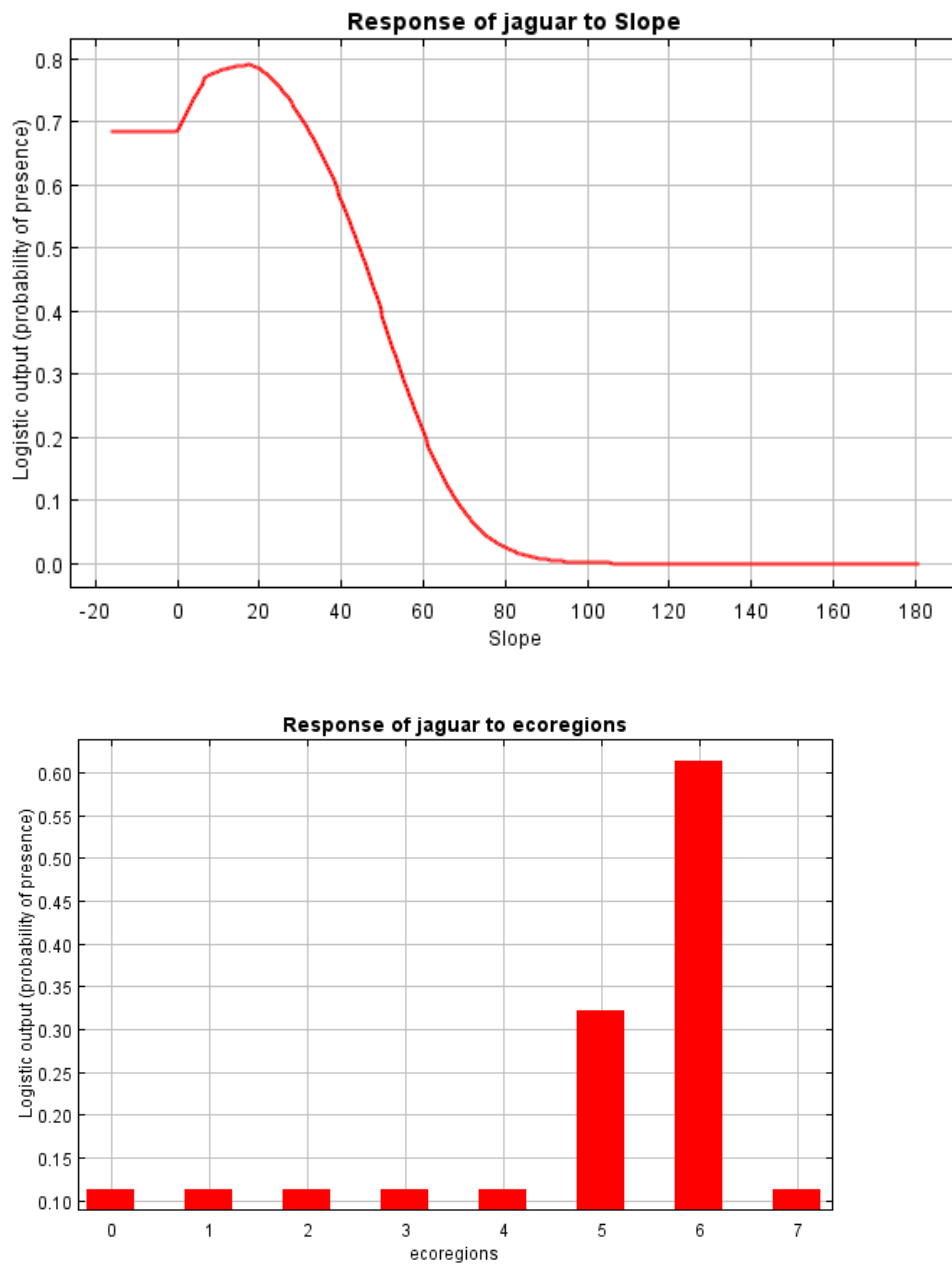


Figure A. 2 The contribution of the main variables to the habitat suitability model. Slopes are in degrees. The ecoregions are 1: Northern Meseta Central desert; 2, Veracruz coastal plain tropical moist forests; 3, Southern Meseta Central desert; 4, Northern Sierra Madre Oriental pine-oak forests; 5 Tamaulipas coastal plain tropical dry forests; 6, Sierra Madre Oriental pine-oak forests; 7, Veracruz montane tropical cloud forests.

Table A.1: Pearson's correlation coefficients for the used predictor variables

	Ecoregions	Elevation	Precipitation	Slope	Temperature	Landcover
Landcover	-0.02	-0.27	0.35	0.04	0.2	1
Temperature	-0.11	-0.57	0.44	-0.03	1	
Slope	0.23	0.2	0.04	1		
Precipitation	-0.1	-0.58	1			
Elevation	0.26	1				
Ecoregions	1					